The Pennsylvania State University

The Graduate School

NOVEL SIGNALS IN STRESS ERYTHROPOIESIS: COORDINATED CONTROL OF WNT, PGE2 AND PERK SIGNALING PATHWAYS REGULATES EXPANSION AND DIFFERENTIATION OF STRESS ERYTHROID PROGENITORS

A Dissertation in

Molecular, Cellular and Integrative Biosciences

by

Yuanting Chen

Submitted in Partial Fulfillment

of the Requirements

for the Degree of

Doctor of Philosophy

May 2020

The dissertation of Yuanting Chen was reviewed and approved* by the following:

Robert F. Paulson
Professor of Veterinary and Biomedical Sciences
Dissertation Advisor
Chair of Committee

K. Sandeep Prabhu
Professor of Immunology and Molecular Toxicology

Zhi-Chun Lai
Professor of Biology & Biochemistry and Molecular Biology

Wendy Hanna-Rose
Professor of Biochemistry and Molecular Biology

Xiaojun Lian
Assistant Professor of Biomedical Engineering & Biology

Melissa Rolls
Professor of Biochemistry and Molecular Biology
Chair of Molecular, Cellular and Integrative Biosciences

ABSTRACT

In response to tissue hypoxia caused by anemia, hemorrhage or infection, the process termed stress erythropoiesis restores tissue oxygenation by rapidly producing large numbers of erythrocytes. In contrast to steady state erythropoiesis, stress erythropoiesis utilizes specialized progenitor cells and distinct set of signals to generate large numbers of erythrocytes. During the early stage of stress erythropoiesis, the immature stress erythroid progenitors (SEPs) rapidly expand without differentiation. The amplifying SEPs maintain their stem cell phenotype until the appearance of transition signals. Upon receiving these signals, SEPs undergo rapid differentiation and give rise to a wave of stress erythroid burst-forming units (BFU-Es), which further develop into mature erythrocytes. The development of SEPs also relies on the regulation derived from the microenvironment. Erythroblastic islands (EBIs) made up of macrophage/monocytes in close contact with developing erythroblasts have been shown to be a necessary niche in erythropoiesis. Our previous work found that SEPs mature in a specific EBI niche. In the stress erythroid niche, monocytes are recruited to the spleen and mature in concert with developing SEPs.

Erythropoietin (Epo) is the key transition signal in stress erythropoiesis. In chapter 2, we discussed the microenvironmental change induced by Epo in regulating SEP differentiation. We found that rather than directly mediating SEPs, Epo signaling acts on EBI macrophages to promote the SEP differentiation by mediating a series of changes in the microenvironment. During the amplifying stage, EBI macrophages generate canonical Wnt ligands, which promote the proliferation of SEPs by targeting β-catenin-dependent gene transcription. Epo induces the transition from proliferating microenvironment to differentiating microenvironment. Two prostaglandins, delta-12-prostaglandin J_2 (Δ^{12}-PGJ_2) and prostaglandin E_2 (PGE_2), are produced by EBI macrophages in response to Epo. Δ^{12}-PGJ_2 activates the peroxisome proliferator-activated receptor gamma (PPARγ), which represses the Wnt expression in macrophages. As another

effector of Epo, PGE_2 drives the differentiation of SEPs simultaneously. As a result, proliferation and differentiation of SEPs become very efficient because of Epo-orchestrated microenvironmental signals.

In chapter 3, we further investigated the mechanism of the PGE_2-mediated SEP differentiation. We demonstrated that the increase in PGE_2 activates the protein kinase RNA-like endoplasmic reticulum kinase (PERK) signaling pathway by regulating intracellular Ca^{2+} flux. PERK belongs to the integrated stress response (ISR) kinase family. We found that the mutation or inhibition of PERK activity causes severe defects in stress erythropoiesis. Perturbation of PERK blocks the transition from amplifying progenitors to differentiating stress BFU-Es in both mouse and human cell cultures. The activation of PERK induces translation of the activating transcription factor 4 (ATF4), which increases the intracellular concentration of amino acids by promoting the expression of amino acid transporter genes. As a microenvironment sensor, the mammalian target of rapamycin complex 1 (mTORC1) is activated in response to the amino acid influx. Consequently, mTORC1 promotes global protein translation in SEPs. Such high rate of protein translation enables the SEP differentiation to generate mature erythrocytes, which eventually alleviates the anemic stress.

In conclusion, the data presented in this thesis identify a key regulatory point in stress erythropoiesis. Unlike the constant production of steady state erythropoiesis, stress erythropoiesis generates a bolus of new erythrocytes, which is designed to maintain homeostasis until steady state erythropoiesis can resume. The initial expansion of immature SEPs represents the first and essential step. There will be inadequate erythrocytes if early progenitors are not efficiently proliferated. Therefore, precise regulation of the expansion and transition of SEPs is vital in stress erythropoiesis. Here we showed that Epo-mediated signal changes in the EBI macrophages promote the transition from proliferating SEPs to differentiating SEPs. These signals also

increase the protein translation in SEPs, allowing the final differentiation of SEPs into mature erythrocytes.

TABLE OF CONTENTS

LIST OF FIGURES

LIST OF TABLES

IMPORTANT ABBREVIATIONS

ATF4: activating transcription factor 4

AGM: aorta-gonad-mesonephros

BFU-Es: erythroid burst-forming units

BM: bone marrow

BMT: bone marrow transplant

BMP4: bone morphogenetic protein 4

CFU-Es: colony-forming units-erythroid

COX: cyclooxygenase

cAMP: cyclic adenosine monophosphate

CReP: constitutive repressor of eIF2α phosphorylation

CHOP: C/EBP homologous protein

CRTH2: chemoattractant receptor-homologous molecule expressed on Th2 cells

CMPs: common myeloid progenitors

DBA: Diamond-Blackfan anemia

Epo: erythropoietin

EpoR: Epo receptor

EBIs: erythroblastic islands

ER: endoplasmic reticulum

EPs: PGE_2 receptors

eIF2α: eukaryotic translation initiation factor 2 alpha

GDF15: growth-differentiation factor 15

GMPs: granulocyte-macrophage progenitors

GCs: glucocorticoids

GR: glucocorticoid receptor

GSK3: glycogen synthase kinase 3

GADD34: growth arrest and DNA damage-inducible protein-34

HSCs: Hematopoietic stem cells

HIF2α: hypoxia. Hypoxia-inducible factor 2 alpha

HH: hedgehog

H-PGDS: hematopoietic prostaglandin D_2 synthase

ISR: integrated stress response

JAK2: Janus kinase 2

MPPs: multipotent progenitors

MEPs: megakaryocyte-erythrocyte progenitors

mTORC1: mammalian target of rapamycin complex 1

mPGES-1: microsomal prostaglandin E synthase-1

Nrf2: nuclear factor erythroid 2-related factor 2

OPP: O-propargyl-puromycin

PB: peripheral blood

PGs: prostaglandins

PGE_2: prostaglandin E_2

PGD_2: prostaglandin D_2

PGH_2: prostaglandin H_2

PGJ_2: prostaglandin J_2

PPARγ: peroxisome proliferator-activated receptor gamma

PERK: protein kinase RNA-like endoplasmic reticulum kinase

PHZ: phenylhydrazine

PKA: protein kinase A

PI3K: phosphoinositide-3-kinase

RPMs: red pulp macrophages

S6: ribosomal S6 protein

SEP: stress erythroid progenitors

Stat5: signal transducer and activator of transcription 5

SCF: stem cell factor

SEEM: stress erythropoiesis expansion media

SEDM: stress erythropoiesis differentiation media

TACs: transit-amplifying cells

4E-BP1: eukaryotic translation initiation factor 4E-binding protein 1

15d-PGJ$_2$:15-deoxy-$\Delta^{12,14}$-prostaglandin J_2

Δ^{12}-PGJ$_2$: delta-12-prostaglandin J_2

ACKNOWLEDGEMENTS

I would like to take this chance to send my endless thanks to the people who have been giving me a lot of help, support and love during my Ph.D. life. My research and this dissertation could not have been accomplished without them.

First and foremost, I would like to thank my advisor Dr. Robert F. Paulson. I am so fortunate to have a mentor who is very knowledgeable and encouraging. Bob is always enthusiastic in science. He shares his insightful thoughts in frontier research all the time, which inspire me to think more of the scientific questions and lead me to a broader picture of my research. Bob always keeps the door open for communications. He never gets tired to discuss with me about the difficulties and interesting ideas in my research. In the past years, Bob taught me how to be a good researcher, encouraged me to present my work to the academic field, understood all my happiness and depressions in the study. I sincerely thank him for giving me valuable advices and significant support in these years.

I would also like to thank all my committee members, Dr. K. Sandeep Prabhu, Dr. Zhi-Chun Lai, Dr. Wendy Hanna-Rose and Dr. Xiaojun Lian for their encouragement and advices during serving on my dissertation committee. I had many collaborations with the members of Dr. Prabhu's group on my projects. Dr. Prabhu has been so generous to give me many help and advices. The collaboration experience was full of joy with his enthusiasm and warmhearted consideration. Dr. Lai is the first Penn State faculty member I met during the graduate recruitment. He made great efforts to help new international graduate students settle down in the brand-new environment. I'm also grateful for his guidance on my research.

The members in Paulson lab has been giving me great support throughout the years. I would like to thank all the previous and present colleagues: Dr. Chang Liao, Dr. Jie Xiang, Baiye Ruan, Ian Huffnegle, Dr. Laura Bennett, Elly Song, Dr. Siyang Hao, James Fraser, Dr. Laura

Goodfield. All of you guys contributed a lot to creating a wonderful working environment in the lab. Jie gave me a lot of help since I joined the lab. She is a great mentor and collaborator. I cannot remember how many times I went to discuss the projects as well as the weekend plans with Chang. We shared a lot of thoughts to each other in both research and life. Ian taught me much more knowledge of motorcycles than I should know. He is such a nice and energetic person that you would always want to talk with. Baiye gave me great support whenever needed. I have been so lucky to have such a great colleague. I've been closely collaborated with Fenghua Qian and Dr. Diwakar Tukaramrao in the Prabhu lab. Both of them are reliable collaborators and great scientists. Fenghua has been so zealous that I've even got used to yell his name in the lab when I need help. He is also a good friend in life that you could discuss a wide range of topics with him.

Thank Dr. Melissa Rolls for making the MCIBS such an active and creative program. Thank all the staff in the Huck Institutes of Life Sciences and Veterinary and Biomedical Sciences. Special thanks to Terrie Young and Margaret Weber for their nice and warm assistance over the years. Many thanks to previous and current staff in flow cytometry facility: Sarah Neering, Brian Dawson and Ruth Nissly.

I'm so grateful for the teaching experience I had in Penn State. I would never know that I enjoy teaching and communicating with students if I haven't been a teaching assistant (TA). I would like to thank Dr. Ola Sodeinde, who is the coordinator of MCRIB 107. He gave great support and guidance for the TAs. He is also very responsible that never missed any questions or issues I brought to him. I learned a lot of teaching philosophies from him during the time we worked together. I would also like to thank all the staff who prepared experimental materials for this laboratory course. Those semesters would never been such smooth without your help. Last but not the least, wish every of my lovely students, who brought me a lot of questions, concerns but much more joy, a great and bright future.

So many thanks to all the friends in and out of State College. I have special thanks to my two oversea friends, Jing Guo and Zedi Niu. The geographical distance has never been an issue for the friendship. Thank you for being such wonderful and perfect friends since we were young girls. Thank you for sharing your life with me and caring about my life, my feelings all the time. My days would be so plain and dim without you.

There are never enough thanks to my family. Many many thanks to my husband, Yong-Jie Hu. I'm extremely lucky to have such a caring man in my life. Yong-Jie, thank you for always being there for me, for understanding me and for backing me up whenever I got tired in life. I could not imagine how life would be without your endless support and love. To my beloved parents, Xinsheng Chen and Xiping Zeng, your unconditional love makes me a stronger person than I ever thought. I could not have done this work without you. To my parents in-laws, Zhongai Hu and Hongying Wu, thank you for welcoming me into the family, treating me as your own kid and all the encouragement and support. Very special thanks to my cat, Sesame. Thank you, my little furry friend, for your love, your company and for bringing so much happiness to my life.

Thank all the people again for helping me and supporting me in this Ph.D. life. It wouldn't be such a wonderful journey without you.

Chapter 1

Introduction

1.1 Hematopoiesis

Hematopoiesis is the process of blood cell development. There are more than 10 types of blood cells in the hematopoietic system[1]. They govern many important functions that ensure the health of the human body, including oxygen transportation, immunity and hemostasis[2,3]. Most of the mature blood cells have limited life spans. Therefore, hematopoiesis is required throughout life to replenish the blood system. Hematopoietic stem cells (HSCs) are the primitive pluripotent stem cells that are capable to self-renewal and differentiate to lineage specific progenitors[4]. The primitive hematopoiesis during development occurs in yolk sac. Definitive HSCs develop in the aorta-gonad-mesonephros (AGM) region and seed the fetal liver during embryogenesis[5]. In adults, hematopoiesis predominately takes place in bone marrow (BM)[5]. However, in pathological circumstances, extramedullary hematopoiesis may also be induced and occurs in liver, lymph nodes and spleen[4]. The classical model of hematopoietic hierarchy is a branched roadmap (Figure 1-1A). Long-term HSCs (LT-HSCs) give rise to progeny that gradually commit to distinct lineages by losing other lineage potentials at each step of differentiation. From 2016, single-cell transcriptome analysis of HSCs and multipotent progenitors (MPPs) provide new insights of hematopoietic development. Rodriguez-Fraticelli et al. identified that LT-HSCs and MPPs are highly heterogeneous populations that includes distinct unilineage and oligolineage clones[6]. The group found that a fraction of LT-HSCs is the source for megakaryocyte progenitors. They also categorized MPPs into four subpopulations based on the transcriptome similarity. MPP1 is close to LT-HSCs that are less lineage primed. MPP2 includes erythroid-primed clones

and megakaryocyte-primed clones. MPP3 mainly has granulocyte/monocytes-primed clones. MPP4 contains lympho-erythromyeloid clones and many multilineage clones. Therefore, the HSC and MPP pool forms a continuum developmental path that mature lineage restricted cells are directly derived from different lineage-primed HSCs or MPPs (Figure 1-1B)[6–10].

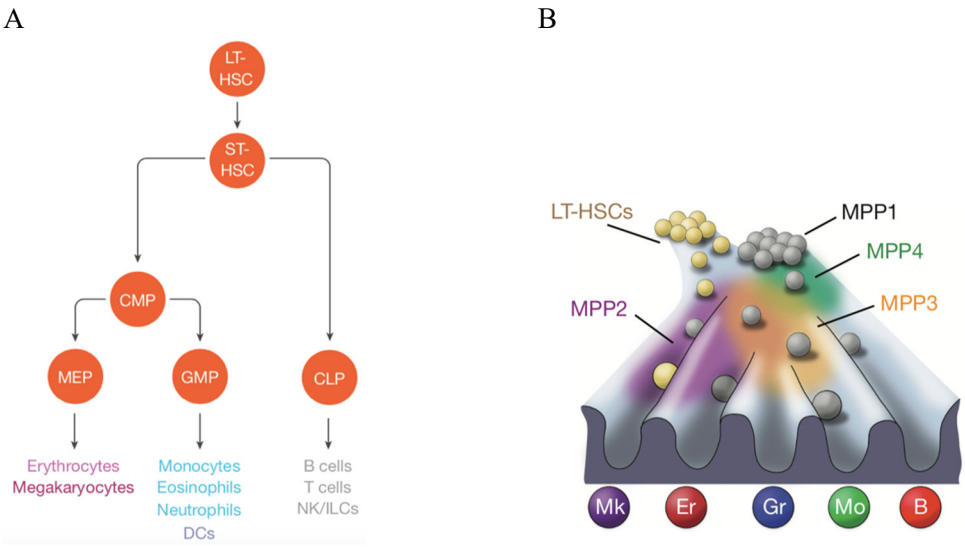

Figure **1-1**: **Models for hematopoietic hierarchy**[6,7]

(A). Classical model of hematopoietic hierarchy. ST-HSCs: short-term HSCs, CMPs: common myeloid progenitors, CLPs: common lymphoid progenitors, MEPs: megakaryocyte-erythrocyte progenitors, GMPs: granulocyte-macrophage progenitors, DCs: dendritic cells, NKs: natural killer cells, ILCs: innate lymphoid cells.

(B). Current model of hematopoietic hierarchy. Mk: megakaryocytes, Er: erythrocytes, Gr: granulocytes, Mo: monocytes, B: B cells.

1.2 Steady state erythropoiesis

Erythrocytes have the average life span of 120 days in human. Under homeostatic conditions, new erythrocytes are generated at the basal rate of approximately 2 x 10^{11} per day to replace damaged or senescent erythrocytes[11]. Erythropoiesis, as one developmental path of HSCs, is the process of generating erythrocytes. There are two waves of erythropoiesis during mammalian development. First, primitive erythropoiesis initiates in the yolk sac. Nucleated erythroblasts are generated and released to the bloodstream. These large size erythroblasts retain proliferation capability and are only observed in the early embryonic circulation. Eventually, the erythroblasts complete enucleation and become mature erythrocytes in circulation. Once switched to the fetal development, the initial definitive erythroid progenitors derived from yolk sac migrate to the fetal liver and give rise to small enucleated erythrocytes. During the following fetal development, these progenitors are replaced by definitive progenitors derived from HSCs in the fetal liver. Around birth, the fetal liver HSCs migrate to BM and maintain lifelong definitive erythropoiesis at this site[11,12] (Figure 1-2). During steady state erythropoiesis, the erythroid lineage committed megakaryocyte-erythrocyte progenitors (MEPs) differentiate into burst-forming units-erythroid (BFU-Es). BFU-Es continue to generate colony-forming units-erythroid (CFU-Es). BFU-Es and CFU-Es were originally defined by colony assays[13,14]. BFU-Es are identified as immature erythroid precursors that give rise to large colonies containing hundreds of cells *in vitro*, whereas CFU-Es are more abundant erythroid precursors and form much smaller colonies than BFU-Es. During the terminal erythropoiesis, pro-erythroblasts (Pro-Es) sequentially differentiate into morphologically recognizable progeny: basophilic erythroblasts (Baso-Es), polychromatophilic erythroblasts (Poly-Es) and orthrochromatic erythroblasts (Ortho-Es)[11]. Along with the successive cell divisions, erythroblasts progressively reduce their size and condense their nucleus, while beginning to accumulate hemoglobin. At the end of maturation,

Ortho-Es undergo nucleus expulsion and organelle clearance, including elimination of mitochondria, endoplasmic reticulum (ER), Golgi apparatus and ribosomes, to become

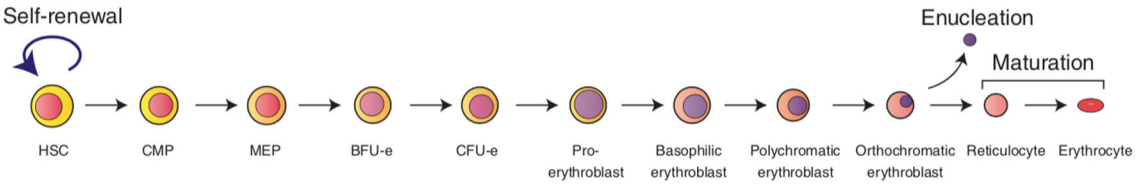

Figure **1-3**: **Development of erythrocytes**[11].

reticulocytes. Reticulocytes continue to reduce in cell size and expel remaining organelles before giving rise to mature erythrocytes[15] (Figure 1-3). The primary function of erythrocytes is to transport oxygen to body tissues. Therefore, mature erythrocytes have biconcave disk shape, which extends the cell surface for gas exchange, and small size, which allows them to travel in the capillaries[12].

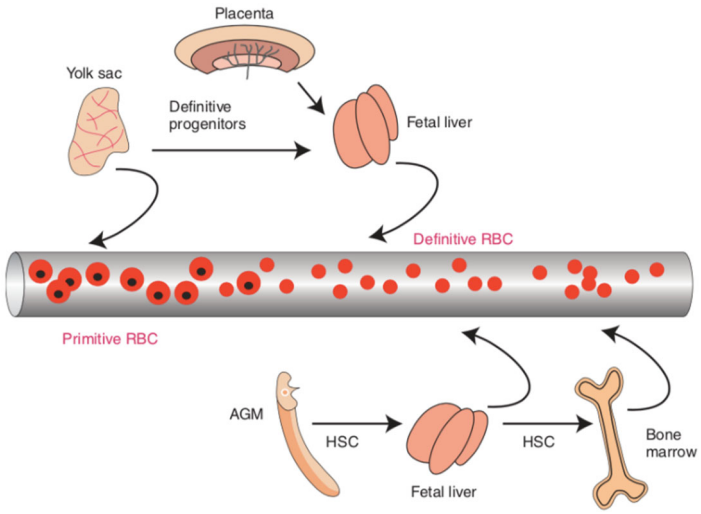

Figure **1-2**: **Ontogeny of erythrocytes**[11].

Primitive erythrocytes are generated in yolk sac from E7.5 to E11/12. Definitive erythroid progenitors derived from yolk sac and placenta migrate to fetal liver at E9 and give rise to definitive erythrocytes. At E10.5, AGM generated HSCs migrate to fetal liver. HSCs continue to migrate to bone marrow at birth and maintain definitive erythropoiesis throughout life.

1.3 Stress erythropoiesis

1.3.1 Overview of stress erythropoiesis

Under many acute circumstances, such as acute anemia, severe hemorrhage and recovery from bone marrow transplant (BMT), increased erythrocyte production is vital for restoring tissue oxygenation and cell survival. Stress erythropoiesis is the predominant process in response to hypoxic stress. In contrast to steady state erythropoiesis, stress erythropoiesis efficiently gives rise to abundant erythrocytes by increasing the erythrocyte production rate up to 10-fold[16]. The strategy of stress erythropoiesis is to rapidly accumulate abundant erythroid progenitors that can synchronously differentiate to generate mature erythrocytes in response to stress signals. As an adaptive stress response, stress erythropoiesis is usually short-term and rapidly declines after restoring erythropoietic homeostasis. In mice, stress erythropoiesis occurs in fetal liver during development, whereas the process takes place in spleen and liver in adults. In humans, the site of stress erythropoiesis is controversial. It has been reported in BM, however, extramedullary erythropoiesis is also observed in anemia patients and BMT patients[17,18]. To fulfill the requirement of generating large numbers of erythrocytes in short-term, stress erythropoiesis utilizes a distinct progenitor population, the stress erythroid progenitors (SEPs). The SEPs undergo a relatively compact developmental path in compare to steady state erythroid progenitors. The entire stress erythropoiesis can be divided into four stages (Figure 1-4). The earliest SEPs derived from ST-HSCs (CD34+Kit+Sca1+Lin-) that migrate from BM to spleen, where they acquire the stress erythroid fate. Next, the immature SEPs rapidly proliferate to expand the pool of early stage SEPs. Previous work in the Paulson lab has revealed unique cell surface markers that identify SEPs in different developmental stages (Figure 1-11)[19]. We found that there are three subtypes of SEPs during the amplification stage. The most immature SEPs

express high level of CD34, CD133, Kit and Sca1(CD34+CD133+Kit+Sca1+ SEPs). The expression of CD34 and CD133 gradually disappear from SEPs as they differentiate to sequentially generate CD34-CD133+Kit+Sca1+ SEPs and CD34-CD133-Kit+Sca1+ SEPs. Although the three SEPs populations represent different developmental stages, they share similar functional properties. All three subtypes are erythroid restricted. They undergo active self-renewal but are unable to differentiate during this stage. Therefore, these SEPs largely retain their stemness and can be serial transplanted. After proliferation, the SEPs transition progenitor cells committed to differentiation. The transition stage relies on several transition signals, among them the erythropoietin (Epo) plays the pivotal role. The amplifying SEPs continue to lose the expression of Sca1 and become stress BFU-E progenitors (CD34-CD133-Kit+Sca1-) in response to increased serum Epo. The final step of stress erythropoiesis is the terminal differentiation of stress BFU-Es. Eventually, a wave of mature erythrocytes is efficiently produced to alleviate anemic stress. It is noteworthy that Kit expression is retained in all stage of SEPs, which distinguishes the SEPs from steady state erythroid progenitors and reflects their ST-HSC origin.

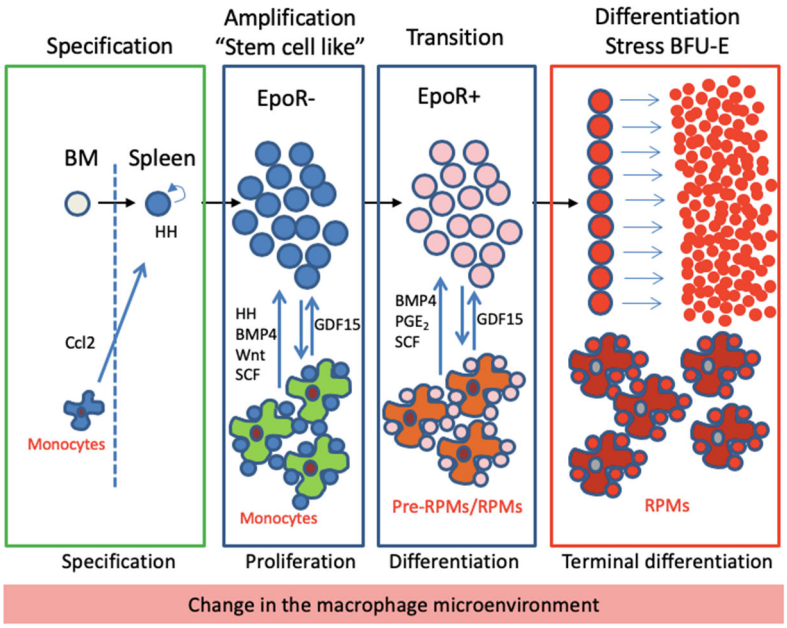

Figure **1-4**: **Schematic of stress erythropoiesis**.

The in vivo stress erythropoiesis process can be divided into four stages. Specification stage: BM derived ST-HSCs migrate to spleen and committed to erythroid restricted progenitors, the SEPs. Amplification stage: early SEPs rapidly expand but are not able to differentiate. Transition stage: transition signals, Epo and hypoxia, induce the transition from amplifying SEPs to differentiating SEPs. Differentiation stage: SEPs efficiently give rise to stress BFU-Es, which continue to differentiate into mature erythrocytes. During the entire process, the microenvironment supports the development of SEPs with required growth factors. Macrophages are the key regulators in the microenvironment. Along with the maturation of SEPs, the macrophage precursors, monocytes, also undergo multiple developmental stages to become mature macrophages. Stress erythropoiesis relies on the close interaction between SEPs and the corresponding niche in all stages. Ccl2: C-C motif chemokine ligand 2. PGE_2: prostaglandin E_2. RPMs: red pulp macrophages.

1.3.2 Microenvironment of stress erythropoiesis

Our increased understanding of the molecular mechanisms of stress erythropoiesis indicates that the development of SEPs requires support from the microenvironment, including microenvironment derived regulatory signals and direct cell-cell interactions. Erythroblastic islands (EBIs) are a necessary niche for regulating the development of erythroid precursors. In line with the sites where erythropoiesis takes place, EBIs are found in BM, spleen and liver in mice[20]. EBIs are composed of a central macrophage and multiple erythroblasts[20]. The developing erythroblasts surround the macrophage to form a ring-shaped structure (Figure 1-5). Studies has shown that the number of surrounding erythroblasts could range from 5 to 30 in human BM[21]. Previous studies also demonstrated a 3-fold increase of erythroid proliferation when there is direct erythroblast-macrophage interaction[22], indicating the important role of central macrophages in supporting the growth of erythroblasts. The most well documented functions of central macrophages are phagocytosis of expelled nuclei from erythroblasts and transferring iron to erythroblasts[23]. In addition, investigations of soluble factors secreted by EBIs revealed that various macrophages derived cytokines, including Ephrin-2, burst-promoting activity (BPA) and insulin-like growth factor-1 (IGF-1), are required for the growth of BFU-Es and CFU-Es[24–26].

Under homeostatic conditions, mature macrophages expressing high levels of F4/80, CD169 and VCAM-1 compose the majority of EBIs[27]. These EBIs maintain a constant number to support the steady state erythropoiesis. Recent work shows that ablation of CD169+ macrophages significantly reduces the EBIs in BM[27]. Notably, depletion of murine CD169+ macrophages also results in severe defects in response to hemolytic anemia and acute blood loss[27]. This observation emphasizes the importance of niche macrophages in regulating stress erythropoiesis. Our recent work demonstrated a novel model where the splenic niche expands and matures in concert with the development of SEPs during stress erythropoiesis (Figure 1-6)[28]. In particular, spleen resident

macrophages secret C-C motif chemokine ligand 2 (Ccl2), which induces the migration of monocytes at the initiation stage of stress erythropoiesis. Mobilized monocytes infiltrate to spleen and sequentially differentiate to pre-red pulp macrophages (pre-RPMs) and red pulp macrophages (RPMs). The maturation of monocytes accompanies the differentiation of SEPs to form unique niche at each stage of stress erythropoiesis. Monocytes and immature pre-RPMs that express more monocytic cell surface markers, CD11b and Ly6C, closely interact with early stage CD133+Kit+Sca1+ SEPs. While mature RPMs having high CD169 and VCAM-1 expression form late stage EBIs with the differentiated Ter119+ erythroblasts. This co-maturation system enables the efficient expansion and differentiation of SEPs through dynamically modulating signals in the microenvironment. Our lab and other groups have identified several important niche signals in stress erythropoiesis (Please see section 1.3.3). However, a more comprehensive understanding of microenvironment derived soluble factors and corresponding signaling transductions remains to be further characterized.

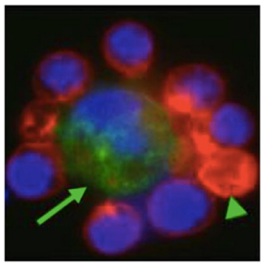

Figure **1-5**: **Immunofluorescence image of EBI from mouse BM**[29].
Red: erythroid marker, green: macrophage maker, blue: DNA probe. Arrow: central macrophage, arrowhead: reticulocytes.

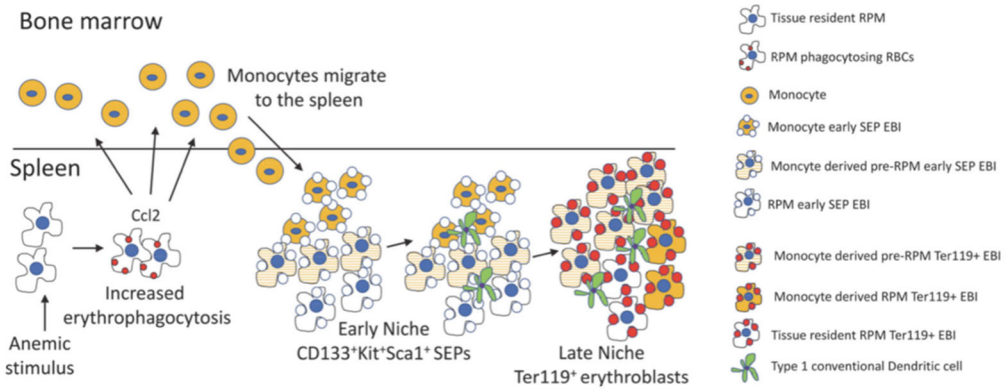

Figure **1-6**: **Model of the splenic stress erythropoiesis niche development after BMT**[28].

1.3.3 Signals in stress erythropoiesis

Epo is a glycoprotein hormone that plays a key role in regulating survival and development of SEPs. In adults, Epo is primarily produced in the kidney and circulates in peripheral blood (PB). Epo production is triggered by low oxygen environment and tissue hypoxia. Hypoxia-inducible factor 2 alpha (HIF2α) is the primary transcription factor that regulates the expression of the Epo gene[30]. Under normal O_2 conditions, two proline residues of HIF2α are hydroxylated by prolyl-4-hydroxylase domain protein (PHD)[31]. Hydroxylated HIF2α binds to von Hippel-Lindau protein (VHL)-E3 ubiquitin ligase complex, which leads to poly-ubiquitination and rapid degradation of HIF2α[31]. The low O_2 environment abrogates the proline hydroxylation process and allows the stabilized HIF2α to translocate to the nucleus where it promotes Epo transcription[31]. Epo targets the Epo receptor (EpoR) expressed on the erythroid progenitors[32]. Our work and recent studies found that macrophages in the EBIs also express EpoR[33], suggesting that Epo may act on the microenvironment to regulate the erythroid

progenitors. Upon binding to Epo, EpoR undergoes conformational change, which activates the tyrosine kinase, Janus kinase 2 (JAK2)[34]. JAK2 continues to phosphorylate the tyrosine residues of EpoR, which provides docking sites for signal transducer and activator of transcription 5 (Stat5)[35]. Recruited Stat5 proteins are phosphorylated, dimerized and translocated to the nucleus to mediate transcription of erythroid genes.

Knockout of EpoR is embryonic lethal but can be rescued by expressing GATA1[36], indicating that the lethality is due to erythropoietic defects. Correspondingly, mice with conditional knockout of Stat5 a/b locus exhibit low hematocrits at E18.5 and in neonatal period[37]. These findings suggest that Epo/EpoR mediated JAK2/Stat5 signaling pathway is indispensable for stress erythropoiesis. It is well documented that Epo has anti-apoptosis function, which promotes the survival of CFU-Es and early erythroblasts[38]. Rhodes et al. found that, in response to a wide range of Epo concentration, the proliferation rate of erythroblasts in EBIs is always significantly higher than erythroblasts cultured alone[22]. Although the number of erythroblasts in both groups increases along with the increased Epo concentration, the apoptosis percentage always remain comparable between groups. These observations indicate that, in addition to the anti-apoptotic effect on erythroblasts, Epo also affects macrophages in the niche to promote the proliferation of erythroblasts. This idea is further supported by a recent study showed that EBI macrophages can be characterized by the EpoR expression[33]. Taken together, current evidence suggest that Epo/EpoR signaling has profound effects on erythroid progenitors, erythroblasts and niche macrophages. Here, we extend the Epo/EpoR findings into stress erythropoiesis and revealed a novel mechanism of Epo dependent microenvironment signaling in the regulation of proliferation and differentiation of SEPs.

In addition to Epo, stress erythropoiesis utilizes distinct signals that are not associated with steady state erythropoiesis. Hedgehog (HH) is required for inducing the BM derived erythroid progenitors to acquire the stress erythroid fate once they migrate to the spleen. HH

signal is also required for priming committed SEPs to further respond to bone morphogenetic protein 4 (BMP4)[39]. The *flexed-tail* (*f*) mutant mice, in which BMP4 signaling is inhibited by a mutation in the BMP signaling pathway component Smad5, exhibit fetal-neonatal anemia that quickly resolves 2 weeks after birth[40,41]. They exhibit a normal erythropoiesis phenotype afterwards, which suggests that BMP4 is not required for steady state erythropoiesis. However, BMP4 is crucial for expanding stress BFU-Es as demonstrated by the delayed recovery in *f/f* mice in response to phenylhydrazine (PHZ) induced hemolytic anemia[42]. Growth-differentiation factor 15 (GDF15) is another indispensable signal for stress erythropoiesis. In the splenic microenvironment, GDF15 maintains BMP4 expression by stabilizing HIF2α. GDF15 also directly acts on SEPs by regulating the expression of metabolic enzymes required for proliferation[43]. The stem cell factor (SCF) and its receptor Kit are required for expansion of BFU-Es. Mice with mutation of Kit receptor are devoid of BMP4 responsive cells in spleen and exhibit delayed recovery after PHZ injection[44]. Previous work in the Paulson lab also demonstrated that SCF, BMP4 and hypoxia together can maximize the expansion of stress BFU-Es[44].

Glucocorticoids (GCs) are steroid hormones that produced by adrenal glands[46]. Mice with mutation in glucocorticoid receptor (GR), $GR^{dim/dim}$ mice, have no obvious defects in steady state erythropoiesis. However, the mutants failed to generate CFU-Es after PHZ injection[45]. Also, $GR^{dim/dim}$ adult mice are unable to increase erythrocyte count and hemoglobin in PB when exposed to hypoxia environment[45]. These findings indicate that GC/GR signaling also plays important roles in stress erythropoiesis[25]. In this dissertation, we will discuss multiple novel signals in stress erythropoiesis.

1.3.4 Tissue regeneration and potential signals in stress erythropoiesis

Hematopoietic reconstitution can also be viewed as a tissue regeneration process. HSCs remain quiescent and undergo slow cell cycle, whereas the MPPs are the main implements of reconstitution. The MPPs act as transit-amplifying cells (TACs) that undergo rapid but limited proliferation then differentiate to downstream lineages. In response to anemic stress, the SEPs resemble one subtype of MPPs that gains erythroid lineage bias and exclusively replenish the erythrocytes. Many other continuous tissues such as hair follicle and intestine share similar tissue regeneration properties in response to injury or other perturbations. For instance, cells locate at the +4 position of the intestinal crypt acquire TAC properties upon damage to the intestinal epithelium[47]. Rather than the crypt resident stem cells, the activated +4 crypt cells contribute to the intestinal epithelium regeneration. Several signaling pathways are commonly required by the regeneration of various tissues. We hypothesize that these signals may also play a role in stress erythropoiesis.

1.3.4.1 Canonical Wnt signaling pathway

The Canonical Wnt signaling pathway has been identified as important regulator of embryonic development and self-renewal of many types of stem cells in adult[48–50]. The initiation of the Wnt signal transduction cascade depends on the ligand-receptor binding (Figure 1-7). In the absence of Wnt ligands, the cytoplasmic β-catenin is bound by a destruction complex composed of Axin, adenomatosis polyposis coli (APC), protein phosphatase 2A (PP2A), glycogen synthase kinase 3 (GSK3) and casein kinase Iα (CK1α). CK1α and GSK3 phosphorylate β-catenin[51]. Phosphorylated β-catenin is recognized by E3 ubiquitin ligase complex. Ubiquitinated β-catenin then gets degraded by proteasome. Once Wnt ligands are

present and bind to the Frizzled/lipoprotein receptor-related protein (Fz/LRP) coreceptor, the canonical Wnt signaling pathway is activated. GSK3β and casein kinase I-γ (CK1γ) phosphorylate LRP, which provides docking site for Axin[51]. In addition, Wnt regulates the phosphorylation of Dishevelled (Dsh, in mammals the protein is Dvl). The exact function of Dsh in Wnt signaling pathway is not clear. However, studies suggest that it may participate in regulating the phosphorylation activity of GSK3β[52]. Together, ligation of Fz/LRP coreceptor disassembles the destruction complex and stabilizes β-catenin in the cytoplasm. β-catenin continues to translocate into the nucleus and promote transcription of canonical Wnt target genes through binding to T-cell factor/lymphoid enhancing factor (TCF/LEF) transcription factor[53].

Canonical Wnt signaling pathway was also well documented as one of the critical niche regulators in retaining cell proliferation in injury repair and regeneration process. Elevated Wnt signaling promotes healing of skin wounds and formation of new hair follicles[54]. In the intestine, induction of Wnt by inhibiting Dickkopf-1 (Dkk1) results in increased proliferation of epithelial cells in wound repair after colitis[55]. In concordance, reduced intestinal regeneration is correlated with decreased Wnt signaling pathway activity in some inflammatory bowel diseases[56].

In hematopoietic system, Wnt ligands can be secreted by both HSCs (autocrine) and the microenvironment (paracrine). It has been demonstrated that canonical Wnt ligand Wnt3a and β-catenin can promote the reconstitution capability of HSC after BMT in mice[57]. Stabilized cytoplasmic β-catenin is the hallmark of activated canonical Wnt signaling pathway. Therefore, genetic manipulation of β-catenin has been widely used to understand roles of canonical Wnt pathway in hematopoiesis. Constitutively activation of β-catenin promotes and retains the self-renewal capacity of hematopoietic precursor for more than 5 months in murine bone marrow[58]. On the other hand, conventional deletion of β-catenin results in embryonic lethality[59]. Conditional deletion of β-catenin in hematopoietic system with Vav-Cre in fetal stage leads to significantly abnormal hematopoiesis[60]. However, inducible β-catenin deletion in adult mouse has no obvious

hematopoietic phenotype[61]. In this dissertation, we demonstrated an important and indispensable role of Wnt/β-catenin in regulating expansion of immature SEPs.

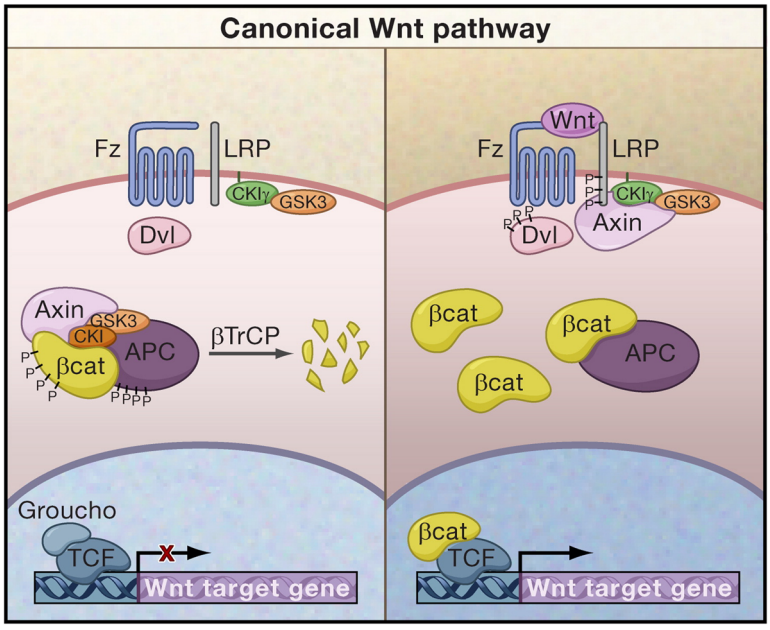

Figure **1-7**: **Canonical Wnt signaling pathway**[51].

1.3.4.2 Prostaglandins

Prostaglandin biosynthesis

Prostaglandins (PGs) are lipid mediators that participate in various physiological and pathological processes. The synthesis of PGs relies on the action of a series of specific enzymes (Figure 1-8). At the beginning of synthetic pathway, phospholipase A_2 (PLA_2) releases arachidonic acid (AA) by hydrolyzing the plasma membrane phospholipids. AA is converted into the unstable metabolite prostaglandin G_2 (PGG_2) with two molecules of oxygen added by the cyclooxygenase (COX) enzymes, COX1 and COX2. Next, PGG_2 is reduced to prostaglandin H_2 (PGH_2) through the peroxidase activity of COX1 and COX2. PGH_2 is a common precursor that

can be converted to thromboxanes (TXs) and other PGs by specific synthases. Depending on the cell types and stimuli, PGH_2 can be catalyzed to prostaglandin E_2 (PGE_2), prostaglandin D_2 (PGD_2), prostaglandin F_{2a} (PGF_{2a}), prostacyclin (PGI_2) and thromboxane A_2 (TXA_2). Upon binding to distinct G protein coupled receptors, PGs and TXA_2 activate a wide range of intracellular signaling pathways to implement their regulatory effects.

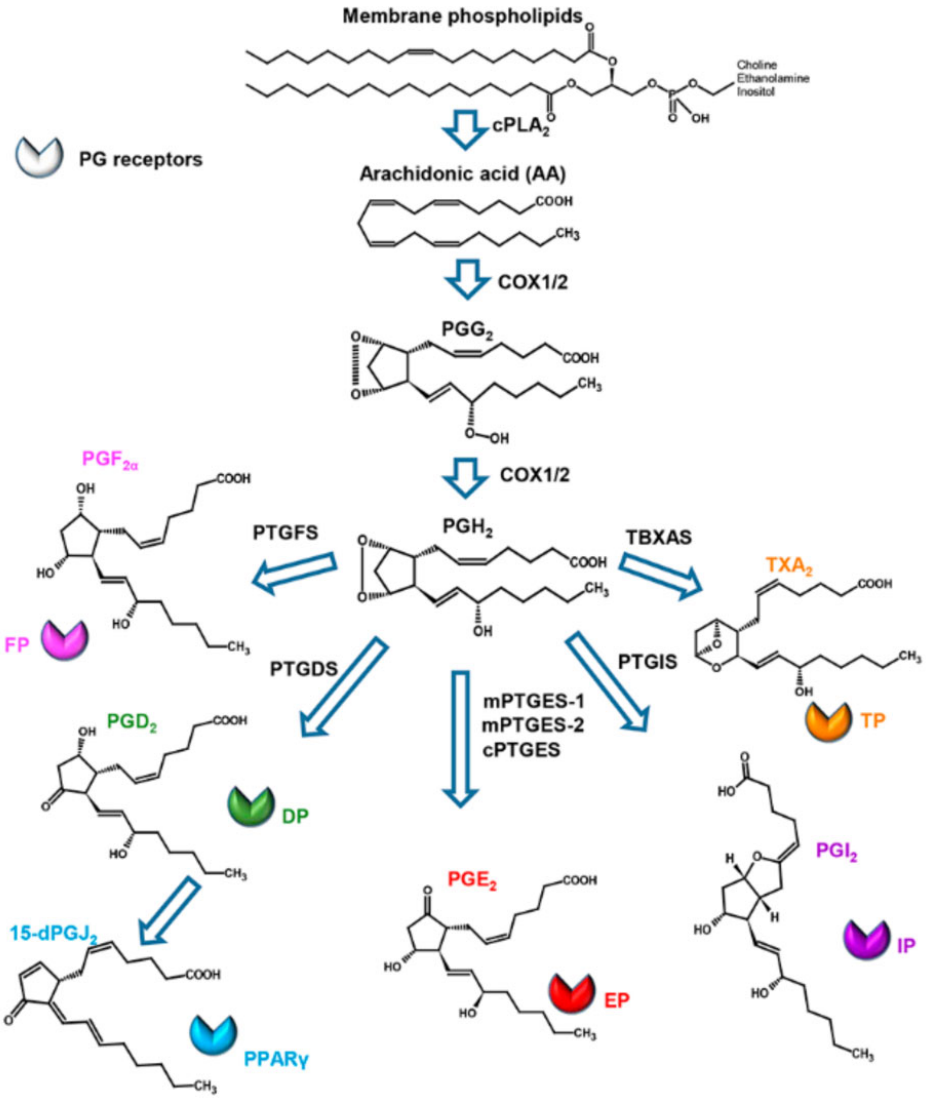

Figure **1-8**: **The prostaglandin biosynthetic pathway**[62].

PGE_2

PGE_2 is the most abundant and widespread PGs in mammals. It regulates various physiological activities including inflammation resolution, potent vasodilation and renal hemodynamics. Three enzymes, microsomal prostaglandin E synthase-1 (mPGES-1), mPGES-2 and cytosolic prostaglandin E synthase (cPGES), can catalyze the synthesis of PGE_2 from PGH_2 (Figure 1-8). mPGES-2 and cPGES are constitutively expressed in cells, while mPGES-1 can be significantly induced upon inflammatory stimulation[63–65]. There are four PGE_2 receptors (EPs), each EP governs distinct signal transduction pathway (Figure 1-9). EP1 receptor induces intracellular Ca^{2+} through coupling with Gq, which activates potential receptor activated Ca^{2+} channels and mobilize extracellular Ca^{2+} flux into the cytoplasm[66]. Both EP2 receptor and EP4 receptor can couple with Gs and sequentially activate adenylyl cyclase, which stimulates the cyclic adenosine monophosphate (cAMP) and protein kinase A (PKA) signaling[67,68]. EP4 receptor can alternately activate phosphoinositide-3-kinase (PI3K) via Gi[69]. Therefore, EP4 receptor shows less affinity to the cAMP-PKA signaling pathway in compare to EP2 receptor. There are multiple isoforms of EP3 due to different mRNA splicing. EP3 receptor is able to regulate different signaling pathways through coupling with distinct G proteins. The known function of EP3 receptor include inhibition of cAMP and mobilizing Ca^{2+} from ER to cytoplasm through increasing inositol 1, 4, 5-trisphosphate (IP3)[70–72].

Recently, Zhang et al. demonstrated an instrumental role of PGE_2 in orchestrating multiple tissue regeneration[73]. With deletion of a prostaglandin-degrading enzyme, 15-hydroxyprostaglandin dehydrogenase (15-PGDH), they observed enhanced hematopoietic capacity in steady state and after bone marrow transplant, promoted resistance to colitis and increased liver regeneration rate in response to partial hepatectomy. It was also documented that PGE_2 has anti-apoptotic effect on CD34+ HSCs[57], enhances long-term and short-term HSC engraftment and repopulation[74], as well as stimulates endogenous heme synthesis[75,76]. In this

dissertation, we characterized a novel role of PGE_2 in regulating stress erythroid differentiation in response to Epo signaling.

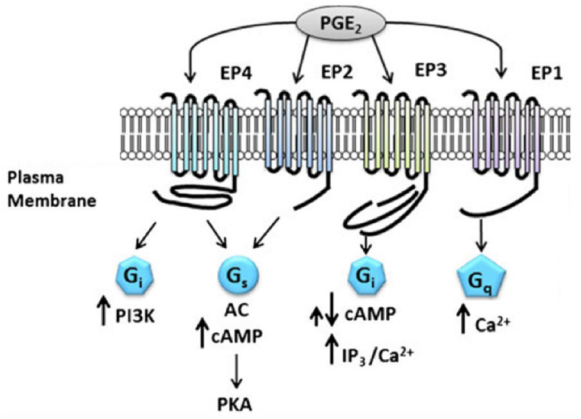

Figure **1-9**: **EP receptor signaling pathway**[77].

PGJ_2 and the ligation of PPARγ

PGJ_2 derives from PGD_2, another metabolite of PGH_2 (Figure 1-8). The generation of PGD_2 depends on two enzymes, hematopoietic prostaglandin D_2 synthase (H-PGDS) and lipocalin prostaglandin D_2 synthase (L-PGDS). H-PGDS is mainly expressed in immune and inflammatory cells, while L-PGDS is localized in central nervous system, vasculature and heart[64,78,79]. PGD_2 can be converted to prostaglandin J_2 (PGJ_2) through spontaneous dehydration. PGJ_2 further isomerizes to delta-12-prostaglandin J_2 (Δ^{12}-PGJ_2), which can be dehydrated to generate 15-deoxy-$\Delta^{12,14}$-prostaglandin J_2 (15d-PGJ_2)[80] (Figure 1-10). PGs of the J_2 series have a reactive cyclopentenone structure that enables their ligand activity. During the injury repair process, PGJ_2 and its derivatives exert anti-inflammatory effects through binding to peroxisome proliferator-activated receptor γ (PPARγ) in addition to other transcription factors, including NF-κB, nuclear factor erythroid 2-related factor 2 (Nrf2) and activator protein 1 (AP-1)[64]. Both Δ^{12}-

PGJ_2 and 15d-PGJ_2 are considered to be the potent endogenous ligand of PPARγ[81–83]. In addition, previous study suggested that the AA metabolism in macrophages is modulated by increased selenium during inflammation[84]. The production of both PGE_2 and TXA_2 are inhibited, while selenium promotes the expression of H-PGDS, which favors the production of Δ^{12}-PGJ_2 and 15d-PGJ_2. Δ^{12}-PGJ_2 and 15d-PGJ_2 activate PPARγ through ligation. Also, PPARγ is able to stimulate the expression of H-PGDS through binding to its promoter. Together, H-PGDS, Δ^{12}-PGJ_2, 15d-PGJ_2 and PPARγ form a positive feedback loop to regulate the resolution of inflammation. Moreover, one of the PGD_2 receptor, chemoattractant receptor-homologous molecule expressed on Th2 cells (CRTH2), is also demonstrated as an important regulator in LPS-induced inflammation[85]. Both Δ^{12}-PGJ_2 and 15d-PGJ_2 have high binding affinity to CRTH2[86,87]. Mutation of CRTH2 leads to increased expression of m-PGES1 in macrophages, indicating that CRTH2 participates in the repression of PGE_2[85]. All evidence suggested that the switching of PGs is important in the resolution of inflammation. On the one hand, CRTH2 regulates the decrease of PGE_2 and other proinflammatory genes. On the other hand, the production of Δ^{12}-PGJ_2 and 15d-PGJ_2, which act as anti-inflammatory lipid mediators, is favorable in the macrophages in response to inflammation. In this dissertation, we extended the investigation of macrophage derived PGE_2 and PGJ_2 into stress erythropoiesis and discussed their new roles in regulating the development of SEPs.

PPARγ belongs to the nuclear receptor family of ligand-activated transcription factors. In addition to natural PG ligands, the synthetic thiazolidinediones (TZDs) are also widely used as PPARγ agonists[88]. Upon binding to its ligands, PPARγ heterodimerizes with the retinoid X receptor (RXR) and form a complex with other transcriptional cofactors[89]. The transcriptional complex binds to the peroxisome proliferator hormone response elements (PPREs) in the promoter region of genes and mediates transcription[89]. PPARγ is detected in a wide range of

tissues, including adipose tissue, adrenal gland, spleen, endothelium and hematopoietic tissue[90–93]. It is known that PPARγ regulates adipogenesis, glucose metabolism, myelopoiesis, the maturation of alternatively activated macrophages and inflammation[92,94–96]. Notably, deletion of PPARγ in hematopoietic cells results in splenomegaly, which indicates ectopic hematopoiesis[97]. PPARγ is also reported to act downstream of Epo to enhance macrophage efferocytosis during acute inflammation[98]. However, little has been known about PPARγ function in stress erythropoiesis and the underling mechanisms. In this dissertation, we revealed a regulatory role of PPARγ in modulating maturation of SEPs by interacting with other signals from the microenvironment.

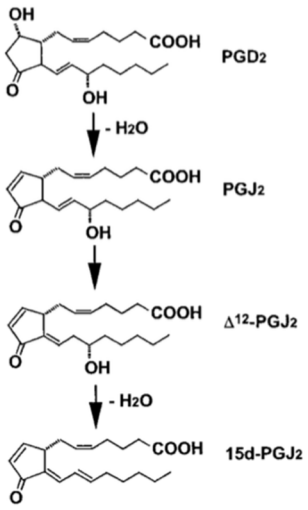

Figure **1-10**: **The PGD_2 metabolic pathway**[80].

1.3.5 Models and methods in study stress erythropoiesis

The Murine model is the most widely used animal model to study stress erythropoiesis. One obvious advantage is that mice share many physiological and pathological features with humans[99]. Furthermore, diverse techniques including transgenesis, genome editing, conventional

and conditional gene knockouts enables multiple ways to manipulate erythroid genes in mouse. Our lab has established *in vitro* culture system to mimic the *in vivo* stress erythropoiesis process[19]. By supplementing factors known to support SEPs in the culture medium, we are able to expand early stage SEPs from unfractionated BM. The three immature SEP populations that proliferate in the stress erythropoiesis expansion media (SEEM) are identified as CD34+CD133+Kit+Sca1+ SEPs, CD34-CD133+Kit+Sca1+ SEPs and CD34-CD133-Kit+Sca1+ SEPs. We are also able to induce differentiation of SEPs by adding Epo and culturing cells at low oxygen condition[19] (Figure 1-11). The SEPs rapidly differentiate into CD34-CD133-Kit+Sca1- stress BFU-E progenitors in this stress erythropoiesis differentiation media (SEDM) culture condition. Notably, human BM mononuclear cells can also give rise to human SEPs that express analogous cell surface markers when cultured in the same condition. We also utilize two *in vivo* models to study stress erythropoiesis[100]. The BMT model allows us to study both the migration of SEPs from BM to spleen and the further extramedullary development of SEPs[100] (Figure 1-12). Recipient mice are lethally irradiated and transplanted with isolated donor BM cells. The spleen and PB are analyzed every 2 - 3 days after BMT to monitor the recovery from irradiation. In this method, donor cells and recipient cells can be easily distinguished. It allows precise analysis of the short-term radioprotection capability of the donor cells and, in some circumstances, allows the analysis of interactions between donor SEPs and recipient microenvironment. The PHZ induced hemolytic anemia model provides a more acute stress erythropoiesis model[100]. The anemic stress is rapidly induced within 24 hours after PHZ injection. The entire stress erythropoiesis response only takes 5 - 7 days from the initiation to full recovery[100]. This model allows us to study the development of resident SEPs and the microenvironment.

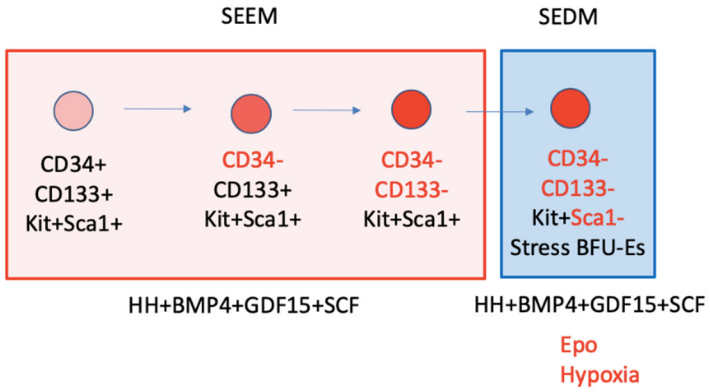

Figure **1-11**: **Schematic of in vitro bone marrow culture and SEP surface markers in different developmental stages**.

Unfractionated BM cells are cultured in stress erythropoiesis expansion media (SEEM) for 5 days to enrich the amplifying SEPs. Growth factors (GDF15, BMP4, SCF, HH) known to regulate stress erythropoiesis are supplemented in culture media. Then cells are switched to stress erythropoiesis differentiation media (SEDM) for 3 days to induce differentiation. Epo is supplemented in SEDM and cells are cultured at 2% O_2. SEPs will gradually lose the expression of CD34, CD133 and Sca1 during development.

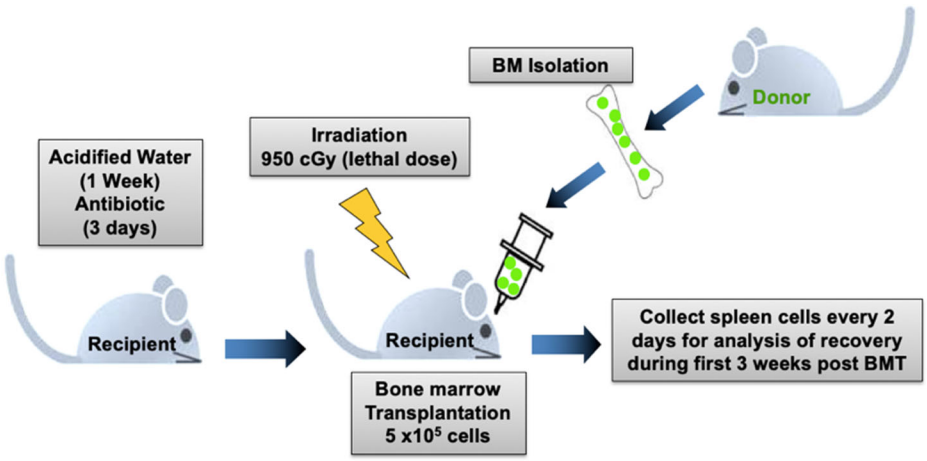

Figure **1-12**: **BMT procedure**.

Recipients are treated with acidified water for 1 week and antibiotic water for 3 days prior to irradiation. Recipients then are lethally irradiated with 950 cGy. Isolated unfractionated BM cells

or sorted SEP cells are injected into the recipient retro-orbitally. The number of donor cells range from $2x10^2$ – $5x10^6$ depend on the experimental design. Blood and spleen samples are collected every 2 days for analysis.

1.4 Integrated stress response and translational regulation

Under conditions of stress, eukaryotes activate a cytoprotective pathway termed the integrated stress response (ISR) to restore homeostasis[101]. There are four kinases that implement ISR in response to distinct stress conditions: Protein kinase RNA-like endoplasmic reticulum kinase (PERK) is located in the ER membrane. ER stresses caused by unfolded proteins, imbalanced redox status and disturbed calcium homeostasis activate PERK[102]. Double-stranded RNA-dependent protein kinase (PKR) mainly responds to the increased dsRNA during viral infection[103]. Heme-regulated eIF2α kinase (HRI) is mainly expressed in the erythroid lineage. Heme deficiency will activate HRI to reduce the production of excess globin, which leads to proteotoxicity[104]. General control non-derepressible 2 (GCN2) is sensitive to nutrient deprivation and UV light irradiation[105,106] (Figure1-13). All four kinases can catalyze the phosphorylation of the α subunit of eukaryotic translation initiation factor 2 alpha (eIF2α) on serine 51. eIF2α, eIF2β and eIF2γ are three subunits of eIF2. The initiation of translation requires the regulation of eIF2 ternary complex (eIF2-TC), which is composed of eIF2, GTP and Met-$tRNA_i^{Met}$ [101]. Phosphorylated eIF2α (P-eIF2α) blocks the exchange of eIF2-GDP to eIF2-GTP, thereby reducing the abundance of eIF2-TC and resulting in reduced initiation of mRNA translation. Through attenuating global protein translation, P-eIF2α helps to alleviate the unfolded or misfolded protein stress, conserve amino acids and reduce metabolic consequences[107,108,109].

Paradoxically, P-eIF2α selectively promotes translation of activating transcription factor 4 (ATF4). ATF4 can form heterodimers with other transcription factors, that then bind to ISR-targeted promoters to enhance the expression of adaptive genes. Target genes of ATF4 are involved in metabolism, protein synthesis, amino acid transport and biosynthesis[110]. Intriguingly, ATF4 knockout mice exhibit severe anemia phenotype in yolk sac and fetal liver[111]. We also found that ATF4 mutants have significantly lower hematocrit after BMT, which indicates delayed recovery and impaired erythropoiesis. All these observations suggest that ISR kinases may play a role in stress erythropoiesis through activating ATF4.

Termination of ISR is another important part of the response. Short-term ISR is considered as adaptive response that the cell can restore homeostasis with timely resuming protein translation. However, prolonged ISR leads to cell death when severe stresses cannot be resolved. Termination of ISR is regulated by dephosphorylation of eIF2α, which requires the protein phosphatase 1 (PP1) complex. PP1 complex is composed of PP1 catalytic subunit (PP1c) and one regulatory subunit. Either protein phosphatase 1 regulatory subunit 15A[112] (PPP1R15A, also known as growth arrest and DNA damage-inducible protein-34, GADD34) or 15B[113] (PPP1R15B, also known as constitutive repressor of eIF2α phosphorylation, CReP) binds to PP1c to exert the phosphatase effect. In mammals, CReP is constitutively expressed in homeostatic cells to maintain normal protein translation, whereas GADD34 is induced by stress[101]. In fact, GADD34 is one of the targets of ATF4[114]. During the late stage of ISR, ATF4 promotes expression of another key transcriptional regulator, C/EBP homologous protein (CHOP). ATF4 and CHOP together induces transcription of GADD34, which in turn dephosphorylates eIF2α through forming GADD34-PP1 complex and resumes the general protein translation.

The Diamond-Blackfan anemia (DBA) is a blood disorder characterized by insufficient erythroid progenitors in BM but no defects on other hematopoietic lineages[115]. The majority of DBA patients have heterozygous mutations in ribosomal protein genes[115]. Consequently, haploinsufficiency of ribosomal proteins selectively impairs the translation of mRNAs in hematopoietic stem and progenitor cells (HSPCs) and results in reduced erythroid progenitor abundance[115]. The findings in DBA implies that erythroid cells are more sensitive to alterations in translation. In stress erythropoiesis, the high rate of erythrocyte generation suggests that SEPs are undergoing active cell division. Therefore, high translational efficiency and appropriate translational regulation is required for stress erythropoiesis. In this dissertation, we demonstrated a novel role of the eIF2α kinase, PERK, in mediating protein translation in SEPs through the cooperation of multiple transcriptional and translational factors.

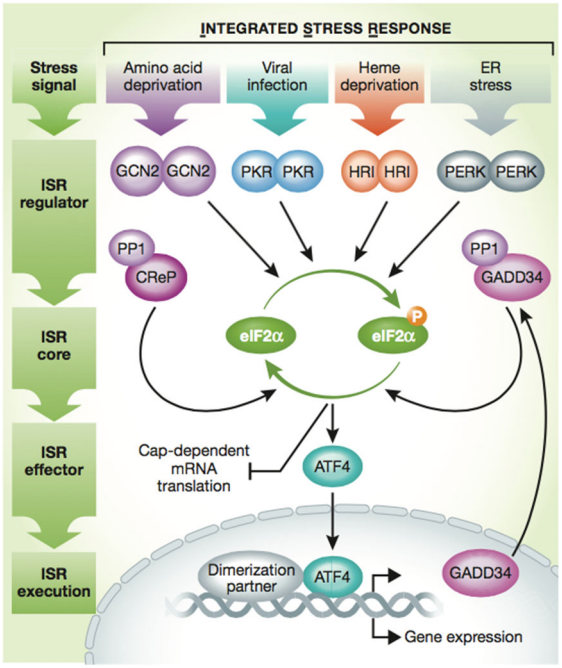

Figure **1-13**: **Model of integrated stress response**[101].

1.5 Hypothesis

In this dissertation, we will discuss several novel signals in the microenvironment and the erythroid progenitors. These signals compose a regulatory network to promote the proliferation and differentiation of SEPs.

Aim1 Investigate Epo regulated microenvironmental signals in stress erythropoiesis

Epo is identified as the humoral factor that regulates erythropoiesis. Through binding to EpoR, Epo regulates the survival, proliferation and differentiation of erythroid progenitors. The microenvironment is required for the maturation of erythroid progenitors. In recent decades, the important role of the EBI macrophage has been well documented. Previous work demonstrated that macrophages are novel target of Epo. However, the molecular mechanisms of EBI macrophages in regulating erythroid progenitors in response to Epo is unclear. Here we discussed the Epo induced microenvironmental changes, including Epo activated signaling pathways in EBI macrophages and the transition of microenvironmental signals produced by EBI macrophages. The precise regulation of microenvironmental signals is crucial for the development of erythroid progenitors in stress erythropoiesis.

Aim 2. Characterize the role of PGE_2-dependent PERK signaling pathway in stress erythropoiesis.

PGE_2 is one of the Epo induced differentiating microenvironmental signals. Our preliminary data showed that inhibition of PGE_2 blocks stress erythropoiesis. In addition, inhibition of the ISR kinase, PERK, causes defects in stress erythropoiesis and blocks the transition from amplifying progenitors to differentiating stress BFU-Es. In this dissertation, we performed analysis to further understand the correlation between PGE_2 and PERK. Also, we

investigated the role of PERK in stress erythropoiesis through analyzing the PERK-dependent translational regulation.

1.6 References

1. Rieger, M. A. & Schroeder, T. Hematopoiesis. *Cold Spring Harbor Perspectives in Biology* (2012). doi:10.1101/cshperspect.a008250
2. Pinho, S. & Frenette, P. S. Haematopoietic stem cell activity and interactions with the niche. *Nature Reviews Molecular Cell Biology* (2019). doi:10.1038/s41580-019-0103-9
3. Jagannathan-Bogdan, M. & Zon, L. I. Hematopoiesis. *Development (Cambridge)* (2013). doi:10.1242/dev.083147
4. Moore, G., Knight, G. & Blann, A. *Haematology*. (OXFORD University Press, 2016).
5. Orkin, S. H. & Zon, L. I. Hematopoiesis: An Evolving Paradigm for Stem Cell Biology. *Cell* (2008). doi:10.1016/j.cell.2008.01.025
6. Rodriguez-Fraticelli, A. E. *et al.* Clonal analysis of lineage fate in native haematopoiesis. *Nature* (2018). doi:10.1038/nature25168
7. Laurenti, E. & Göttgens, B. From haematopoietic stem cells to complex differentiation landscapes. *Nature* (2018). doi:10.1038/nature25022
8. Tusi, B. K. *et al.* Population snapshots predict early haematopoietic and erythroid hierarchies. *Nature* (2018). doi:10.1038/nature25741
9. Karamitros, D. *et al.* Single-cell analysis reveals the continuum of human lympho-myeloid progenitor cells article. *Nature Immunology* (2018). doi:10.1038/s41590-017-0001-2
10. Notta, F. *et al.* Distinct routes of lineage development reshape the human blood hierarchy across ontogeny. *Science* (2016). doi:10.1126/science.aab2116
11. Dzierzak, E. & Philipsen, S. Erythropoiesis: Development and differentiation. *Cold Spring Harbor Perspectives in Medicine* (2013). doi:10.1101/cshperspect.a011601
12. Testa, U. Apoptotic mechanisms in the control of erythropoiesis. *Leukemia* (2004). doi:10.1038/sj.leu.2403383
13. Gregory, C. J. & Eaves, A. C. Human marrow cells capable of erythropoietic differentiation in vitro: definition of 3 erythroid colony responses. *Blood* (1977). doi:10.1182/blood.v49.6.855.bloodjournal496855
14. Gregory, C. J. & Eaves, A. C. Three stages of erythropoietic progenitor cell differentiation distinguished by a number of physical and biologic properties. *Blood* (1978). doi:10.1182/blood.v51.3.527.bloodjournal513527
15. Moras, M., Lefevre, S. D. & Ostuni, M. A. From erythroblasts to mature red blood cells: Organelle clearance in mammals. *Frontiers in Physiology* (2017). doi:10.3389/fphys.2017.01076
16. Socolovsky, M. Molecular insights into stress erythropoiesis. *Current Opinion in Hematology* (2007). doi:10.1097/MOH.0b013e3280de2bf1
17. Bresnick, E. H. *et al.* Mechanisms of erythrocyte development and regeneration: Implications for regenerative medicine and beyond. *Development (Cambridge)* (2018). doi:10.1242/dev.151423
18. Haidar, R., Mhaidli, H. & Taher, A. T. Paraspinal extramedullary hematopoiesis in

patients with thalassemia intermedia. *European Spine Journal* (2010). doi:10.1007/s00586-010-1357-2

19. Xiang, J., Wu, D. C., Chen, Y. & Paulson, R. F. In vitro culture of stress erythroid progenitors identifies distinct progenitor populations and analogous human progenitors. *Blood* (2015). doi:10.1182/blood-2014-07-591453

20. BESSIS, M. L'ílot érythroblastique, unité fonctionnelle de la moelle osseuse. *Revue d'hématologie* (1958).

21. Lee, S. H. *et al.* Isolation and immunocytochemical characterization of human bone marrow stromal macrophages in hemopoietic clusters. *Journal of Experimental Medicine* (1988). doi:10.1084/jem.168.3.1193

22. Rhodes, M. M., Kopsombut, P., Bondurant, M. C., Price, J. O. & Koury, M. J. Adherence to macrophages in erythroblastic islands enhances erythroblast proliferation and increases erythrocyte production by a different mechanism than erythropoietin. *Blood* (2008). doi:10.1182/blood-2007-06-098178

23. Chasis, J. A. & Mohandas, N. Erythroblastic islands: Niches for erythropoiesis. *Blood* (2008). doi:10.1182/blood-2008-03-077883

24. Terasawa, T., Ogawa, M., Porter, P. N., Golde, D. W. & Goldwasser, E. Effect of burst-promoting activity (BPA) and erythropoietin on hemoglobin biosynthesis in culture. *Blood* (1980). doi:10.1182/blood.v56.6.1106.bloodjournal5661106

25. Sawada, K., Krantz, S. B., Dessypris, E. N., Koury, S. T. & Sawyer, S. T. Human colony-forming units-erythroid do not require accessory cells, but do require direct interaction with insulin-like growth factor I and/or insulin for erythroid development. *Journal of Clinical Investigation* (1989). doi:10.1172/JCI114070

26. Kurtz, A., Hartl, W., Jelkmann, W., Zapf, J. & Bauer, C. Activity in fetal bovine serum that stimulates erythroid colony formation in fetal mouse livers is insulinlike growth factor I. *Journal of Clinical Investigation* (1985). doi:10.1172/JCI112149

27. Chow, A. *et al.* CD169 + macrophages provide a niche promoting erythropoiesis under homeostasis and stress. *Nature Medicine* (2013). doi:10.1038/nm.3057

28. Liao, C., Sandeep Prabhu, K. & Paulson, R. F. Monocyte-derived macrophages expand the murine stress erythropoietic niche during the recovery from anemia. *Blood* (2018). doi:10.1182/blood-2018-06-856831

29. Lee, G. *et al.* Targeted gene deletion demonstrates that the cell adhesion molecule ICAM-4 is critical for erythroblastic island formation. *Blood* (2006). doi:10.1182/blood-2006-03-006759

30. Scortegagna, M. *et al.* HIF-2α regulates murine hematopoietic development in an erythropoietin-dependent manner. *Blood* (2005). doi:10.1182/blood-2004-05-1695

31. Haase, V. H. Regulation of erythropoiesis by hypoxia-inducible factors. *Blood Reviews* (2013). doi:10.1016/j.blre.2012.12.003

32. Sathyanarayana, P. *et al.* EPO receptor circuits for primary erythroblast survival. *Blood* (2008). doi:10.1182/blood-2007-10-119743

33. Li, W. *et al.* Identification and transcriptome analysis of erythroblastic island macrophages. *Blood* (2019). doi:10.1182/blood.2019000430

34. Witthuhn, B. A. *et al.* JAK2 associates with the erythropoietin receptor and is tyrosine phosphorylated and activated following stimulation with erythropoietin. *Cell* (1993). doi:10.1016/0092-8674(93)90414-L

35. Quelle, F. W. *et al.* Erythropoietin induces activation of Stat5 through association with specific tyrosines on the receptor that are not required for a mitogenic response. *Molecular and Cellular Biology* (1996). doi:10.1128/mcb.16.4.1622

36. Suzuki, N. *et al.* Erythroid-specific expression of the erythropoietin receptor rescued its null mutant mice from lethality. *Blood* (2002). doi:10.1182/blood-2002-01-0124

37. Cui, Y. *et al.* Inactivation of Stat5 in Mouse Mammary Epithelium during Pregnancy Reveals Distinct Functions in Cell Proliferation, Survival, and Differentiation. *Molecular and Cellular Biology* (2004). doi:10.1128/mcb.24.18.8037-8047.2004

38. Koury, M. J. & Bondurant, M. C. Erythropoietin retards DNA breakdown and prevents programmed death in erythroid progenitor cells. *Science* (1990). doi:10.1126/science.2326648

39. Perry, J. M. *et al.* Maintenance of the BMP4-dependent stress erythropoiesis pathway in the murine spleen requires hedgehog signaling. *Blood* (2009). doi:10.1182/blood-2008-03-147892

40. Bateman, A. E. & Cole, R. J. Colony forming cells in the livers of prenatal flexed (f/f) anaemic mice. *Cell Proliferation* (1972). doi:10.1111/j.1365-2184.1972.tb01013.x

41. Mixter, R. & Hunt, H. R. Anemia in the Flexed Tailed Mouse, Mus Musculus. *Genetics* (1933).

42. Lenox, L. E., Perry, J. M. & Paulson, R. F. BMP4 and Madh5 regulate the erythroid response to acute anemia. *Blood* (2005). doi:10.1182/blood-2004-02-0703

43. Hao, S. *et al.* Gdf15 regulates murine stress erythroid progenitor proliferation and the development of the stress erythropoiesis niche. *Blood Advances* (2019). doi:10.1182/bloodadvances.2019000375

44. Perry, J. M., Harandi, O. F. & Paulson, R. F. BMP4, SCF, and hypoxia cooperatively regulate the expansion of murine stress erythroid progenitors. *Blood* (2007). doi:10.1182/blood-2006-04-016154

45. Bauer, A. *et al.* The glucocorticoid receptor is required for stress erythropoiesis. *Genes and Development* (1999). doi:10.1101/gad.13.22.2996

46. Hattangadi, S. M., Wong, P., Zhang, L., Flygare, J. & Lodish, H. F. From stem cell to red cell: Regulation of erythropoiesis at multiple levels by multiple proteins, RNAs, and chromatin modifications. *Blood* (2011). doi:10.1182/blood-2011-07-356006

47. Li, N. & Clevers, H. Coexistence of quiescent and active adult stem cells in mammals. *Science* (2010). doi:10.1126/science.1180794

48. Loh, K. M., van Amerongen, R. & Nusse, R. Generating Cellular Diversity and Spatial Form: Wnt Signaling and the Evolution of Multicellular Animals. *Developmental Cell* (2016). doi:10.1016/j.devcel.2016.08.011

49. Anastas, J. N. & Moon, R. T. WNT signalling pathways as therapeutic targets in cancer. *Nature Reviews Cancer* (2013). doi:10.1038/nrc3419

50. Nusse, R. & Varmus, H. Three decades of Wnts: A personal perspective on how a scientific field developed. *EMBO Journal* (2012). doi:10.1038/emboj.2012.146

51. Clevers, H. & Nusse, R. Wnt/β-catenin signaling and disease. *Cell* (2012). doi:10.1016/j.cell.2012.05.012

52. Wallingford, J. B. & Habas, R. The developmental biology of Dishevelled: An enigmatic protein governing cell fate and cell polarity. *Development* (2005). doi:10.1242/dev.02068

53. Cadigan, K. M. & Waterman, M. L. TCF/LEFs and Wnt signaling in the nucleus. *Cold Spring Harbor Perspectives in Biology* (2012). doi:10.1101/cshperspect.a007906

54. Ito, M. *et al.* Wnt-dependent de novo hair follicle regeneration in adult mouse skin after wounding. *Nature* (2007). doi:10.1038/nature05766

55. Koch, S. *et al.* The Wnt antagonist Dkk1 regulates intestinal epithelial homeostasis and wound repair. *Gastroenterology* (2011). doi:10.1053/j.gastro.2011.03.043

56. Wehkamp, J. *et al.* The Paneth Cell α-Defensin Deficiency of Ileal Crohn's Disease Is Linked to Wnt/Tcf-4. *The Journal of Immunology* (2007). doi:10.4049/jimmunol.179.5.3109

57. Goessling, W. *et al.* Genetic Interaction of PGE2 and Wnt Signaling Regulates Developmental Specification of Stem Cells and Regeneration. *Cell* (2009). doi:10.1016/j.cell.2009.01.015

58. Templin, C. *et al.* Establishment of immortalized multipotent hematopoietic progenitor cell lines by retroviral-mediated gene transfer of β-catenin. *Experimental Hematology* (2008). doi:10.1016/j.exphem.2007.10.005

59. Tan, X. *et al.* β-catenin deletion in hepatoblasts disrupts hepatic morphogenesis and survival during mouse development. *Hepatology* (2008). doi:10.1002/hep.22225

60. Lento, W., Congdon, K., Voermans, C., Kritzik, M. & Reya, T. Wnt signaling in normal and malignant hematopoiesis. *Cold Spring Harbor Perspectives in Biology* (2013). doi:10.1101/cshperspect.a008011

61. Cobas, M. *et al.* β-Catenin Is Dispensable for Hematopoiesis and Lymphopoiesis. *Journal of Experimental Medicine* (2004). doi:10.1084/jem.20031615

62. Di Costanzo, F., Di Dato, V., Ianora, A. & Romano, G. Prostaglandins in marine organisms: A review. *Marine Drugs* (2019). doi:10.3390/md17070428

63. Mancini, J. A. *et al.* Cloning, Expression, and Up-regulation of Inducible Rat Prostaglandin E Synthase during Lipopolysaccharide-induced Pyresis and Adjuvant-induced Arthritis. *Journal of Biological Chemistry* (2001). doi:10.1074/jbc.M006865200

64. Ricciotti, E. & Fitzgerald, G. A. Prostaglandins and inflammation. *Arteriosclerosis, Thrombosis, and Vascular Biology* (2011). doi:10.1161/ATVBAHA.110.207449

65. Tanioka, T., Nakatani, Y., Semmyo, N., Murakami, M. & Kudo, I. Molecular identification of cytosolic prostaglandin E2 synthase that is functionally coupled with cyclooxygenase-1 in immediate prostaglandin E2 biosynthesis. *Journal of Biological Chemistry* (2000). doi:10.1074/jbc.M003504200

66. Tabata, H. *et al.* Possible coupling of prostaglandin E receptor EP1 to TRP5 expressed in Xenopus laevis oocytes. *Biochemical and Biophysical Research Communications* (2002).

doi:10.1016/S0006-291X(02)02455-5

67. Ichikawa, A., Sugimoto, Y. & Tanaka, S. Molecular biology of histidine decarboxylase and prostaglandin receptors. *Proceedings of the Japan Academy Series B: Physical and Biological Sciences* (2010). doi:10.2183/pjab.86.848

68. Regan, J. W. EP2 and EP4 prostanoid receptor signaling. in *Life Sciences* (2003). doi:10.1016/j.lfs.2003.09.031

69. Fujino, H. & Regan, J. W. EP 4 prostanoid receptor coupling to a pertussis toxin- sensitive inhibitory G protein. *Molecular Pharmacology* (2006). doi:10.1124/mol.105.017749

70. Kotelevets, L. *et al.* A new mRNA splice variant coding for the human EP3-I receptor isoform. *Prostaglandins Leukotrienes and Essential Fatty Acids* (2007). doi:10.1016/j.plefa.2007.09.005

71. Kotani, M. *et al.* Molecular cloning and expression of multiple isoforms of human prostaglandin E receptor EP3 subtype generated by alternative messenger RNA splicing: Multiple second messenger systems and tissue-specific distributions. *Molecular Pharmacology* (1995).

72. Dey, I., Lejeune, M. & Chadee, K. Prostaglandin E 2 receptor distribution and function in the gastrointestinal tract. *British Journal of Pharmacology* (2006). doi:10.1038/sj.bjp.0706923

73. Zhang, Y. *et al.* Inhibition of the prostaglandin-degrading enzyme 15-PGDH potentiates tissue regeneration. *Science* (2015). doi:10.1126/science.aaa2340

74. Hoggatt, J., Singh, P., Sampath, J. & Pelus, L. M. Prostaglandin E2 enhances hematopoietic stem cell homing, survival, and proliferation. *Blood* (2009). doi:10.1182/blood-2009-01-201335

75. Dunn, C. D. R. Prostaglandins and erythropoiesis: structure/action relationships and identification of the prostaglandin responsive cells. *Blut* (1981). doi:10.1007/BF00996847

76. Ortega, J. A., Dukes, P. P., Ma, A., Shore, N. A. & Malekzadeh, M. H. A clinical trial of prostaglandin E2 to increase erythropoiesis in anemia of end stage renal disease. A preliminary report. *Prostaglandins, Leukotrienes and Medicine* (1984). doi:10.1016/0262-1746(84)90124-0

77. Reader, J., Holt, D. & Fulton, A. Prostaglandin E 2 EP receptors as therapeutic targets in breast cancer. *Cancer and Metastasis Reviews* (2011). doi:10.1007/s10555-011-9303-2

78. Herlong, J. L. & Scott, T. R. Positioning prostanoids of the D and J series in the immunopathogenic scheme. *Immunology Letters* (2006). doi:10.1016/j.imlet.2005.10.004

79. Song, W. L. *et al.* Lipocalin-like prostaglandin D synthase but not hemopoietic prostaglandin D synthase deletion causes hypertension and accelerates thrombogenesis in mice. *Journal of Pharmacology and Experimental Therapeutics* (2018). doi:10.1124/jpet.118.250936

80. Shibata, T. *et al.* 15-Deoxy-δ 12,14-prostaglandin J 2. A prostaglandin D 2 metabolite generated during inflammatory processes. *Journal of Biological Chemistry* (2002). doi:10.1074/jbc.M110314200

81. Powell, W. S. 15-Deoxy-Δ 12,14 -PGJ 2 : Endogenous PPARγ ligand or minor eicosanoid degradation product? *Journal of Clinical Investigation* (2003). doi:10.1172/JCI19796

82. Nosjean, O. & Boutin, J. A. Natural ligands of PPARγ: Are prostaglandin J2 derivatives really playing the part? *Cellular Signalling* (2002). doi:10.1016/S0898-6568(01)00281-9

83. Ward, C. *et al.* Prostaglandin D 2 and Its Metabolites Induce Caspase-Dependent Granulocyte Apoptosis That Is Mediated Via Inhibition of IκBα Degradation Using a Peroxisome Proliferator-Activated Receptor-γ-Independent Mechanism . *The Journal of Immunology* (2002). doi:10.4049/jimmunol.168.12.6232

84. Gandhi, U. H. *et al.* Selenoprotein-dependent up-regulation of hematopoietic prostaglandin D2 synthase in macrophages is mediated through the activation of peroxisome proliferator-activated receptor (PPAR) gamma. *The Journal of biological chemistry* **286**, 27471–82 (2011).

85. Diwakar, B. T. *et al.* Crth2 receptor signaling down-regulates lipopolysaccharide-induced NF-κB activation in murine macrophages via changes in intracellular calcium. *FASEB journal : official publication of the Federation of American Societies for Experimental Biology* (2019). doi:10.1096/fj.201802608R

86. Hata, A. N., Zent, R., Breyer, M. D. & Breyer, R. M. Expression and Molecular Pharmacology of the Mouse CRTH2 Receptor. *Journal of Pharmacology and Experimental Therapeutics* **306**, 463 LP – 470 (2003).

87. Pettipher, R. The roles of the prostaglandin D2 receptors DP1 and CRTH2 in promoting allergic responses. *British Journal of Pharmacology* **153**, S191–S199 (2008).

88. Spiegelman, B. M. PPAR-γ: Adipogenic regulator and thiazolidinedione receptor. *Diabetes* (1998). doi:10.2337/diabetes.47.4.507

89. Tyagi, S., Gupta, P., Saini, A., Kaushal, C. & Sharma, S. The peroxisome proliferator-activated receptor: A family of nuclear receptors role in various diseases. *Journal of Advanced Pharmaceutical Technology and Research* (2011). doi:10.4103/2231-4040.90879

90. Ricote, M. *et al.* Expression of the peroxisome proliferator-activated receptor γ (PPARγ) in human atherosclerosis and regulation in macrophages by colony stimulating factors and oxidized low density lipoprotein. *Proceedings of the National Academy of Sciences of the United States of America* (1998). doi:10.1073/pnas.95.13.7614

91. Fajas, L. *et al.* The organization, promoter analysis, and expression of the human PPARγ gene. *Journal of Biological Chemistry* (1997). doi:10.1074/jbc.272.30.18779

92. Tontonoz, P., Hu, E., Devine, J., Beale, E. G. & Spiegelman, B. M. PPAR gamma 2 regulates adipose expression of the phosphoenolpyruvate carboxykinase gene. *Molecular and Cellular Biology* (1995). doi:10.1128/mcb.15.1.351

93. Kliewer, S. A. *et al.* Differential expression and activation of a family of murine peroxisome proliferator-activated receptors. *Proceedings of the National Academy of Sciences of the United States of America* (1994). doi:10.1073/pnas.91.15.7355

94. Heim, M. *et al.* Phytanic acid, a natural peroxisome proliferator-activated receptor (PPAR) agonist, regulates glucose metabolism in rat primary hepatocytes. *The FASEB journal : official publication of the Federation of American Societies for Experimental Biology* (2002). doi:10.1096/fj.01-0816fje

95. Mitroulis, I. *et al.* Modulation of Myelopoiesis Progenitors Is an Integral Component of Trained Immunity. *Cell* (2018). doi:10.1016/j.cell.2017.11.034

96. Stienstra, R. *et al.* Peroxisome proliferator-activated receptor γ activation promotes infiltration of alternatively activated macrophages into adipose tissue. *Journal of Biological Chemistry* (2008). doi:10.1074/jbc.M710314200

97. Wan, Y., Chong, L. W. & Evans, R. M. PPAR-γ regulates osteoclastogenesis in mice. *Nature Medicine* (2007). doi:10.1038/nm1672

98. Luo, B. *et al.* Phagocyte respiratory burst activates macrophage erythropoietin signalling to promote acute inflammation resolution. *Nature Communications* (2016). doi:10.1038/ncomms12177

99. An, X., Schulz, V. P., Mohandas, N. & Gallagher, P. G. Human and murine erythropoiesis. *Current Opinion in Hematology* (2015). doi:10.1097/MOH.0000000000000134

100. Bennett, L. F., Liao, C. & Paulson, R. F. Stress erythropoiesis model systems. in *Methods in Molecular Biology* (2018). doi:10.1007/978-1-4939-7428-3_5

101. Pakos-Zebrucka, K. *et al.* The integrated stress response. *EMBO reports* (2016). doi:10.15252/embr.201642195

102. Chong, W. C., Shastri, M. D. & Eri, R. Endoplasmic reticulum stress and oxidative stress: A vicious nexus implicated in bowel disease pathophysiology. *International Journal of Molecular Sciences* (2017). doi:10.3390/ijms18040771

103. Lemaire, P. A., Anderson, E., Lary, J. & Cole, J. L. Mechanism of PKR Activation by dsRNA. *Journal of Molecular Biology* (2008). doi:10.1016/j.jmb.2008.05.056

104. Chen, J. J. & London, I. M. Regulation of protein synthesis by heme-regulated eIF-2α kinase. *Trends in Biochemical Sciences* (1995). doi:10.1016/S0968-0004(00)88975-6

105. Deng, J. *et al.* Activation of gcn2 in uv-irradiated cells inhibits translation. *Current Biology* (2002). doi:10.1016/S0960-9822(02)01037-0

106. Vazquez de Aldana, C. R., Wek, R. C., Segundo, P. S., Truesdell, A. G. & Hinnebusch, A. G. Multicopy tRNA genes functionally suppress mutations in yeast eIF-2 alpha kinase GCN2: evidence for separate pathways coupling GCN4 expression to unchanged tRNA. *Molecular and Cellular Biology* (1994). doi:10.1128/mcb.14.12.7920

107. Harding, H. P., Zhang, Y., Bertolotti, A., Zeng, H. & Ron, D. Perk is essential for translational regulation and cell survival during the unfolded protein response. *Molecular Cell* (2000). doi:10.1016/S1097-2765(00)80330-5

108. Zhang, P. *et al.* The GCN2 eIF2 Kinase Is Required for Adaptation to Amino Acid Deprivation in Mice. *Molecular and Cellular Biology* (2002). doi:10.1128/mcb.22.19.6681-6688.2002

109. Harding, H. P. *et al.* An integrated stress response regulates amino acid metabolism and resistance to oxidative stress. *Molecular Cell* (2003). doi:10.1016/S1097-2765(03)00105-9

110. Han, J. *et al.* ER-stress-induced transcriptional regulation increases protein synthesis leading to cell death. *Nature Cell Biology* (2013). doi:10.1038/ncb2738

111. Masuoka, H. C. & Townes, T. M. Targeted disruption of the activating transcription factor 4 gene results in severe fetal anemia in mice. *Blood* (2002). doi:10.1182/blood.V99.3.736

112. Novoa, I., Zeng, H., Harding, H. P. & Ron, D. Feedback inhibition of the unfolded protein response by GADD34-mediated dephosphorylation of eIF2α. *Journal of Cell Biology* (2001). doi:10.1083/jcb.153.5.1011

113. Jousse, C. *et al.* Inhibition of a constitutive translation initiation factor 2α phosphatase, CReP, promotes survival of stressed cells. *Journal of Cell Biology* (2003). doi:10.1083/jcb.200308075

114. Dey, S. *et al.* Both transcriptional regulation and translational control of ATF4 are central to the integrated stress response. *Journal of Biological Chemistry* (2010). doi:10.1074/jbc.M110.167213

115. Khajuria, R. K. *et al.* Ribosome Levels Selectively Regulate Translation and Lineage Commitment in Human Hematopoiesis. *Cell* (2018). doi:10.1016/j.cell.2018.02.036

Chapter 2

Epo-receptor Signaling in Macrophage Alters the Splenic Niche to Promote Erythroid Differentiation.

Yuanting Chen*[1], Jie Xiang*[1,6], Fenghua Qian[2], Bastihalli T. Diwakar[3,7], Baiye Ruan[2], Siyang Hao[1], K. Sandeep Prabhu[1-4] and Robert F. Paulson[1-4].

This thesis chapter is modified from a submitted manuscript in *Blood* Journal. Figure 2-1A-F,K and Figure 2-2 are provided by Jie Xiang. Figure 2-3B is provided by Siyang Hao. The remaining figures are done by Yuanting Chen.

Affiliations

[1]Graduate Program in Molecular, Cellular and Integrative Biosciences, Huck Institutes of the Life Sciences, The Pennsylvania State University, University Park, PA 16802, USA
[2]Graduate Program in Pathobiology, The Pennsylvania State University, University Park, PA 16802, USA
[3]Department of Veterinary and Biomedical Sciences, The Pennsylvania State University, University Park, PA 16802, USA
[4]Center for Molecular Immunology and Infectious Disease, The Pennsylvania State University, University Park, PA 16802, USA
*Authors contributed equally.

Present Address

[6]University of Michigan Kidney Epidemiology and Cost Center, Ann Arbor, MI, USA.
[7]Department of Pharmacology & Experimental Therapeutics, College of Pharmacy & Pharmaceutical Sciences, Frederic & Mary Wolfe Center, The University of Toledo, OH, USA.

Acknowledgements

We would like to thank the members of the Paulson and Prabhu labs for their insight and comments on the work. In particular, Dr. Chang Liao for her help with the analysis of EBIs by imaging flow cytometry. Dr. Lothar Hennighausen for providing the Stat5$^{fx/fx}$ mice. This work was supported, in part, by grants from the National Institutes of Health R01 DK080040 (R.F.P), R01 DK077152, Office of Dietary Supplements (K.S.P) and USDA-NIFA Hatch project numbers PEN04581, Accession number 1005468 (R.F.P) and PEN04605, Accession number 1010021 (KSP).

Author contributions

YC, JX, KSP and RFP designed experiments and analyzed data. YC, JX, FQ, BTD, BR and SH performed the experiments. YC and RFP wrote the manuscript. All authors commented on the manuscript.

Conflict of Interest

RFP is a consultant with Rubius Therapeutics. All other authors have declared that no conflict of interest exists.

Abstract

In response to anemic stress, stress erythropoiesis rapidly generates new erythrocytes to restore tissue oxygenation. Stress erythropoiesis is best understood in mice where it is extramedullary occurring primarily in the spleen. However, both human and mouse stress erythropoiesis utilize signals and progenitor cells that are distinct from steady state erythropoiesis. Immature stress erythroid progenitors (SEPs) are derived from short-term hematopoietic stem cells (ST-HSCs). Although the SEPs are capable of self-renewal, they are erythroid restricted. Inflammation and anemic stress induce the rapid proliferation of SEPs, but they do not differentiate until serum erythropoietin (Epo) levels increase. Here we show that rather than directly regulating SEPs, Epo promotes this transition from proliferation to differentiation by acting on macrophages in the splenic niche. During the proliferative stage, macrophages produce canonical Wnt ligands that promote proliferation and inhibit differentiation. Epo/Stat5 dependent signaling induces the production of bioactive lipid mediators in macrophages. Increased production of prostaglandin J2 (PGJ_2) activates peroxisome proliferator-activated receptor gamma (PPARγ) dependent repression of Wnt expression, while increased production of prostaglandin E2 (PGE_2) promotes the differentiation of SEPs.

2.1 Introduction

Bone marrow steady state erythropoiesis produces new erythrocytes at a constant rate that matches the rate of clearance of senescent red blood cells[1, 2]. Blood loss, inflammation or infection disrupts this homeostasis. When challenged by these conditions, a regenerative process termed stress erythropoiesis generates new erythrocytes[3]. Unlike steady state erythropoiesis, stress erythropoiesis generates a synchronous wave of new erythrocytes that maintains homeostasis until bone marrow steady state erythropoiesis can resume. This process requires the proliferation of transient amplifying cells to generate large numbers of committed erythroid progenitors[4, 5]. Stress erythropoiesis utilizes progenitor cells and signals that are distinct from steady state erythropoiesis[5-8]. In mice, stress erythroid progenitors (SEPs) are directly derived from bone marrow short-term hematopoietic stem cells (ST-HSCs- CD34+Kit+Sca1+Lin-)[4], which migrate to the spleen and are restricted to the stress erythroid lineage by signals produced by the splenic microenvironment[8]. This population of progenitors, CD34+CD133+Kit+Sca1+ (CD34+CD133+KS) cells, acts as a transient amplifying population[5]. Despite being erythroid restricted during this stage, the progenitors do not differentiate. The rise in serum Epo concentration drives the transition from proliferating progenitors to committed stress burst-forming units-erythroid (BFU-Es), which lose expression of CD34, CD133 and Sca1 and synchronously differentiate into erythrocytes[4, 5].

In addition to specialized SEPs, the splenic microenvironment regulates stress erythropoiesis[9-12]. The splenic stress erythropoiesis niche is a complex and dynamic structure made up of erythroblastic islands (EBIs), which are composed of a central monocyte/macrophage surrounded by developing erythroid progenitors. Stress erythropoiesis is severely compromised when macrophages are eliminated in vitro or in vivo[5, 9, 11]. Monocytes are recruited to spleen during stress erythropoiesis where they mature in concert with immature SEPs in EBIs[10]. The

generation of new erythrocytes therefore requires the interplay between the development and expansion of the niche, which must occur in conjunction with the proliferation and development of SEPs.

EBI macrophages express the Epo receptor[13, 14]. Our previous work showed that Epo was the signal that promoted the transition from proliferating immature SEPs to committed erythroid progenitors suggesting that Epo signaling in macrophages could promote this transition[5]. Here we show that Epo dependent activation of Stat5 in splenic macrophages leads to a change in signals from canonical Wnt signaling to prostaglandins. Wnt2b and Wnt8a promote the proliferation of the immature SEPs and inhibit their differentiation. Epo antagonizes Wnt expression by increasing the production of PGJ_2, which activates PPARγ dependent repression of Wnt expression. Simultaneously, Epo increases the production of PGE_2, which independently promotes the differentiation of SEPs. These data establish a role for Epo signaling in macrophages in regulating stress erythropoiesis.

2.2 Material and Methods

Mice

C57BL/6 mice, C57BL/6-Tg (UBC-GFP) 30Scha/J mice, B6.SJL-Ptprc^{a}Pepc^{b}/BoyJ, B6.129-Ctnnb1^{tm2Kem}/KnwJ mice and B6;129-Gt (ROSA)26Sor$^{tm1(cre/ERT)Nat}$/J mice (Rosa26-CreERT mice) were purchased from The Jackson Laboratory. All strains were back crossed onto C57BL/6 background. C57BL/6 mice with a floxed allele of Stat5a and Stat5b (referred to as Stat5$^{fx/fx}$ mice) were obtained from Dr. Lothar Hennighausen [47]. All animal procedures are approved by Institutional Animal Care and Use Committee (IACUC) of the Pennsylvania State University.

Stress erythropoiesis Cultures

Isolated murine bone marrow cells were cultured in stress erythropoiesis expansion media (SEEM) for 5 days and switched to stress erythropoiesis differentiation media (SEDM) for 3 days. SEEM contains Gibco IMDM (Invitrogen) supplemented with 10% fetal bovine serum (Gemini Bio-Products), 1% penicillin-streptomycin, 10 μg/ml insulin, 200 μg/ml transferrin, 2mM L-glutamine, 0.01g/ml bovine serum albumin, 7 μl/L 2-mercaptoethanol, 30 ng/ml GDF15 (Novoprotein), 15 ng/ml BMP4 (R&D systems), 50 ng/ml SCF (Goldbio) and 25 ng/ml SHH (GoldBio). SEDM contains Gibco IMDM, all supplements in SEEM and 3U/ml Epo. Cells were incubated at 2% O_2, 5% CO_2 when cultured in SEDM. Sorted murine spleen cells were cultured in SEEM and SEDM for indicated period of time.

Murine bone marrow derived macrophage (BMDM) cultures

L929 cell line was cultured in DMEM supplemented with 10% fetal bovine serum and 1% penicillin-streptomycin. L929 supernatants were filtered and collected after 7 days. Isolated murine bone marrow cells were cultured in DMEM with 10% fetal bovine serum, 1% penicillin-streptomycin and 10% L929 supernatants for 5 days to generate BMDMs. Media were changed every 2 to 3 days.

Human BMDM culture

Human bone marrow mononuclear cells (MNCs) (ReachBio) were thawed at 37°C water according to the ReachBio instructions. MNCs were enumerated and cell concentrations were adjusted to 5×10^5 cells/mL. MNCs were cultured in Gibco RPMI-1640 (Invitrogen) supplemented with 10% fetal bovine serum (Gemini Bio-Products), 1% penicillin-streptomycin, 2 mM L-glutamine and recombinant human macrophage colony-stimulating factor (M-CSF) (GoldBio). 10 ng/mL M-CSF were supplemented for the first 24 hours and 25 ng/mL M-CSF were supplemented for the following culture period. Media were changed every 2 to 3 days. Human BMDMs were enriched after 10 to 15 days.

Lipid extraction and liquid chromatography–tandem mass spectrometry (LC-MS/MS) analysis

Prostaglandins (PGs) were extracted from BMDMs and BMDM cell culture supernatants by using C18 Sep-pak cartridges (Waters). Briefly, culture supernatants were acidified with 1N HCl and loaded on to the Sep-Pak cartridge, bound PGs were eluted with methanol, evaporated under the stream of nitrogen gas and stored in ethyl acetate at −80° C until further analysis. For intracellular PGs, cell pellets were washed twice with DPBS, suspended in 1 mL of 80% methanol and homogenized with 0.1 mm zirconium beads using a bead beater homogenizer under standard cycle conditions. Homogenates were centrifuged at 20000 x g for 10 mins at 4˚ C. Supernatants were transferred to a clean brown glass vial, evaporated under nitrogen, dissolved in ultrapure water, acidified and extracted as described above. After extraction, PGs were suspended in 70% methanol and analyzed by LC-MS/MS. Quantitative analysis of Δ^{12}-PGJ_2 and PGE_2 was

performed using a calibration curve generated by respective standards in multiple reaction monitoring (MRM) mode. Following mass transitions were used to detect each PG: Δ^{12}-PGJ_2 (332.8/188.9; 332.8/314.9; 332.8/271.3 m/z) and PGE_2 (351/315; 351/271; 351/189). Data acquisition and analysis were performed using Analyst software (version 1.5; AB Sciex). PGs were normalized to cell number.

Tamoxifen dependent deletion of floxed mouse alleles.

Homozygous floxed mice were crossed with Rosa26-CreERT mice to generate floxed;Rosa26-CreERT mutants. To delete Stat5 in vivo, Tamoxifen was injected into mice every day for 5 days (75 mg/kg). Isolated bone marrow cells were treated with 1μM 4-hydroxytamoxifen (Sigma Aldrich) for 24 hours to induce deletion of Stat5 and β-catenin in vitro.

BMT and complete blood count assay

For BMT, $Stat5^{fx/fx}$;Rosa26-CreERT and β-$catenin^{fx/fx}$;Rosa26-CreERT bone marrow cells were isolated and cultured in SEEM with 4-OHT for 24 hours to generate $Stat5^{\Delta/\Delta}$ cells and β-$catenin^{\Delta/\Delta}$ cells. $Stat5^{fx/fx}$ or β-$catenin^{fx/fx}$ cells were also treated with 4-OHT as control. Recipient mice were lethally irradiated (950 cGy) and transplanted with unfractionated or sorted donor bone marrow cells with indicated cell numbers. Peripheral blood was collected retro-orbitally on indicated days and transferred to blood collection tubes coated with EDTA (BD). Hemavet 950 was used for hematological analysis.

Phenylhydrazine (PHZ) treatment and monocytes transfer

Resident splenic macrophages were depleted with chlodronate liposomes (ClodronateLiposomes. org). A single dose of chlodronate (100µl/10g body weight) is injected retro-orbitally. Donor monocytes were purified by using EasySep Monocyte Enrichment Kit (Stem Cell Technologies). 24 hours after chlodronate administration, $1x10^6$ monocytes were transferred into recipients retro-orbitally. Recipient mice were injected with a single dose of PHZ (100mg/kg body weight) intraperitoneally 24 hours after monocytes transfer.

Splenic EBI isolation

The isolation of splenic EBIs isolation was done as previously described[10]. In brief, spleens were minced and digested in 0.075% (*m/v*) Collagenase IV (Gibco 17104019) and 0.004% (*m/v*) DNase I (Invitrogen DN25) in RPMI1640 for 30min at 37ₒC. The suspension was gently passed through an 18-guage needle several times and cells were washed by centrifugation. Cell pellets were resuspended with 1mL RPMI1640 containing 0.004% DNaseI and layered on top of 30% (*v/v*) FBS in Iscove's Modified Dulbecco's Medium (IMDM) followed by gravity sedimentation for 45 minutes at room temperature. The supernatant was carefully removed and the pellet was processed with Percoll (Sigma) gradient centrifugation (50%(*v/v*)/100%(*v/v*)) at 400*g* for 20min. The interface between the 50% and 100% Percoll was collected, washed with PBS, and processed for flow cytometry and imaging flow cytometry.

Immunocytochemistry

Spleen macrophages and BMDMs were fixed with 4% formaldehyde (Sigma-Aldrich) for 20 min at room temperature (RT). Cells were washed with PBST (PBS containing 0.1% Tween20) and permeabilized by 0.3% Triton X-100. Samples were blocked with 1% BSA in PBST for 30 min at RT and incubated with primary antibodies (F4/80, 123102, Biolegend and Phospho-Stat5a/b, ab32364, Abcam) at 4 °C overnight. Secondary antibodies (FITC-conjugated goat anti-rabbit IgG, sc-2012, Santa Cruz Biotechnology and Alexa 647-conjugated goat anti-rabbit IgG, A21244, Life Technologies) were applied for 1h in dark. After washing with PBST for 3 times, samples were mounted in Prolong Gold Antifade Mountant with DAPI (P-36931, Life Technologies). FV1000 confocal microscope (Olympus) was used for imaging.

Stress BFU-E colony assay

Isolated spleen cells or in vitro cultured bone marrow cells were plated in methylcellulose media (M3334, StemCell Technologies). Stress BFU-Es were scored after 5 days incubation. Stress BFU-E culture conditions and stress BFU-E colony enumeration procedures were previously described (1).

PKH26 cell membrane labeling

Bone marrow cells were isolated and immediately labeled with PHK26 by following the manufacture instructions (PHK26 Red Fluorescent Cell Linker Kits, Sigma-Aldrich). Cells were collected and stained with other cell surface markers before flow cytometry analysis. PKH26

were detect by using LSR-II Fortessa Flow cytometer (BD Biosciences) with 561nm laser and 575/26 filter.

Flow cytometry and cell sorting

Cells were collected and labeled with indicated antibodies. A list of antibodies was provided in Table **2-1**. Dead cells were determined by zombie yellow fixable viability dye (BioLegend) staining. LSR-II Fortessa Flow cytometer (BD Biosciences) was used for flow cytometry analysis. All flow cytometry data were analyzed with FlowJo software. Astrios (Becton Dickinson) cell sorter was used for cell sorting.

Table **2-1**: **Flow cytometry antibody list.**

Antibodies	**Fluorochrome**	**Source**	**Catalog No.**
CD34	Alexa Fluor 647	BD	560230
CD133	PE	eBiosciences	12133182
CD133	PE-Cy7	BioLegend	141210
Kit (c-kit)	Brilliant Violet 421	BioLegend	1058282
Sca1 (Ly-6A/E)	APC-Cy7	BioLegend	108126
Sca1 (Ly-6A/E)	FITC	Biolegend	108106
Phospho-Stat5	Alexa Fluor 647	BD	562074
F4/80	PE-Cy7	Biolegend	123114
CD16/32	N/A	Biolegend	101302

Epo and PGE_2 ELISA assay

Peripheral blood was collected by cardiac puncture and transferred to serum separator tubes (BD). Serum samples were separated by centrifuge, collected and stored at -80 ˚C before use. Serum Epo concentrations were measured by Mouse Erythropoietin Quantikine ELISA Kit (R&D systems). Spleens were collected and weighed on indicated days after BMT. Cells were homogenized in PBS and PGE_2 levels were measured by ELISA immediately. Splenic and serum PGE_2 concentrations were measured by Prostaglandin E_2 Express EIA Kit (Cayman Chemical Company) and Prostaglandin E_2 Metabolite EIA Kit (Cayman Chemical Company), respectively.

Quantitative reverse transcription PCR (RT-qPCR)

Total RNA was isolated by using TriZol reagent (Invitrogen). Complementary DNA (cDNA) was generated by using the qScript cDNA SuperMix (Quanta Biosciences). qPCR was done by using StepOnePlus Real-Time PCR System (Applied Biosystems). A list of TaqMan probes is provided in supplemental Table **2-2**.

Table **2-2**: **TaqMan probe list.**

Gene	**Catalog No.**
18s	Hs99999901_s1
EpoR	Mm00833882_m1
Wnt1	Mm01300555_g1
Wnt2	Mm00470018_m1
Wnt2b	Mm00437330_m1
Wnt3	Mm03053665_s1

Wnt3a	Mm00437337_m1
Wnt4	Mm01194003_m1
Wnt5a	Mm00437347_m1
Wnt5b	Mm01183986_m1
Wnt6	Mm00437353_m1
Wnt7a	Mm00437354_m1
Wnt7b	Mm01301717_m1
Wnt8a	Mm01157914_g1
Wnt8b	Mm00442107_m1
Wnt9a	Mm00460518_m1
Wnt9b	Mm00457102_m1
Wnt10a	Mm00437325_m1
Wnt10b	Mm00442104_m1
Wnt11	Mm00437328_m1
Wnt16	Mm00446420_m1
Wnt2b(human)	Hs00921614_m1
Wnt8a(human)	Hs00230534_m1
Hpgds	Mm00479846_m1
PPARγ	Mm00440940_m1
Ptges	Mm00452105_m1

Gene Set Enrichment Analysis (GSEA)

Microarray data transcriptomics analysis was done previously[2]. The data were deposited into NCBI's Gene Expression Omnibus (GEO) for public access via GEO accession number, GSE122390. Gene expression profile was visualized by Transcriptome Analysis Console (TAC) software (Affymetrix). Normalized dataset was also processed with Gene Set Enrichment Analysis (GSEA) in order to determine statistically differentially expressed gene sets in the two groups of SEPs. Hallmark gene sets were accessed from Molecular Signatures Database (MSigDB).

Statistics

Quantitative data were represented as means ± SEM. Statistical analysis was described in figure legends. Significant level was set as α=0.05. ns, not significant, *p<0.05, **p<0.01, ***p<0.001, ****p<0.0001.

2.3 Results

Epo/Stat5 signaling is required for macrophage regulated SEP development

The most immature CD34+CD133+KS SEPs rapidly proliferate in the spleen during the initial stage of recovery from bone marrow transplantat (BMT). This expansion occurs prior to increased Epo production in kidney[4, 5]. The expansion of this population is recapitulated in vitro when bone marrow cells are cultured in stress erythropoiesis expansion media (SEEM) that lacks Epo[5]. Although Epo induces the immature SEPs to commit to differentiation, the cells express

very low amounts of Epo receptor (EpoR) mRNA (Figure 2-1A), which is consistent with previous work showing that these progenitors were unable to generate stress BFU-E colonies when plated in methylcellulose media containing Epo[5]. These findings suggest that the target of Epo is not the immature SEPs. In contrast, primary F4/80+ macrophages isolated from spleen and in vitro cultured bone marrow derived macrophages (BMDMs) expressed significant levels of EpoR mRNA (Figure 2-1A). The expression levels were not as high as the more mature SEPs, $CD34^{neg}CD133^{neg}$Kit+Sca1+ cells (CD34-CD133-KS SEPs), that are able to differentiate. However, this observation is consistent with recent work showing that EpoR expression marks the EBI macrophages[13, 14]. Treatment of BMDMs with Epo induces Stat5 phosphorylation as measured by flow cytometry and immunofluorescence (Figure 2-1B). Primary spleen F4/80+ macrophages treated with Epo induced Stat5 phosphorylation and that signal was lost in $Stat5^{\Delta/\Delta}$ macrophages (Figure 2-1C). To demonstrate a role for EpoR/Stat5 signaling in macrophages in regulating the transition to committed erythroid progenitors, we cultured wildtype CD34+CD133+KS cells on control $Stat5^{fx/fx}$ or mutant $Stat5^{\Delta/\Delta}$ macrophages for 5 days and then added Epo to the cultures. The CD34+CD133+KS SEPs grown on control macrophages matured into CD34-CD133-KS cells, while the CD34+CD133+KS grown on mutant BMDMs failed to transition (figure 2-1D). This failure to mature was also evident when the cells were plated for stress BFU-Es. Cells grown on $Stat5^{\Delta/\Delta}$ macrophages were unable to generate BFU-E colonies when cultured in Epo alone condition. They also produced significantly fewer colonies when plated in media containing Epo + SCF + BMP4 at 2% O_2. This culture condition maximizes the SEP potential of generating stress BFU-Es. (Figure 2-1E). However, the SEPs generated with the mutant macrophages were not defective as transplant of purified SEPs generated with control or $Stat5^{\Delta/\Delta}$ BMDMs were equally able to provide short-term radioprotection (Figure 2-1F).

To assess the role of Epo/Stat5 dependent signaling in the splenic niche, we treated congenic CD45.1+ mice with clodronate liposomes to eliminate resident splenic macrophages. We then transferred purified $Stat5^{fx/fx}$ or $Stat5^{\Delta/\Delta}$ Ly6C+Ly6G-CD11b+CD45.2+ monocytes into the clodronate treated mice[10, 15]. These mice were then treated with phenylhydrazine (PHZ) to induce anemia. At 48 hours after treatment, $Stat5^{\Delta/\Delta}$ and $Stat5^{fx/fx}$ contributed to similar percentages of donor derived immature EBIs (F4/80+CD133+$Ter119^{lo/neg}$), but $Stat5^{\Delta/\Delta}$ monocytes contributed to significantly fewer mature EBIs (F4/80+$CD133^{lo/neg}$Ter119+). However, by 72 hours after treatment, the difference in mature EBIs was lost, which may reflect that the signals induced by Epo signaling in recipient derived macrophages rescued the $Stat5^{\Delta/\Delta}$ mutant phenotype (Figure 2-1G). Analysis of the EBIs by imaging flow cytometry showed that $Stat5^{\Delta/\Delta}$ EBIs had fewer associated Ter119+ cells (Figure 2-1H, 2-1I). These differences in EBIs occurred despite the observation that serum Epo concentrations in recipients that received mutant or control monocytes were not different at 48 or 72 hours (Figure 2-1J). These data were consistent with BMT experiments. During recovery from BMT, the splenic niche contains both recipient derived and donor derived monocytes and macrophages[10]. Transplanting control unfractionated bone marrow into a $Stat5^{\Delta/\Delta}$ recipient mouse led to a defect in erythroid short-term radioprotection. However, the most severe phenotype was observed when $Stat5^{\Delta/\Delta}$ donor cells were transplanted into $Stat5^{\Delta/\Delta}$ recipients. These mice failed to reach normal hematocrit levels by 24 days after transplant (Figure 2-1K). These data suggest that loss of Epo/Stat5 dependent signaling in recipient and donor derived monocytes and macrophages compromises stress erythropoiesis.

A

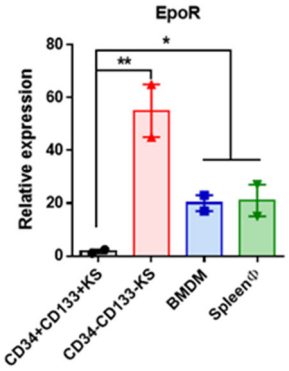
EpoR
Relative expression
80
60
40
20
0
*
**
CD34+CD133+KS
CD34-CD133-KS
BMDM
Spleen

B

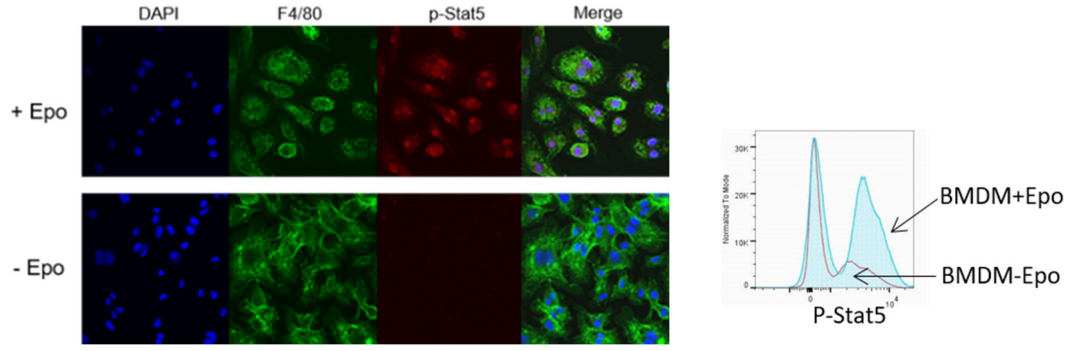
DAPI
F4/80
p-Stat5
Merge
+ Epo
- Epo
BMDM+Epo
BMDM-Epo
P-Stat5

C

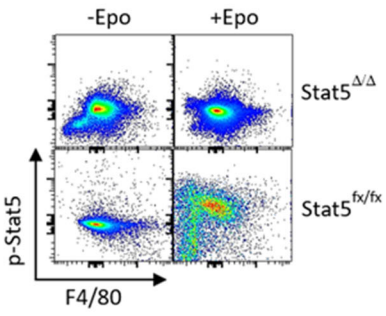
-Epo
+Epo
Stat5Δ/Δ
Stat5fx/fx
p-Stat5
F4/80

D

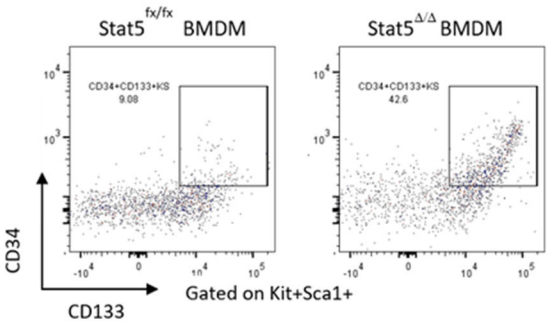
Stat5fx/fx BMDM
Stat5Δ/Δ BMDM
CD34+CD133+KS
9.08
CD34+CD133+KS
42.6
CD34
CD133
Gated on Kit+Sca1+

E

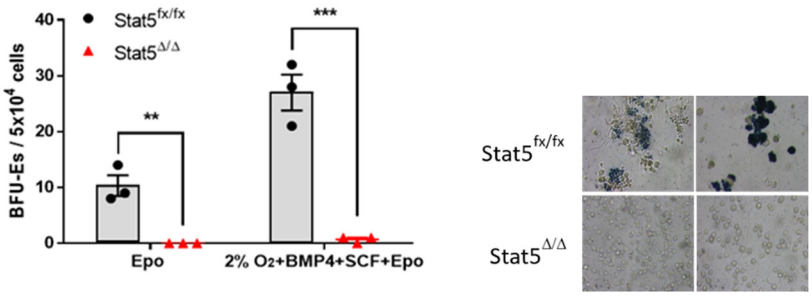
Stat5fx/fx
Stat5Δ/Δ
BFU-Es / 5x10^4 cells
40
30
20
10
0
**
***
Epo
2% O2+BMP4+SCF+Epo
Stat5fx/fx
Stat5Δ/Δ

F

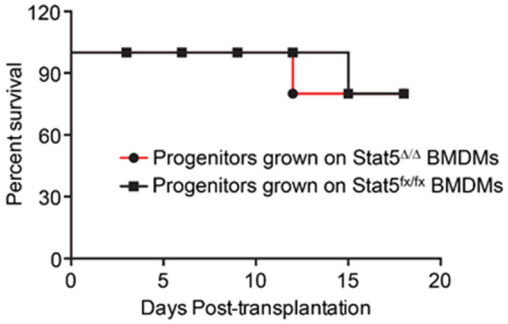
Percent survival
120
90
60
30
0
0
5
10
15
20
Days Post-transplantation
Progenitors grown on Stat5Δ/Δ BMDMs
Progenitors grown on Stat5fx/fx BMDMs

G

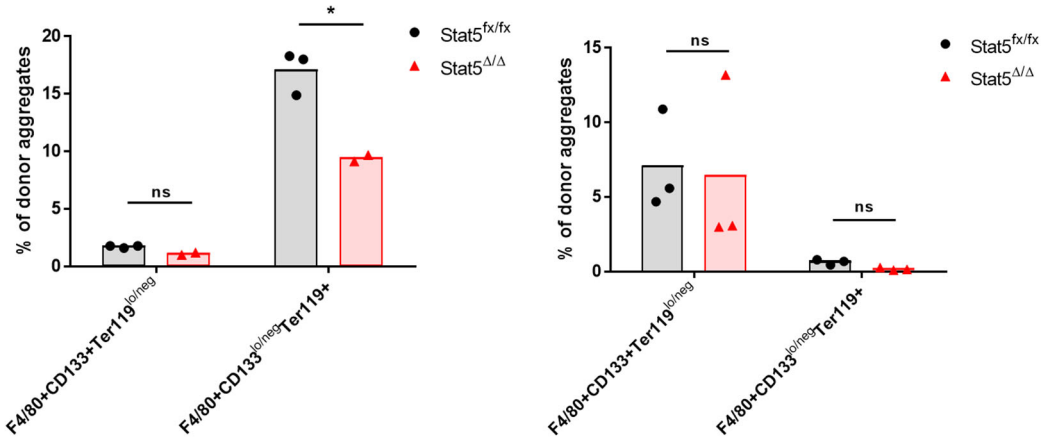
% of donor aggregates
20
15
10
5
0
ns
*
Stat5fx/fx
Stat5Δ/Δ
F4/80+CD133+Ter119lo/neg
F4/80+CD133lo/neg Ter119+
% of donor aggregates
15
10
5
0
ns
ns
Stat5fx/fx
Stat5Δ/Δ
F4/80+CD133+Ter119lo/neg
F4/80+CD133lo/neg Ter119+

H

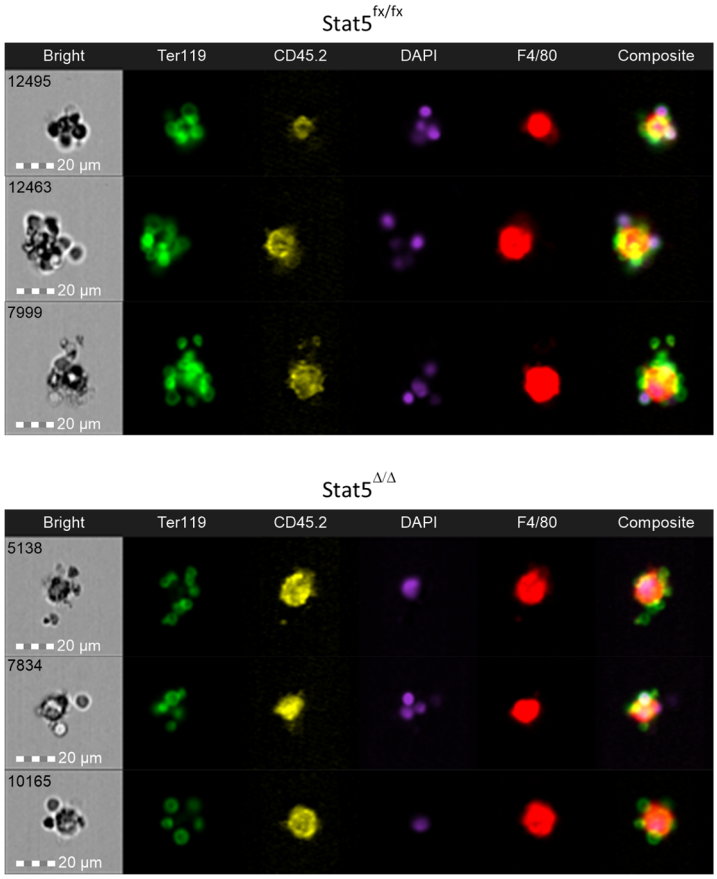
Stat5fx/fx
Bright
Ter119
CD45.2
DAPI
F4/80
Composite
12495
20 µm
12463
20 µm
7999
20 µm
Stat5Δ/Δ
Bright
Ter119
CD45.2
DAPI
F4/80
Composite
5138
20 µm
7834
20 µm
10165
20 µm

I

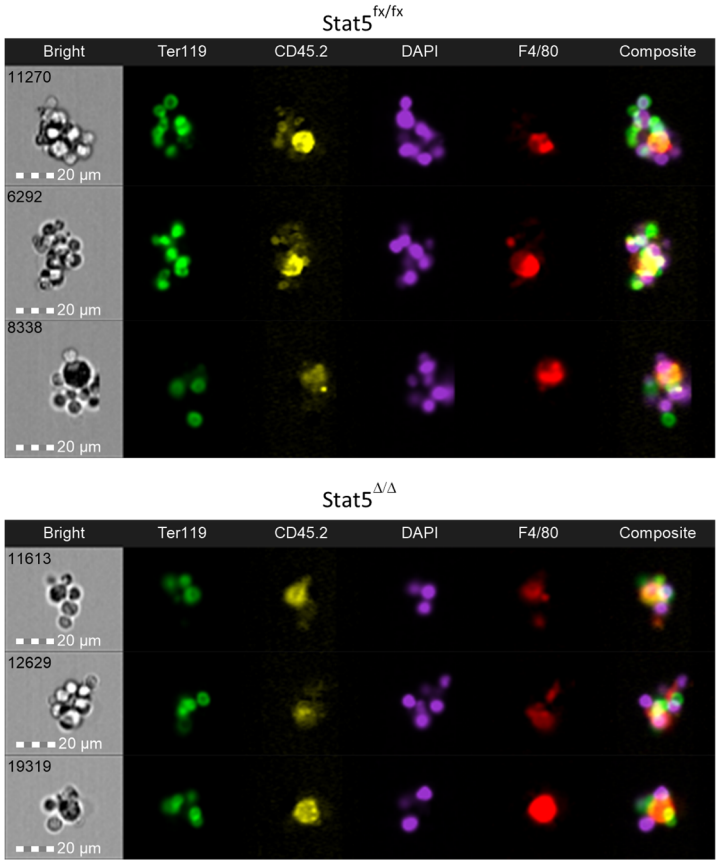
Stat5fx/fx
Bright
Ter119
CD45.2
DAPI
F4/80
Composite
11270
20 µm
6292
20 µm
8338
20 µm
Stat5Δ/Δ
Bright
Ter119
CD45.2
DAPI
F4/80
Composite
11613
20 µm
12629
20 µm
19319
20 µm

J

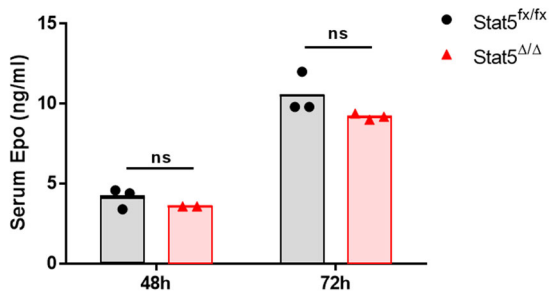
Serum Epo (ng/ml)
15
10
5
0
ns
ns
48h
72h
Stat5fx/fx
Stat5Δ/Δ

K

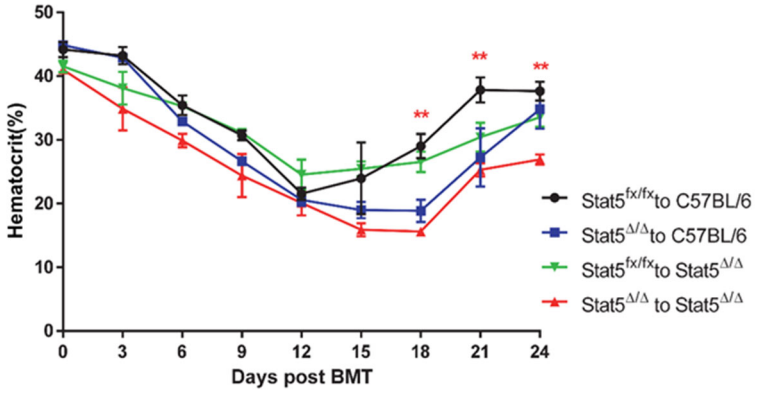

Figure **2-1**: **Differentiation of SEPs requires activation of macrophages through Epo-dependent Stat5 activation**.

(A). mRNA expression of EpoR in sorted SEPs (CD34+CD133+KS and CD34-CD133-KS), BMDMs and sorted primary F4/80+ spleen macrophages (spleen ϕ). Student t-test (2-tailed). Data represent means ± SEM. * $p<0.05$, ** $p< 0.01$.

(B). Immunocytochemistry analysis of co-localization of phosphorylated Stat5, F4/80 and DAPI in BMDMs (Left). Flow cytometry analysis of phosphorylated Stat5 in BMDMs treated ± Epo (Right).

(C). Flow cytometry analysis of Stat5 phosphorylation in F4/80+ spleen macrophages isolated from $Stat5^{fx/fx}$ or $Stat5^{\Delta/\Delta}$ mice treated ± Epo.

(D). Flow cytometry analysis of CD34+CD133+KS SEPs co-cultured with $Stat5^{fx/fx}$ BMDMs or $Stat5^{\Delta/\Delta}$ BMDMs. CD34 and CD133 expression is shown on cells gated on Kit+Sca1+.

(E). Stress BFU-E colony number (left) and representative BFU-E morphology (right) of SEPs co-cultured with $Stat5^{fx/fx}$ BMDMs or $Stat5^{\Delta/\Delta}$ BMDMs. Student t-test (2-tailed). Data represent means ± SEM. ** $p< 0.01$.

(F). Sorted CD34+CD133+KS donor bone marrow cells were cultured on $Stat5^{fx/fx}$ or $Stat5^{\Delta/\Delta}$ BMDMs in SEEM media. Lethally irradiated C57BL/6 recipient mice were transplanted with 5,000 cultured CD34+CD133+KS donor cells. n=5 mice per group

(G). Quantification of flow cytometry analysis of early stage F4/80+CD133+$Ter119^{lo/neg}$ EBIs and late stage F4/80+$CD133^{lo/neg}$Ter119+ EBIs after 48 hours PHZ treatment (left) and 72 hours PHZ treatment (right). F4/80, CD133 and Ter119 expressions are shown on aggregates gated on

CD45.2+ (donor). Student t-test (2-tailed). Data represent means ± SEM. * $p < 0.05$, ns, not significant.

Macrophage-derived Wnt/β-catenin signaling promotes SEP proliferation

These observations support a role for Epo signaling in macrophages in promoting the transition from proliferating SEPs to differentiating SEPs. During liver regeneration, macrophages express canonical Wnt signals, which influence neighboring hepatic progenitor cells by promoting their proliferation and determining their developmental fate[16]. We tested whether Wnt signaling plays a similar role in stress erythropoiesis. First, we examined the mRNA expression of canonical and non-canonical Wnts in both in vitro cultured BMDMs in response to Epo stimulation and in primary F4/80+ spleen macrophages isolated at different days post BMT. Non-canonical Wnts did not exhibit significant changes in expression (Figure 2-2A). In contrast, the expression of most canonical Wnts exhibited significant fluctuations in response to Epo in vitro and in vivo. Wnt2b, Wnt7, Wnt8a and Wnt9b exhibited the most significant changes in expression (Figure 2-2A, 2-2B). To further characterize the role of Wnt signaling in stress erythropoiesis in more detail, we focused on two canonical Wnts, Wnt2b and Wnt8a, which showed a sensitive response to Epo in vitro and in vivo. Analysis of Wnt2b and Wnt8a mRNA expression in the spleen following BMT showed that the two Wnt ligands peaked at day 4 after transplant and rapidly decreased by day 6. The decrease in expression of Wnt2b and Wnt8a corresponded to the increase in serum Epo concentration that peaked at day 6. Additionally, the expression of Wnt2b and Wnt8a remained repressed while Epo levels are elevated during the recovery (Figure 2-2C). Furthermore, isolated murine F4/80+ spleen macrophages treated with

Epo rapidly decreased the expression of Wnt2b and Wnt8a (Figure 2-2D left). However, splenic macrophages isolated from $Stat5^{\Delta/\Delta}$ mice were unable to decrease Wnt2b and Wnt8a expression in response to Epo stimulation (Figure 2-2E). We extended these observations to human stress erythropoiesis. Unfractionated human bone marrow cells cultured in SEEM expressed Wnt2b and Wnt8a mRNA, whereas these expression levels were significantly decreased within 24 hours after Epo treatment (Figure 2-2D right). These observations demonstrate that Epo negatively regulates the expression of Wnt2b and Wnt8a.

Our observation that Wnt2b and Wnt8a expression occurs prior to the Epo induced transition to differentiation suggested that Wnt signaling may play a role in the expansion of immature SEP populations. To investigate this possibility, we performed in vitro stress erythropoiesis expansion cultures and manipulated canonical Wnt signaling. Murine bone marrow cells cultured in SEEM media were treated with and without BIO, a GSK3 inhibitor that activates canonical Wnt signaling[17]. Addition of BIO to the cultures resulted in an expansion of the CD34+CD133+KS population of early SEPs and maintained this population even when Epo was added to the culture (Figure 2-2F). BIO also blocked the Epo-dependent development of stress BFU-Es in these cultures (Figure 2-2G). However, this block to differentiation was reversible. When immature CD34+CD133+KS SEPs expanded in SEEM + BIO cultures were switched to SEEM + Epo media lacking BIO, these cultures responded to Epo and induced differentiation into stress BFU-Es. Treatment with BIO resulted in an increased frequency of stress BFU-Es when compared to cultures that were not expanded in BIO (Figure 2-2H). In contrast, when we inhibited Wnt signaling with WIF1, which binds to Wnt proteins and inhibits their activity[18], we observed a significant increase in the frequency of stress BFU-Es in the absence of Epo. When WIF1 was added to SEEM + Epo culture, we observed an increase in stress BFU-E frequency over the addition of Epo alone (Figure 2-2I).

β-catenin dependent transcription is a hallmark of canonical Wnt signaling[19, 20]. To further demonstrate a role for Wnt signaling in the proliferation of SEPs, we analyzed the effects of blocking Wnt signaling by using a conditional allele of β-catenin, that could be deleted in culture using a tamoxifen inducible Cre (β-catenin$^{fx/fx}$;Rosa-CreERT)[21, 22]. Previously, we showed that labeling bone marrow cells cultured in SEEM with the fluorescent membrane dye PKH26, allowed us to identify a faster dividing PKH26^{low} and a slower dividing PKH26^{high} population of SEPs. PKH26^{low} cells are more mature SEPs (CD34-CD133-KS), while PKH26^{high} cells are corresponded primarily to CD34+CD133+KS SEPs[23]. We analyzed cell proliferation by labeling β-catenin$^{\Delta/\Delta}$ and control cells with PKH26 and cultured the cells for 5 days. We observed a substantially lower proliferation rate in β-catenin$^{\Delta/\Delta}$ SEPs. When we analyzed specific SEP subpopulations, all populations exhibited significant decreases in cell proliferation with the greatest effect on the more mature faster dividing populations (Figure 2-3A). Gene set enrichment analysis showed that PKH26^{low} cells were positively correlated for Wnt signaling and target genes increased by β-catenin[24] (Figure 2-3B).Deleting β-catenin in a bone marrow culture could also potentially affect Wnt dependent signaling in the stroma. To control for stromal effects, we plated equal number of GFP+ control and β-catenin$^{fx/fx}$;Rosa-CreERT bone marrow cells in a co-culture system. The cells were expanded in SEEM for 2 days followed by 4-hydroxytamoxifen (4-OHT) treatment for 24 hours. Then cells were washed and cultured in SEEM for 2 additional days. We compared the proliferation of GFP+ control cells with the β-catenin$^{\Delta/\Delta}$ (GFP-) cells. Prior to 4-OHT treatment, nearly equal proportions of GFP+ and GFP- cells were observed in the culture. However, after deletion of β-catenin, the proportion of GFP-;β-catenin$^{\Delta/\Delta}$ cells was significantly lower than GFP+ control cells (Figure 2-3C). Analysis of the SEP populations showed that the GFP-;β-catenin$^{\Delta/\Delta}$ cells contained a similar percentage of CD34+CD133+KS cells, but the percentages of more mature progenitors, CD34-CD133-KS cells, were decreased similar to what

we observed in Figure 2-3A (Figure 2-3D). Furthermore, the total numbers of these populations were all severely decreased (Figure 2-3D). Switching the cultures to Epo containing stress erythropoiesis differentiation media (SEDM) led to significantly fewer stress BFU-Es in the GFP-;β-catenin$^{\Delta/\Delta}$ cells when compared to the GFP+ control cells (Figure 2-3E). These data demonstrate that mutating β-catenin leads to defects in the proliferation of immature SEPs severely impacts the ability of committed progenitors to generate erythrocytes.

We next extended this in vitro analysis to an in vivo stress erythropoiesis model, erythroid short-term radioprotection after BMT. Donor cells rapidly proliferate in the spleen resulting in increased spleen weights after transplant[4, 5]. However, mice transplanted with unfractionated β-catenin$^{\Delta/\Delta}$ bone marrow cells exhibited significantly smaller spleens and had fewer donor derived cells during the recovery period (Figure 2-3F). This defect manifested as a significantly delayed erythroid recovery, but the recovery of WBC counts was not different from control transplanted mice (Figure 2-3 G-J). The slow generation of new erythrocytes was a result of a defect in the production of stress BFU-Es in the spleen (Figure 2-3K). Donor bone marrow cells contribute to the microenvironment as well as SEPs. To control for the effects of mutating β-catenin on the microenvironment, we transplanted purified immature CD133+Kit+Sca1+ β-catenin$^{\Delta/\Delta}$ or β-catenin$^{fx/fx}$ SEPs with an equal number of GFP+ wildtype SEPs into irradiated recipients. Mutant and control SEPs homed to the spleen with similar efficiency at 24 hours after transplant (Figure 2-4A). Mice transplanted with mutant SEPs showed decreased survival as only 50% survived to 8 days (Figure 2-4B). Expansion of CD133+Kit+Sca1+ SEPs and CD133-Kit+Sca1+ SEPs were significantly decreased in the mutant transplants (Figure 2-4C), which lead to decreased spleen weight, hematocrit and hemoglobin concentration (Figure 2-4 D-H). In addition, RBC counts were less but not significantly decreased, but WBC counts were similar. The extent of the anemia induced a higher level of serum Epo concentration in the mutant

transplants (Figure 2-4I). Taken together, these data show that mutation of β-catenin in SEPs impairs their proliferation, which compromises short-term radioprotection after BMT.

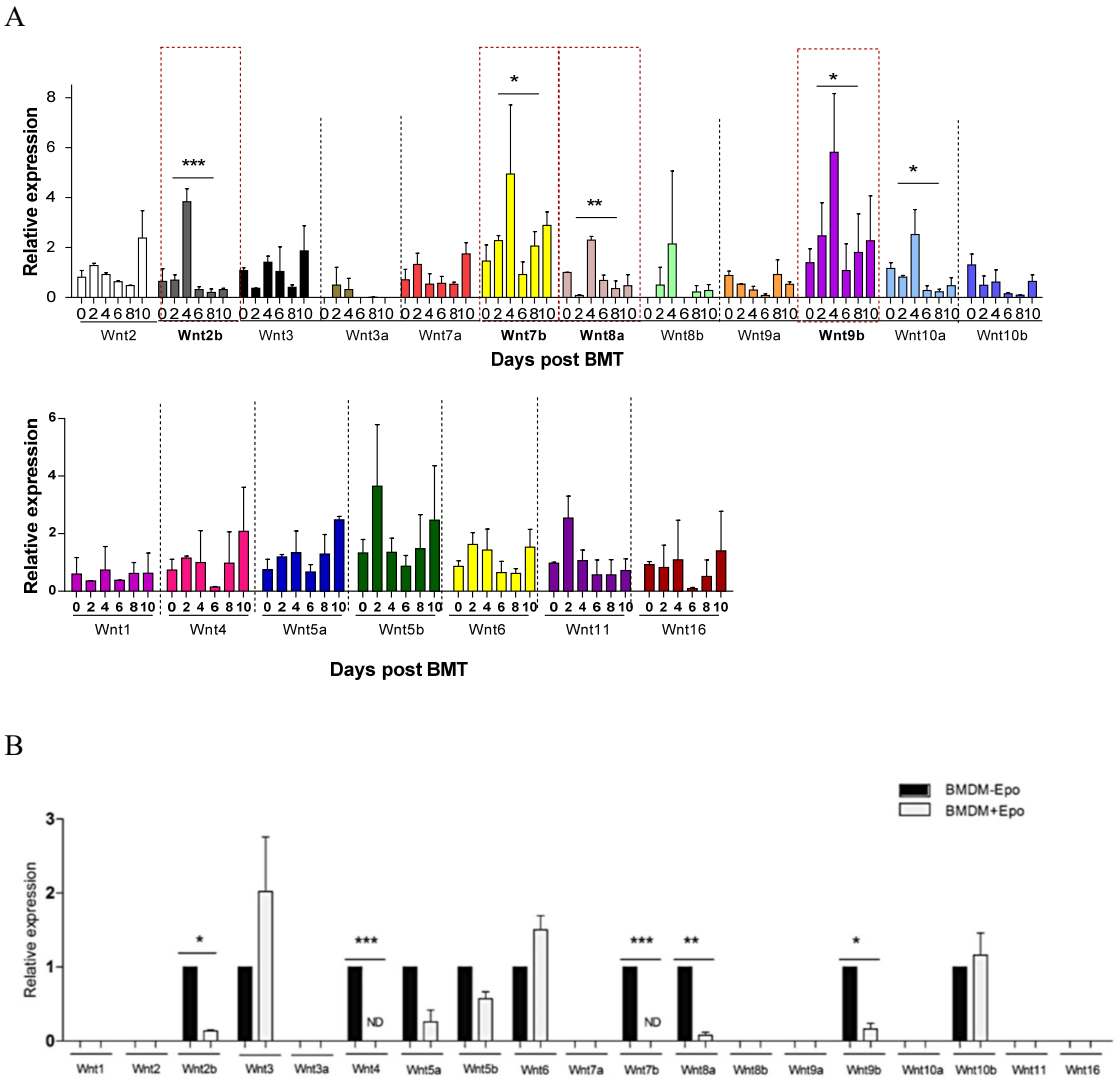

C

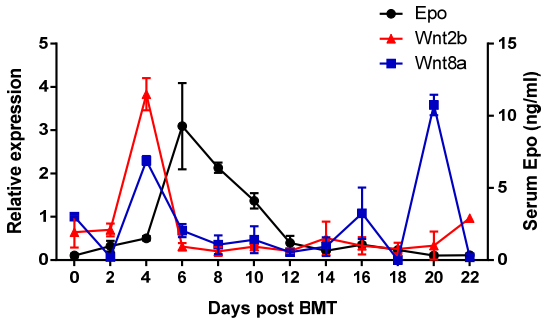
Epo
Wnt2b
Wnt8a
Relative expression
Serum Epo (ng/ml)
Days post BMT

D

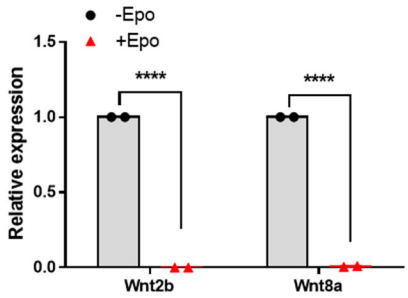
-Epo
+Epo
Relative expression
****
****
Wnt2b
Wnt8a

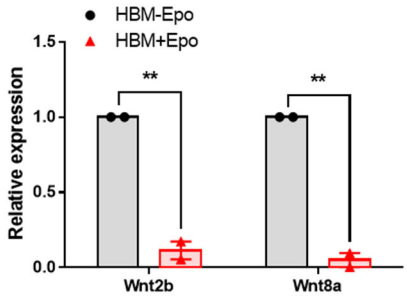
HBM-Epo
HBM+Epo
Relative expression
**
**
Wnt2b
Wnt8a

E

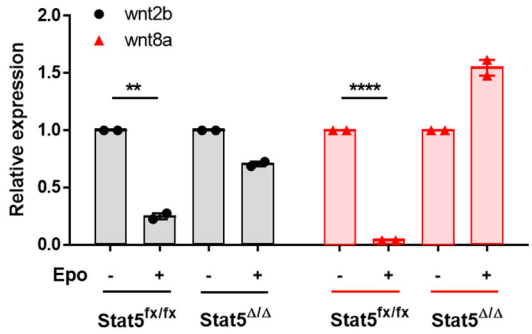
wnt2b
wnt8a
Relative expression
**
****
Epo
Stat5fx/fx
Stat5Δ/Δ
Stat5fx/fx
Stat5Δ/Δ

F

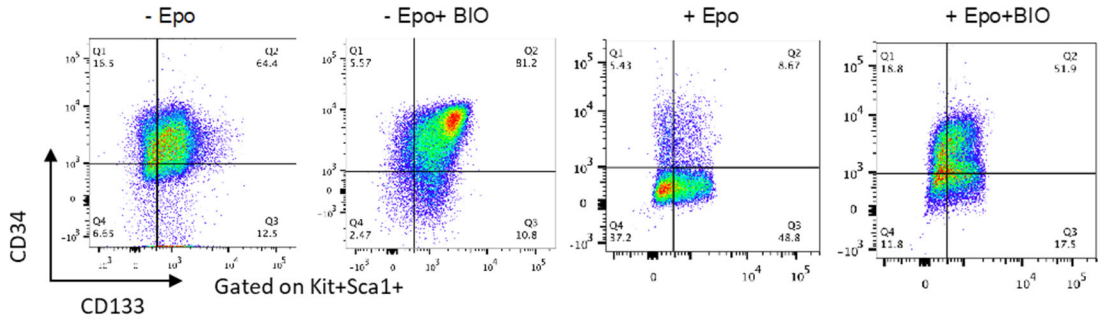
- Epo
- Epo+ BIO
+ Epo
+ Epo+BIO
CD34
CD133
Gated on Kit+Sca1+

G

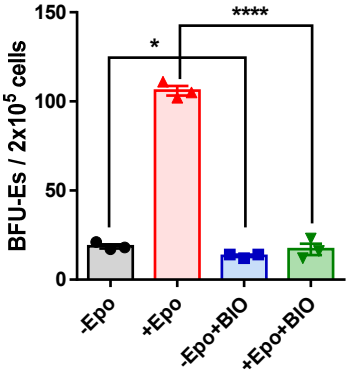
BFU-Es / 2x10^5 cells
-Epo
+Epo
-Epo+BIO
+Epo+BIO

H

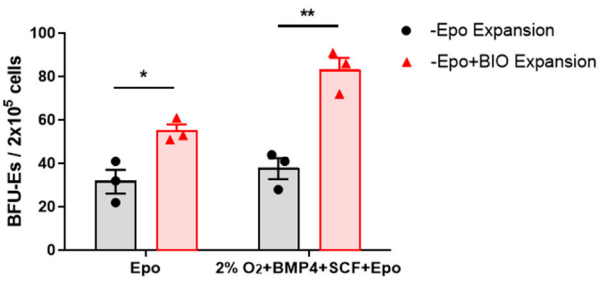
BFU-Es / 2x10^5 cells
-Epo Expansion
-Epo+BIO Expansion
Epo
2% O2+BMP4+SCF+Epo

I

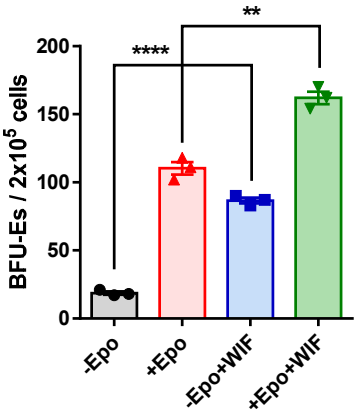
BFU-Es / 2x10^5 cells
-Epo
+Epo
-Epo+WIF
+Epo+WIF

Figure **2-2**: **Epo negatively regulates Wnt signaling, which promotes early SEPs expansion**.
(A). mRNA expression of canonical Wnt ligands (top) and non-canonical Wnt ligands (bottom) in spleen cells from day 0 to day10 after BMT. 500,000 isolated C57/BL6 bone marrow cells were transplanted into lethally irradiated C57/BL6 recipient. Samples were collected every 2 days for analysis. n=2 mice per time point. One-way ANOVA. Data represent means ± SEM. * $p< 0.05$, ** $p< 0.01$, *** $p< 0.001$.
(B). mRNA expression of canonical and non-canonical Wnt ligands in BMDMs treated ± Epo for 24 hours. n=3 per group. ND, not detected. Two-way ANOVA followed by Bonferroni's multiple comparisons. Data represent means ± SEM. * $p< 0.05$, ** $p< 0.01$, *** $p< 0.001$.
(C). ELISA analysis of serum Epo (right Y axis) and Wnt2b and Wnt8a mRNA expression (left Y axis) in spleen cells on indicated days post BMT. For each time point, n=3 mice per group.
(D). Wnt2b and Wnt8a mRNA expression in sorted spleen F4/80+ macrophages treated ± Epo for 24 hours (Left). mRNA expression of Wnt2b and Wnt8a in unfractionated human bone marrow cells cultured in SEEM for 5 days then treated ± Epo for 24 hours (Right). Student t-test (2-tailed). Data represent means ± SEM. ** $p< 0.01$.
(E). mRNA expression of Wnt2b (left) and Wnt8a (right) in ex vivo cultured spleen macrophages from $Stat5^{fx/fx}$ and $Stat5^{\Delta/\Delta}$ mice treated as indicated ± Epo for 24 hours. Student t-test (2-tailed). Data represent means ± SEM. ** $p< 0.01$, **** $p< 0.0001$.
(F). Representative flow cytometry analysis of CD34 and CD133 expression on Kit+Sca1+ SEPs from murine bone marrow cells cultured in SEEM ± 1μM BIO and ± Epo.
(G). Stress BFU-E colony assay of in vitro cultured SEPs treated ± Epo and ± BIO as shown in panel C. Student t-test (2-tailed). Data represent means ± SEM. * $p<0.05$, **** $p< 0.0001$.
(H). Stress BFU-E colony assay of SEPs expanded in SEEM media + BIO. The SEPs were then switched into SEDM media without BIO and stress BFU-Es were assayed after 3 days. Student t-test (2-tailed). Data represent means ± SEM. * $p< 0.05$, ** $p<0.01$.
(I). Stress BFU-E colony assay of SEPs expanded in SEEM ± Epo, + 100ng/ml WIF1 or treated with Epo + WIF1. Student t-test (2-tailed). Data represent means ± SEM. ** $p<0.01$, **** $p< 0.0001$.

A

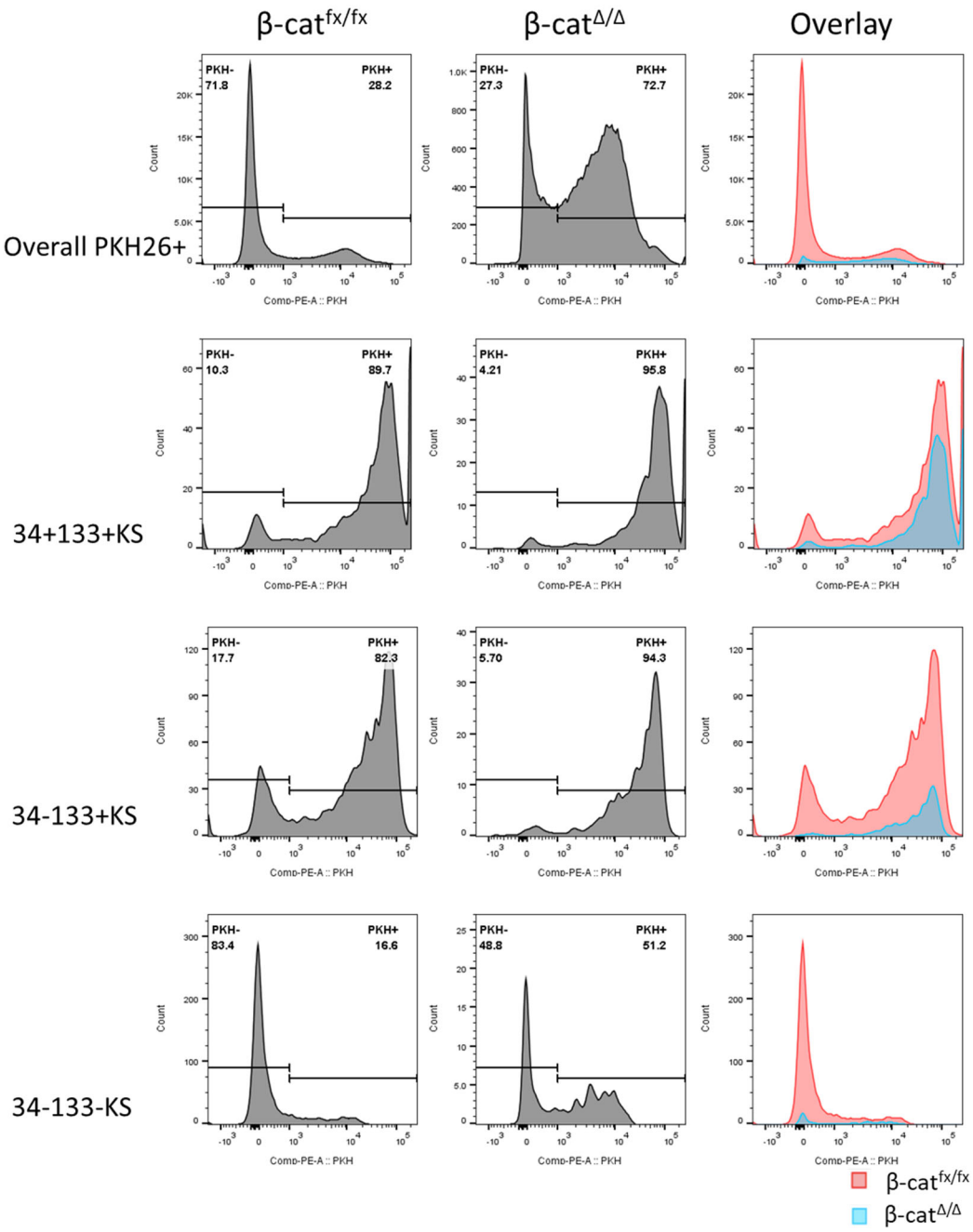
β-cat^fx/fx
β-cat^Δ/Δ
Overlay
Overall PKH26+
34+133+KS
34-133+KS
34-133-KS
PKH-
PKH+
71.8
28.2
27.3
72.7
10.3
89.7
4.21
95.8
17.7
82.3
5.70
94.3
83.4
16.6
48.8
51.2
Count
Comp-PE-A :: PKH
β-cat^fx/fx
β-cat^Δ/Δ

B

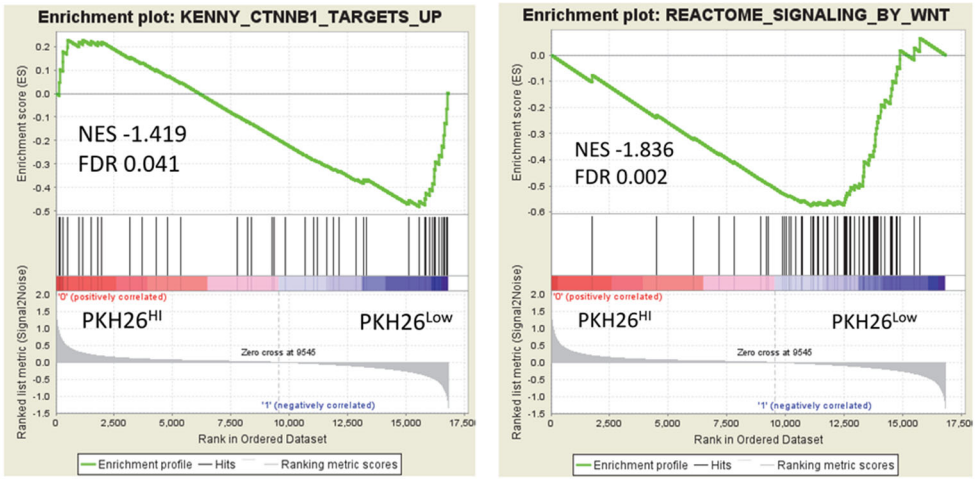
Enrichment plot: KENNY_CTNNB1_TARGETS_UP
NES -1.419
FDR 0.041
Enrichment score (ES)
Ranked list metric (Signal2Noise)
'0' (positively correlated)
PKH26HI
PKH26Low
Zero cross at 9545
'1' (negatively correlated)
Rank in Ordered Dataset
Enrichment profile
Hits
Ranking metric scores
Enrichment plot: REACTOME_SIGNALING_BY_WNT
NES -1.836
FDR 0.002
Enrichment score (ES)
Ranked list metric (Signal2Noise)
'0' (positively correlated)
PKH26HI
PKH26Low
Zero cross at 9545
'1' (negatively correlated)
Rank in Ordered Dataset
Enrichment profile
Hits
Ranking metric scores

C

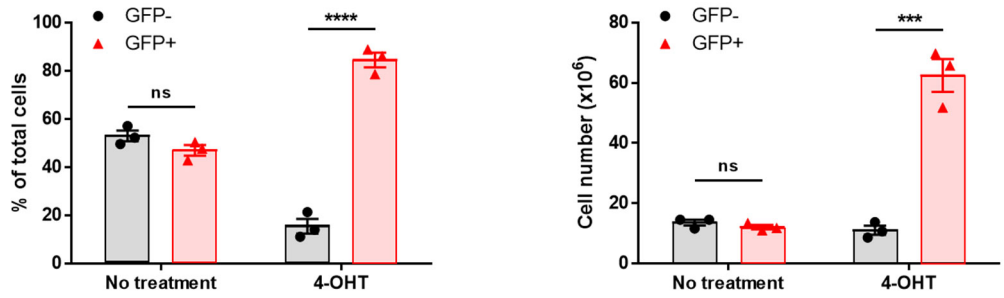
GFP-
GFP+
% of total cells
ns
****
No treatment
4-OHT
GFP-
GFP+
Cell number (x10^6)
ns
***
No treatment
4-OHT

D

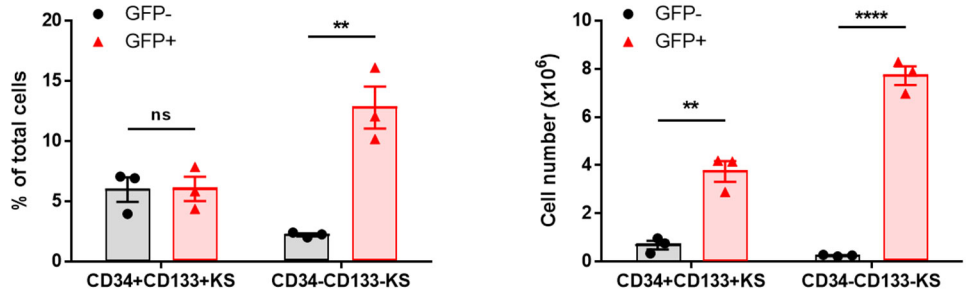
GFP-
GFP+
% of total cells
ns
**
CD34+CD133+KS
CD34-CD133-KS
GFP-
GFP+
Cell number (x10^6)
**
****
CD34+CD133+KS
CD34-CD133-KS

E

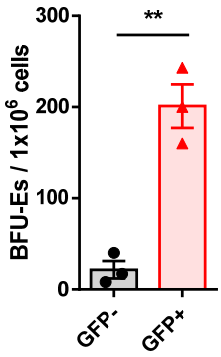
**
BFU-Es / 1x10^6 cells
300
200
100
0
GFP-
GFP+

F

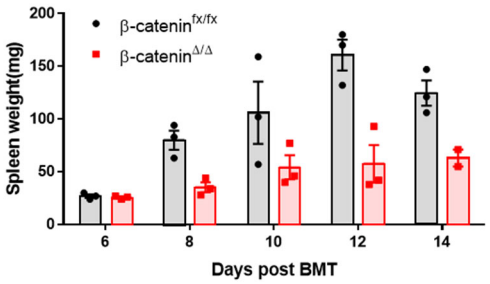
β-catenin^fx/fx
β-catenin^Δ/Δ
Spleen weight(mg)
200
150
100
50
0
6
8
10
12
14
Days post BMT

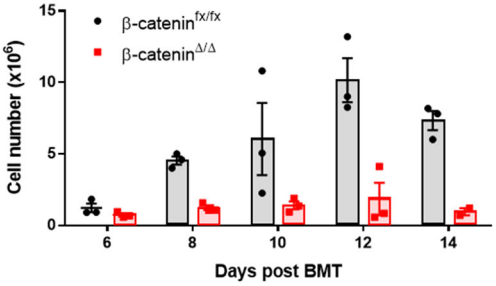
β-catenin^fx/fx
β-catenin^Δ/Δ
Cell number (x10^6)
15
10
5
0
6
8
10
12
14
Days post BMT

G

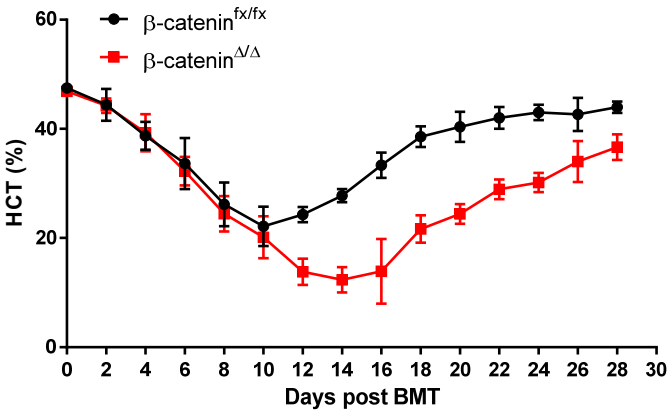
β-catenin^fx/fx
β-catenin^Δ/Δ
HCT (%)
60
40
20
0
0
2
4
6
8
10
12
14
16
18
20
22
24
26
28
30
Days post BMT

H

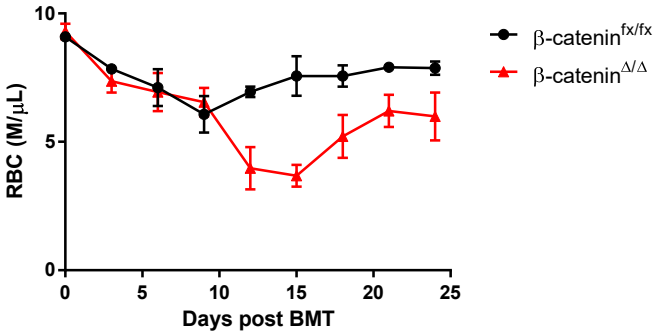

I

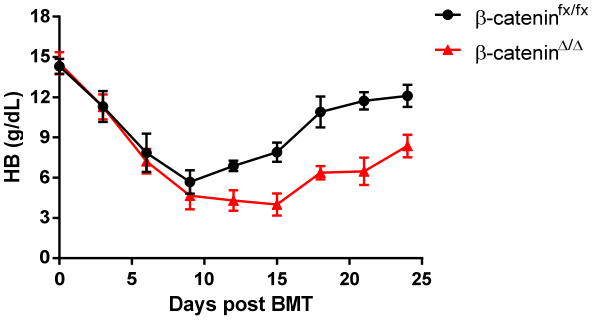

J

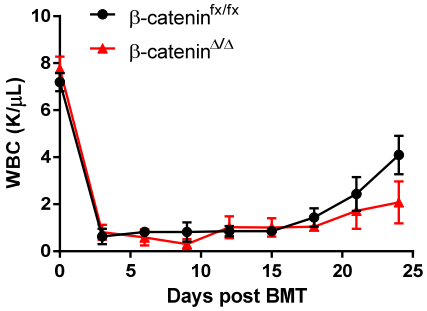

K

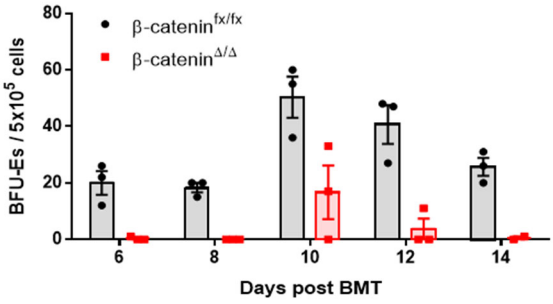

Figure **2-3**: **Macrophage-derived Wnt signaling regulates SEP proliferation through β-catenin dependent signaling pathway.**

(A). Analysis of SEP proliferation using loss PKH26 fluorescent intensity in control β-catenin$^{fx/fx}$ and β-catenin$^{\Delta/\Delta}$ bone marrow cells cultured in SEEM media. Cells were labeled with PKH26

after isolation and cultured in SEEM for 5 days before analysis. Representative PKH26 fluorescence is shown for all cell populations (Top), CD34+CD133+KS (second), CD34-CD133+KS (third), CD34-CD133-KS (bottom).

(B). Analysis of microarray data by gene set enrichment analysis. Expression data from our previous microarray analysis comparing PKH26^{lo}CD133-Kit+Sca1+ (PKH26^{low}) and PKH26^{hi}CD133+Kit+Sca1+ (PKH26^{high}) SEPs (NCBI Gene Expression Omnibus (GEO) accession number, GSE122390). Normalized datasets were processed with Gene Set Enrichment Analysis (GSEA) in order to determine statistically differentially expressed gene sets in the two groups of SEPs. Hallmark gene sets were accessed from Molecular Signatures Database (MSigDB). Targets up-regulated by β-catenin (Left) and Reactome Signaling by Wnt (right).

(C) β-catenin$^{fx/fx}$;Rosa26-CreERT bone marrow cells were co-cultured with GFP+ control bone marrow cells (1:1 ratio) for 2 days then treated ± 4-OHT for 24 hours. The cells were then washed and plated in fresh SEEM without 4-OHT for 2 days. Proportion (left) and total cell number (right) of GFP+ population (control cells) versus GFP- population (β-catenin$^{\Delta/\Delta}$ cells) in co-culture. Student t-test (2-tailed). Data represent means ± SEM. ns, not significant, *** $p< 0.001$, **** $p< 0.0001$.

(D). Flow cytometry analysis of 4-OHT treated co-cultures described in panel C. Proportion (left) and total cell number (right) of CD34+CD133+KS population (GFP+ or GFP-) and CD34-CD133-KS population (GFP+ or GFP-). Student t-test (2-tailed). Data represent means ± SEM. ns, not significant, ** $p< 0.01$, **** $p< 0.0001$.

(E). Production of stress BFU-Es by β-catenin$^{\Delta/\Delta}$ SEPs. Co-cultures as described in panel C were switched into SEDM media and cultured for 3 days, after which GFP+ cells and GFP- SEPs were isolated by FACS and plated for stress BFU-Es. Student t-test (2-tailed). Data represent means ± SEM. ** $p< 0.01$.

(F-K). Analysis of erythroid short-term radioprotection after BMT with β-catenin$^{\Delta/\Delta}$ or control unfractionated donor bone marrow cells. 500,000 bone marrow cells isolated from β-catenin$^{fx/fx}$;Rosa-CreERT or β-catenin$^{fx/fx}$ control mice were treated with 4-OHT for 24 hours before transplanted to lethally irradiated C57BL/6 recipients. (F). Analysis of spleen weight (left), total spleen cell number (right). (G). Analysis of hematocrit during the recovery time. (H). Analysis of RBC count. (I). Analysis of hemoglobin level. (J). Analysis of WBC count. (K). Analysis of stress BFU-Es in the spleen on the indicated days after transplant. For each time point, n=3 mice per group.

A

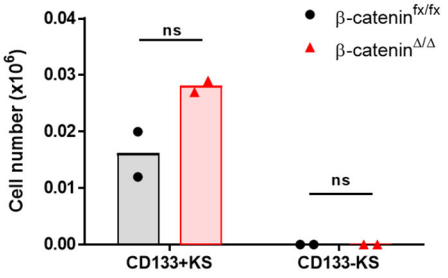
Cell number (x10^6)
0.04
0.03
0.02
0.01
0.00
ns
ns
β-catenin^fx/fx
β-catenin^Δ/Δ
CD133+KS
CD133-KS

B

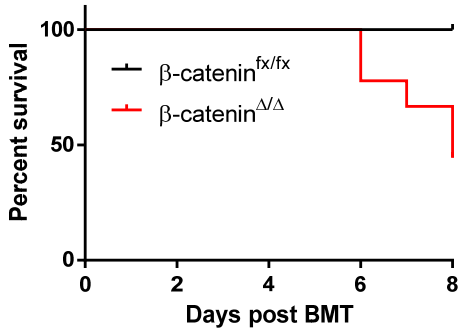
Percent survival
100
50
0
β-catenin^fx/fx
β-catenin^Δ/Δ
0
2
4
6
8
Days post BMT

C

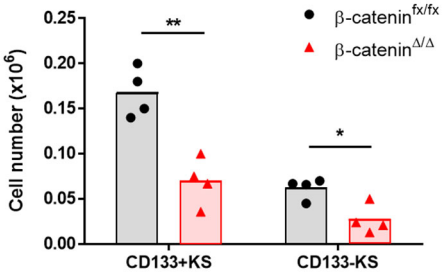
Cell number (x10^6)
0.25
0.20
0.15
0.10
0.05
0.00
**
*
β-catenin^fx/fx
β-catenin^Δ/Δ
CD133+KS
CD133-KS

D

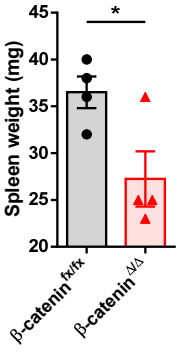
Spleen weight (mg)
45
40
35
30
25
20
*
β-catenin^fx/fx
β-catenin^Δ/Δ

E

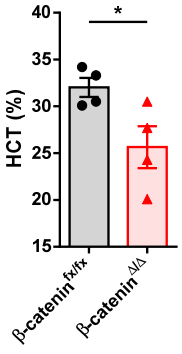
HCT (%)
40
35
30
25
20
15
*
β-catenin^fx/fx
β-catenin^Δ/Δ

F

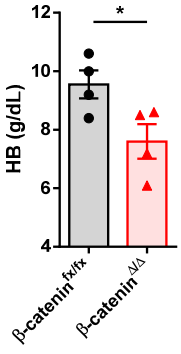
HB (g/dL)
12
10
8
6
4
*
β-catenin^fx/fx
β-catenin^Δ/Δ

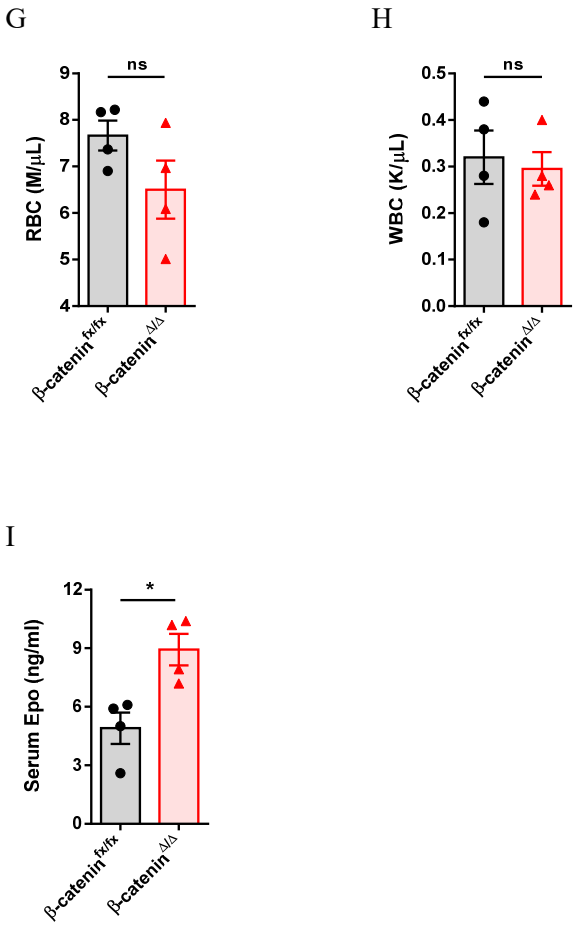

Figure **2-4**: **β-catenin dependent signaling pathway is required for SEP proliferation.**

Analysis of erythroid short-term radioprotection after BMT by sorted β-catenin$^{\Delta/\Delta}$ and control SEPs. 50,000 GFP cells and 50,000 sorted CD133+KS cells isolated from β-catenin$^{fx/fx}$ or β-catenin$^{\Delta/\Delta}$ mice were transplanted to lethally irradiated CD45.1 C57BL/6 recipients.

(A) Flow cytometry analysis of donor SEP homing on day 1 after BMT. CD133, Kit and Sca1 expressions are shown on cells gated on GFP-CD45.2+.

(B). Survival of recipients received β-catenin$^{fx/fx}$ or β-catenin$^{\Delta/\Delta}$ CD133+KS cells. n=9 mice per group.

(C). Flow cytometry analysis of donor derived GFP- SEPs in spleen on day 8 after BMT. Student t-test (2-tailed). Data represent means ± SEM. * $p<0.05$, ** $p< 0.01$.

(D). Analysis of spleen weight on day 8.

(E). Analysis of hematocrit on day 8.

(F). Analysis of hemoglobin level on day 8.

(G) Analysis of RBC count on day 8.

(H) Analysis of WBC count on day 8.

(I). Serum Epo level measurement by ELISA on day 8 after BMT. Student t-test (2-tailed). Data represent means ± SEM. * $p< 0.05$.

Epo induces the production of the PPARγ ligand, Δ^{12}-PGJ_2, to inhibit macrophage Wnt expression

Epo signaling in macrophages resolves inflammation[25, 26] and promotes the clearance of dead cells by increasing the expression of PPARγ expression[27]. Additionally, PPARγ has been shown to antagonize Wnt signaling[28, 29]. We tested whether Epo treatment of BMDMs could induce PPARγ expression. Treatment over a 72-hour time course led to a 10-fold increase in PPARγ expression. PPARγ is a nuclear hormone receptor that responds to known endogenous and synthetic ligands. Hematopoietic prostaglandin D synthase (HPGDS) is an enzyme downstream of cyclooxygenases that generates prostaglandin D2, which is non-enzymatically converted to delta-12-prostaglandin J2 (Δ^{12}-PGJ_2) and its metabolite 15-deoxy-$\Delta^{12,14}$-prostaglandin J2 (15d-PGJ_2) by dehydration[30]. Δ^{12}-PGJ_2 and 15d-PGJ_2 are endogenous PPARγ ligands[31, 32]. BMDMs treated with Epo also showed a 3-fold increase in HPGDS expression, which correlated with increased levels of Δ^{12}-PGJ_2 in the media (Figure 2-5A). $Stat5^{\Delta/\Delta}$ mice fail to produce Δ^{12}-PGJ_2 in response to Epo further demonstrating that Epo induces the production of these PPARγ ligands (Figure 2-5B). The observed increase in PPARγ expression requires the production of Δ^{12}-PGJ_2 as

blocking HPGDS activity with the inhibitor HQL79[33] abrogated the Epo dependent increase in PPARγ expression (Figure 2-5C). Treatment of cultures with the synthetic PPARγ ligand, pioglitazone[34], was as effective as Epo treatment in repressing the expression of Wnt2b and Wnt8a. In contrast, the PPARγ antagonist GW9662[35] blocked the ability of Epo to decrease Wnt expression as did inhibiting Δ^{12}-PGJ_2 production with HQL79 (Figure 2-5D). We extended this analysis to human BMDMs and showed that Epo increased the production of Δ^{12}-PGJ_2 at both 48 hours and 72 hours in each of 4 distinct human bone marrow samples. Similarly, pioglitazone was as effective as Epo treatment in repressing Wnt2b and the effect of Epo was blocked by GW9662 and HQL79 in the human BMDMs (Figure 2-5E). Unlike human stress erythropoiesis cultures (Figure 2-2D right panel), Wnt8a expression was not detectable in human BMDM cultures. These data demonstrate that Epo signaling promotes the production of Δ^{12}-PGJ_2, which in turn leads to the PPARγ dependent repression of Wnt2b and Wnt8a expression.

We next tested whether altering PPARγ activity affects the expansion and transition to differentiation in in vitro stress erythropoiesis cultures. Culturing SEPs in SEEM in presence of pioglitazone resulted in decreased percentages of the most immature CD34+CD133+KS SEPs coupled with an increase in more mature CD34-CD133-Kit+Sca1- (CD34-CD133-K+S-) SEPs (Figure 2-6A). Furthermore, when SEPs were switched to stress erythropoiesis differentiation media (SEDM), addition of GW9662 blocked the transition and led to an increased percentage of immature CD34+CD133+KS SEPs (Figure 2-6B). When we assayed stress BFU-E formation, pioglitazone increased the frequency of stress BFU-Es in the absence of Epo, while GW9662 or HQL79 blocked the Epo dependent increase in stress BFU-Es (Figure 2-6C). These data show that PPARγ acts downstream of Epo to promote the SEP transition to differentiation by antagonizing Wnt signaling during stress erythropoiesis.

A

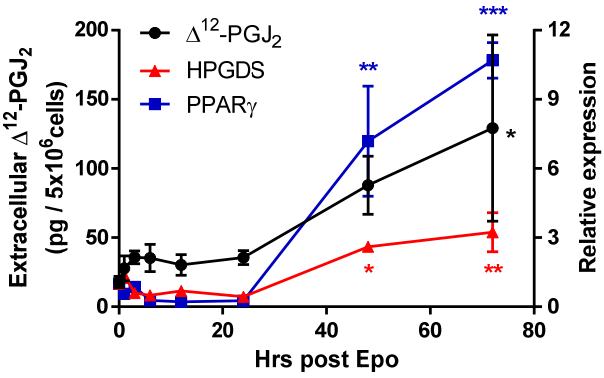
Δ12-PGJ2
HPGDS
PPARγ
Extracellular Δ12-PGJ2 (pg / 5x10^6cells)
Relative expression
Hrs post Epo
0
20
40
60
80
50
100
150
200
3
6
9
12
*
**
***

B

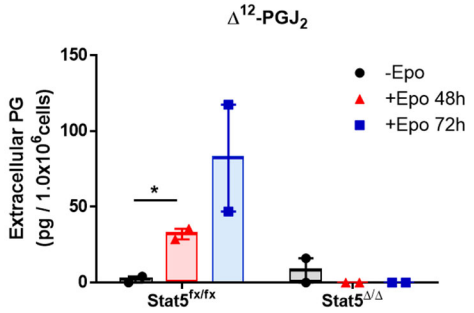
Δ12-PGJ2
-Epo
+Epo 48h
+Epo 72h
Extracellular PG (pg / 1.0x10^6cells)
Stat5fx/fx
Stat5Δ/Δ
*
50
100
150

C

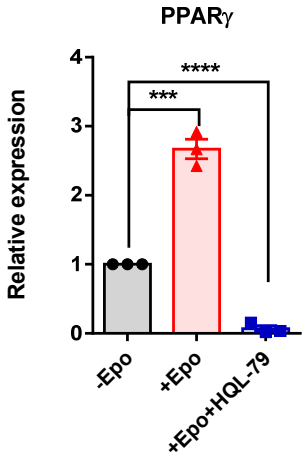
PPARγ
Relative expression
****
***
-Epo
+Epo
+Epo+HQL-79
1
2
3
4

D

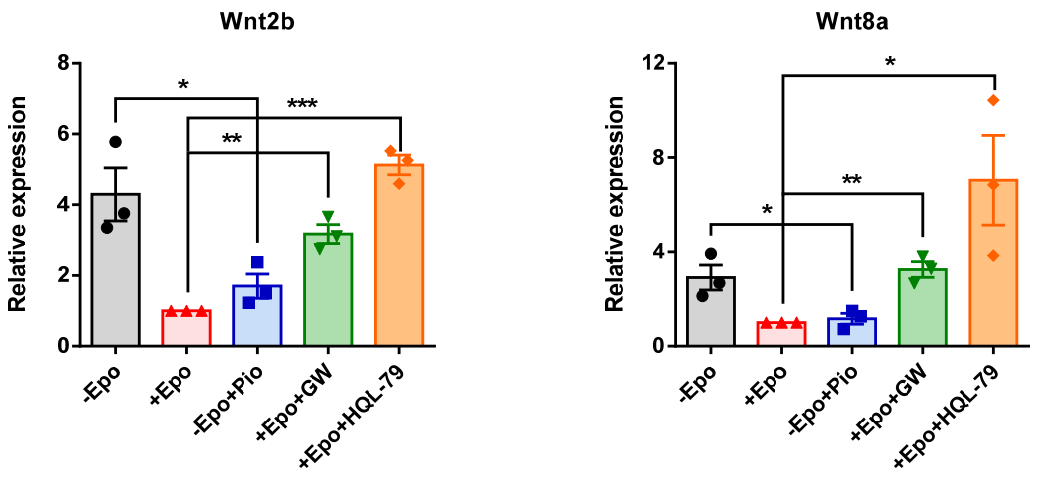

E

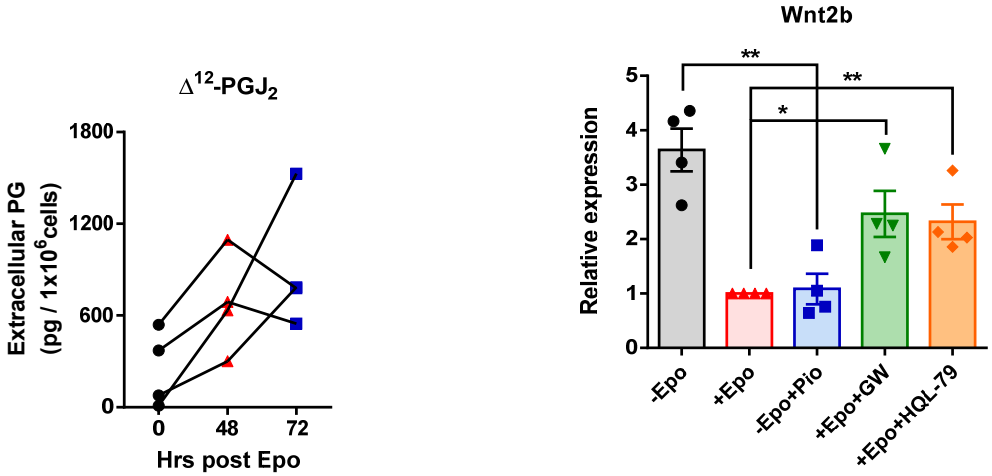

Figure **2-5**: **Epo dependent PPARγ signaling represses Wnt signaling.**

(A). mRNA expression of HPGDS and PPARγ (right Y axis) and liquid chromatography–tandem mass spectrometry (LC-MS/MS) analysis of extracellular Δ^{12}-PGJ_2 (left Y axis) of mouse BMDMs at indicated time points after Epo treatment. One-way ANOVA followed by Dunnett's multiple comparisons. Data represent means ± SEM. * $p< 0.05$, ** $p< 0.01$, *** $p< 0.001$. * represent P values of comparisons between indicated time points and 0 time point. Red stars*, HPGDS. Blue stars*, PPARγ. Black stars*, Δ^{12}-PGJ_2. n=3 per time point.

(B). LC-MS/MS analysis of extracellular Δ^{12}-PGJ_2 in $Stat5^{fx/fx}$ and $Stat5^{\Delta/\Delta}$ BMDMs at the indicated times after Epo treatment. Two-way ANOVA followed by Bonferroni's multiple comparisons. Data represent means ± SEM. * $p< 0.05$.

(C). mRNA expression of PPARγ in mouse BMDMs treated ± Epo or Epo + 25μM HQL79 (HPGDS antagonist). Student t-test (2-tailed). Data represent means ± SEM. *** $p< 0.001$, **** $p< 0.0001$.

(D). mRNA expression of Wnt2b (left) and Wnt8a (right) in mouse BMDMs treated with Epo, 1μM Pio (Pioglitazone, PPARγ agonist), 1μM GW (GW9662, PPARγ antagonist) or HQL79 as indicated. Student t-test (2-tailed). Data represent means ± SEM. * $p< 0.05$, ** $p< 0.01$, *** $p< 0.001$.

(E). LC-MS/MS analysis of extracellular Δ^{12}-PGJ_2 of human BMDMs on the indicated time points before and after Epo treatment (Left). mRNA expression of Wnt2b in human BMDMs treated with Epo, Pio, GW or HQL-79 as indicated (Right). Student t-test (2-tailed). Data represent means ± SEM. * $p< 0.05$, ** $p< 0.01$.

A

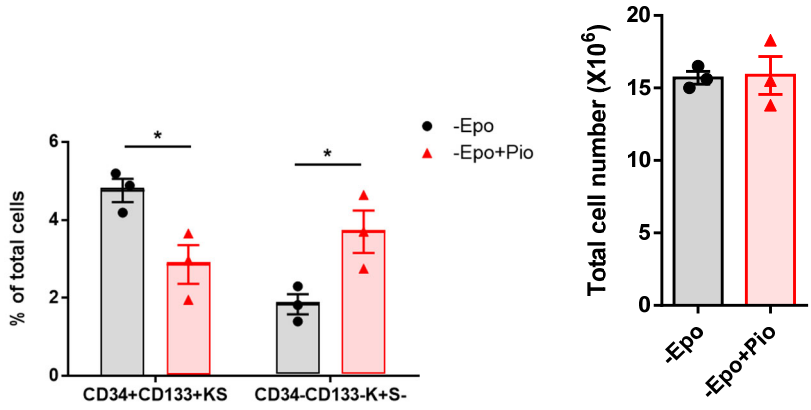

B

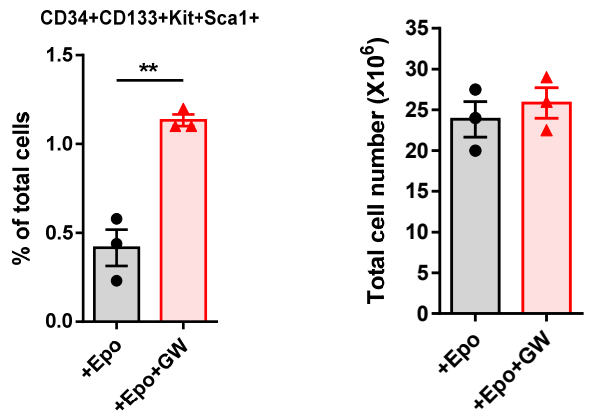

C

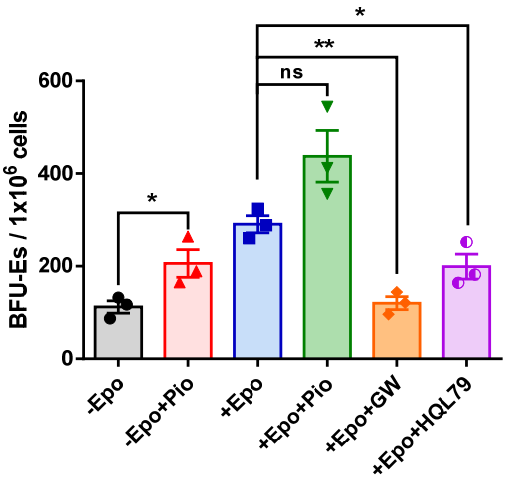

Figure **2-6**: **Epo-dependent PPARγ signaling promote SEP differentiation.**

Analysis of the effects of manipulating PPARγ signaling in in vitro stress erythropoiesis cultures. Unfractionated bone marrow cells were cultured in SEEM or SEDM with indicated treatments (A). Flow cytometry analysis of in vitro cultured SEPs in SEEM ± 1μM Pio. Percentage of CD34+CD133+KS SEPs and CD34-CD133-K+S- SEPs in total cell population (Left). Total cell numbers after culture (Right). Student t-test (2-tailed). Data represent means ± SEM. * $p < 0.05$. (B). Flow cytometry analysis of in vitro cultured SEPs in SEDM with or without 1μM GW. Percentage of CD34+CD133+KS SEPs in total cell population (Left). Total cell numbers after culture (Right). Student t-test (2-tailed). Data represent means ± SEM. ** $p < 0.01$.

(C). Stress BFU-E colony assay of in vitro cultured SEPs expanded in SEEM and then treated with Epo, Pio, GW or HQL-79 as indicated. Student t-test (2-tailed). Data represent means ± SEM. ns, not significant, * $p< 0.05$, ** $p< 0.01$.

Epo-dependent production of PGE_2 promotes differentiation of SEPs.

In addition to PGJ_2, other bioactive eicosanoids are generated by synthases acting downstream of cyclooxygenases 1 and 2 (COX-1, COX-2) [36]. We observed that Epo treatment of murine BMDMs increased the expression of prostaglandin E synthase (PTGES or mPGES-1). PGE_2 is known to promote the generation of erythroid and multilineage progenitor cells, which suggests that PGE_2 may play a role in regulating differentiation of SEPs[37-40]. We examined PGE_2 production in murine BMDMs after Epo treatment and observed a significant increase in PGE_2 production at 48 hours and 72 hours after Epo treatment, which was synchronized with the increased mRNA expression of PTGES (Figure 2-7A). These data show that PGE_2 and Δ^{12}-PGJ_2 were produced simultaneously from macrophages, implying that Epo regulates both prostaglandins in parallel. In vivo, during the recovery from BMT, PGE_2 production in the spleen follows the increase in serum Epo levels (Figure 2-7B). Furthermore, human BMDMs derived from 4 distinct donors each showed increased extracellular PGE_2 after Epo treatment. (Figure 2-7C). Although Epo appears to increase both PGJ_2 and PGE_2 simultaneously, PGE_2 had no effect on the expression of Wnt2b and Wnt8a (Figure 2-7D). Similarly, PPARγ dependent repression of Wnt signaling does not affect the increase in PGE2 production. When we examined PTGES expression in cells cultured with the PPARγ antagonist GW9662 or the Wnt pathway activator BIO. PTGES was consistently increased in SEDM regardless of whether the cells were treated

with GW9662 or BIO. The data demonstrate that PGE2 production is directly regulated by Epo and is not a consequence of increased Δ12-PGJ2 (Figure 2-7E). To define the function of PGE2 in regulating development of SEPs, we analyzed the effects of PGE2 treatment on SEPs in vitro. Addition of 16,16-dimethyl-PGE2 (dmPGE2) to bone marrow cells cultured in SEEM media decreased the percentage of the most immature SEPs (CD34+CD133+KS cells) (Figure 2-7F). In contrast, when we inhibited PTGES with CAY10526 in cells grown in SEDM, we observed a significant decrease in total cell number accompanied with a moderately increased percentage of immature SEPs. This observation shows that there was an inhibition of differentiation when PGE2 production was suppressed (Figure 2-7G). Analysis of stress BFU-E production showed that in the absence of Epo, exogenously added dmPGE2 could induce a significant increase in stress BFU-Es and when dmPGE2 was added with Epo we observed a significant increase in stress BFU-Es over Epo alone. Conversely, if we inhibited PTGES with CAY10526, the number of stress BFU-Es induced by Epo was significantly decreased (Figure 2-7H). These data support a role for PGE2 in promoting the differentiation of stress BFU-Es that is independent of Δ12-PGJ2 and PPARγ dependent suppression of Wnt expression. These two signals work together as addition of WIF1 to inhibit Wnt signaling and PGE_2 to promote differentiation in SEEM induces a significant increase in stress BFU-Es in the absence of Epo (Figure 2-7I).

A

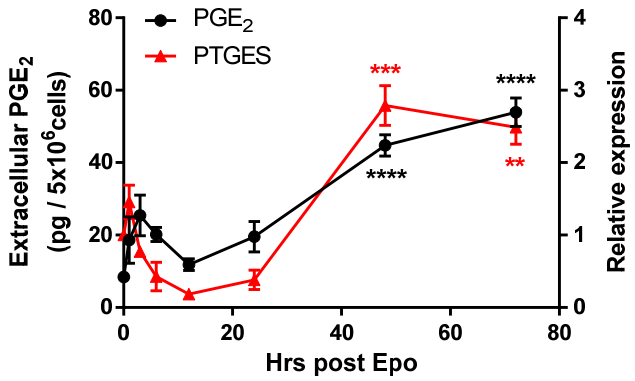
PGE2
PTGES
Extracellular PGE2
(pg / 5x10^6cells)
Relative expression
Hrs post Epo
***
****
****
**

B

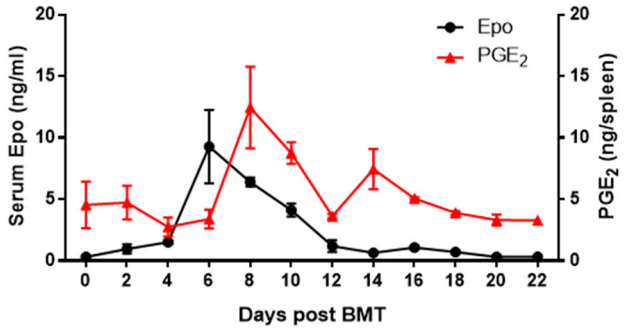
Epo
PGE2
Serum Epo (ng/ml)
PGE2 (ng/spleen)
Days post BMT

C

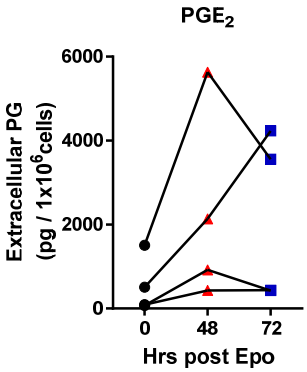
PGE2
Extracellular PG
(pg / 1x10^6cells)
Hrs post Epo

D

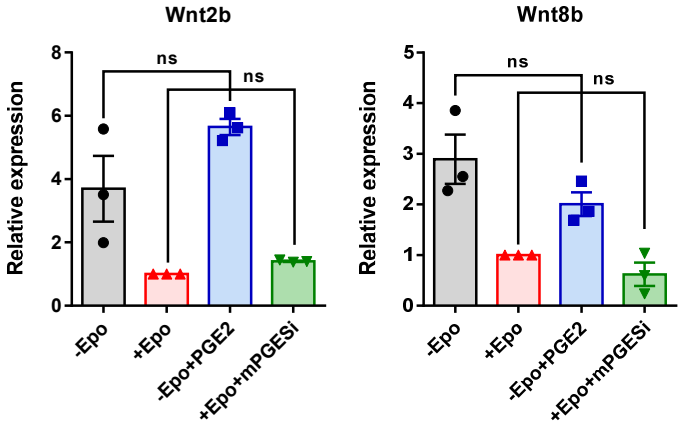
Wnt2b
Wnt8b
Relative expression
ns
-Epo
+Epo
-Epo+PGE2
+Epo+mPGESi

E

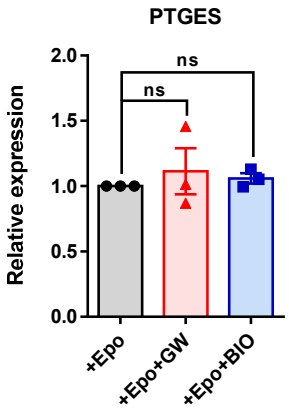
PTGES
Relative expression
2.0
1.5
1.0
0.5
0.0
ns
ns
+Epo
+Epo+GW
+Epo+BIO

F

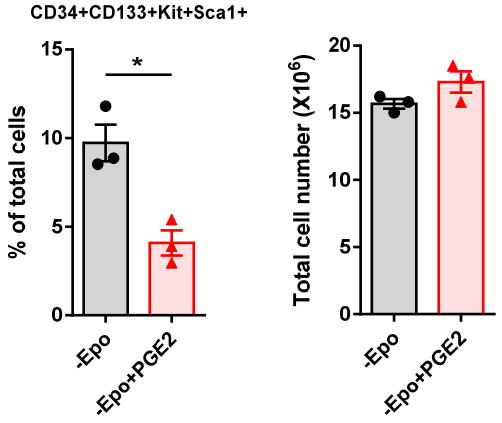
CD34+CD133+Kit+Sca1+
% of total cells
15
10
5
0
*
-Epo
-Epo+PGE2
Total cell number (X10^6)
20
15
10
5
0
-Epo
-Epo+PGE2

G

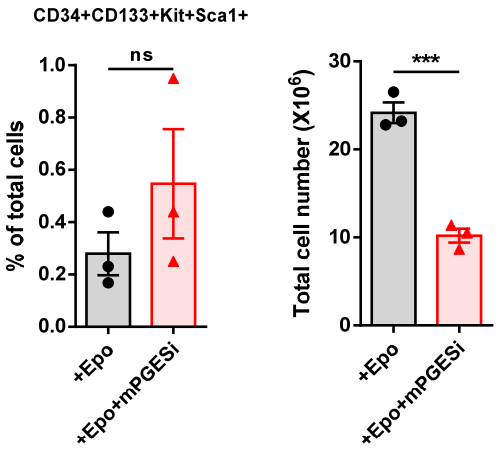
CD34+CD133+Kit+Sca1+
% of total cells
1.0
0.8
0.6
0.4
0.2
0.0
ns
+Epo
+Epo+mPGESi
Total cell number (X10^6)
30
20
10
0
***
+Epo
+Epo+mPGESi

H

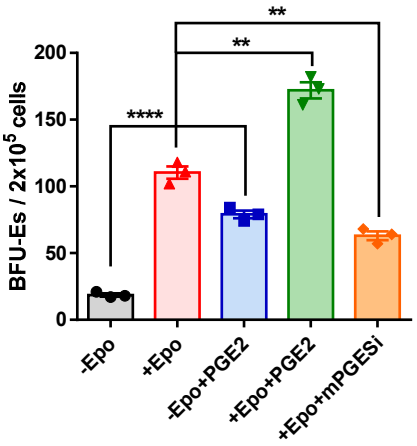
BFU-Es / 2x10^5 cells
200
150
100
50
0
**
**
****
-Epo
+Epo
-Epo+PGE2
+Epo+PGE2
+Epo+mPGESi

I

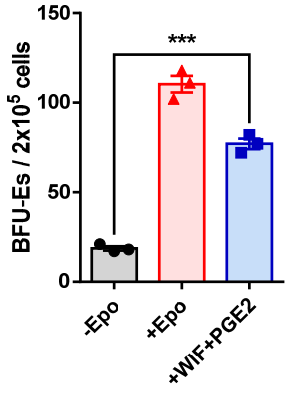
BFU-Es / 2x10^5 cells
150
100
50
0
***
-Epo
+Epo
+WIF+PGE2

Figure **2-7**: **Epo-dependent macrophage derived PGE_2 signaling enhances SEP differentiation.**

(A). LC-MS/MS analysis of extracellular PGE_2 (left Y axis) and mRNA expression of PTGES (right Y axis) in mouse BMDMs at the indicated time points before and after Epo treatment. One-way ANOVA followed by Dunnett's multiple comparisons. Data represent means ± SEM. ** p< 0.01, *** p< 0.001, **** p< 0.0001. * represent P values of comparisons between indicated time points and 0 time point. Red stars*, PTGES. Black stars*, PGE_2. n=3 per time point.

(B). ELISA analysis of serum Epo and spleen PGE_2 on indicated days after BMT. 500,000 unfractionated bone marrow cells were transplanted to C57BL/6 recipients. For each time point, n=3 mice per group.

(C). LC-MS/MS analysis of extracellular PGE_2 of human BMDMs on the indicated time points before and after Epo treatment. Student t-test (2-tailed). Data represent means ± SEM.

(D). mRNA expression of Wnt2b (left) and Wnt8a (right) in BMDMs treated with Epo, PGE_2 or mPGESi as indicated for 24 hours. Student t-test (2-tailed). Data represent means ± SEM. ns, not significant.

(E). mRNA expression of PTGES in BMDMs treated with Epo, GW or BIO as indicated. Student t-test (2-tailed). Data represent means ± SEM. ns, not significant.

(F and G). Analysis of manipulating PGE_2 signaling in in vitro SEP cultures. (F). SEPs cultured in SEEM were treated ± 50 nM 16,16-dimethyl PGE_2 (PGE_2). Flow cytometry analysis of in vitro cultured SEPs. Percentage of CD34+CD133+KS SEPs in total cell population (Left). Total cell numbers after culture (Right). (G). SEPs were cultured in SEDM ± 10 μM CAY10526 (mPGESi, the PTGES inhibitor). Flow cytometry analysis of in vitro cultured SEPs. Percentage of CD34+CD133+KS SEPs in total cell population (Left). Total cell numbers after culture (Right). Student t-test (2-tailed). Data represent means ± SEM. ns, not significant, * p< 0.05, *** p< 0.001.

(H and I). Stress BFU-E colony assay of in vitro cultured bone marrow cells. Cells were expanded in SEEM and treated with Epo, PGE_2, mPGESi or WIF1 as indicated. Student t-test (2-tailed). Data represent means ± SEM. ** p< 0.01, *** p< 0.001, **** p< 0.0001.

2.4 Discussion

In contrast to steady state erythropoiesis, stress erythropoiesis is not a continuous process. Progenitor cells proliferate in the spleen and then synchronously differentiate to generate a wave of new erythrocytes. Furthermore, it takes 21 days before a second wave of erythrocytes can be generated[8]. Precise regulation of the proliferation and differentiation of SEPs is required to generate enough erythrocytes to maintain homeostasis. Here we have identified a novel paradigm where Epo produced by the kidney alters signals produced by the splenic niche to induce differentiation. Macrophage-derived canonical Wnt ligands increase at the early stage of stress erythropoiesis. These signals in combination with previously identified factors, SCF, BMP4, GDF15 and Hedgehog, drive the efficient proliferation of immature SEPs. These observations fit previous data showing that BMP and Wnt dependent transcription factors work in concert with lineage specific transcription factors during regeneration[41]. Epo acts on the splenic niche to switch the predominant niche signal from proliferation to differentiation. Niche macrophages produce lipid messengers in response to Epo. Increased Δ^{12}-PGJ_2 production activates PPARγ activity, which inhibits the expression of canonical Wnts and decreases proliferation. Subsequently, increased PGE_2 production promotes differentiation. The central player in this transition to differentiation is Epo signaling, which orchestrates arachidonic acid metabolism in macrophages to generate distinct bioactive eicosanoids (Figure 2-8).

These data also underscore the key role of macrophages in the niche. The correlation between macrophages and erythroid progenitor cells has been intensively studied since EBIs were first reported by Marcel Bessis[42-45]. Depletion of macrophages severely compromises stress erythropoiesisin vitro and in vivo[5, 9, 11]. The splenic niche expands with the proliferation of SEPs. Anemic stress induces pro-inflammatory signals that induce tissue resident red pulp macrophages to recruit monocytes into the spleen. Lineage tracing analysis showed that the recruited

monocytes contribute to the majority of the EBIs. These monocytes mature in concert with the SEPs. Immature SEPs are present in EBIs containing a central macrophage expressing more monocyte-like markers, while late stage progenitors interact with EBIs containing cells expressing red-pulp macrophage markers[10, 23]. These data coupled with our findings suggest that there is coordinate regulation of niche development, the expansion and differentiation of SEPs and the expression of Epo in the kidney, which ensures that the timing of niche maturation and expansion of SEP populations is optimal to generate erythrocytes to maintain homeostasis.

Recent work from Li et al. showed that EBI niche macrophages are characterized by their expression of EpoR[13]. Our data are consistent with those observations and suggest that Epo dependent signaling in EBIs plays a key role in regulating proliferation and differentiation of SEPs. However, this observation also points to the potential for aberrant EpoR signaling in macrophages to contribute to the pathology of hematological disease. Expression of the $Jak2^{V617F}$ protein in myeloid cells causes erythrocytosis and expansion of EBIs in the splenic niche suggesting that enhanced EpoR signaling in macrophages contributes to the development of myeloproliferative disease[46]. This role for pathological macrophage signals was further demonstrated when depletion of macrophages was shown to alleviate the erythrocytosis in a murine model of Polycythemia[9, 11]. These defects in regulation by niche macrophages is not limited to over production of erythrocytes. The anemia in murine beta-thalassemia model ($Hbb^{th3/+}$ mice) is characterized by inefficient erythropoiesis and the accumulation of immature erythroid progenitors. Depletion of macrophages with clodronate liposomes ameliorates the disease suggesting that the inefficient erythropoiesis in $Hbb^{th3/+}$ mice results from improper macrophages dependent regulation of differentiation[11]. These data highlight the crucial role of the macrophages in the EBI niche and underscore the potential for manipulating the niche as a treatment for anemia and polycythemia.

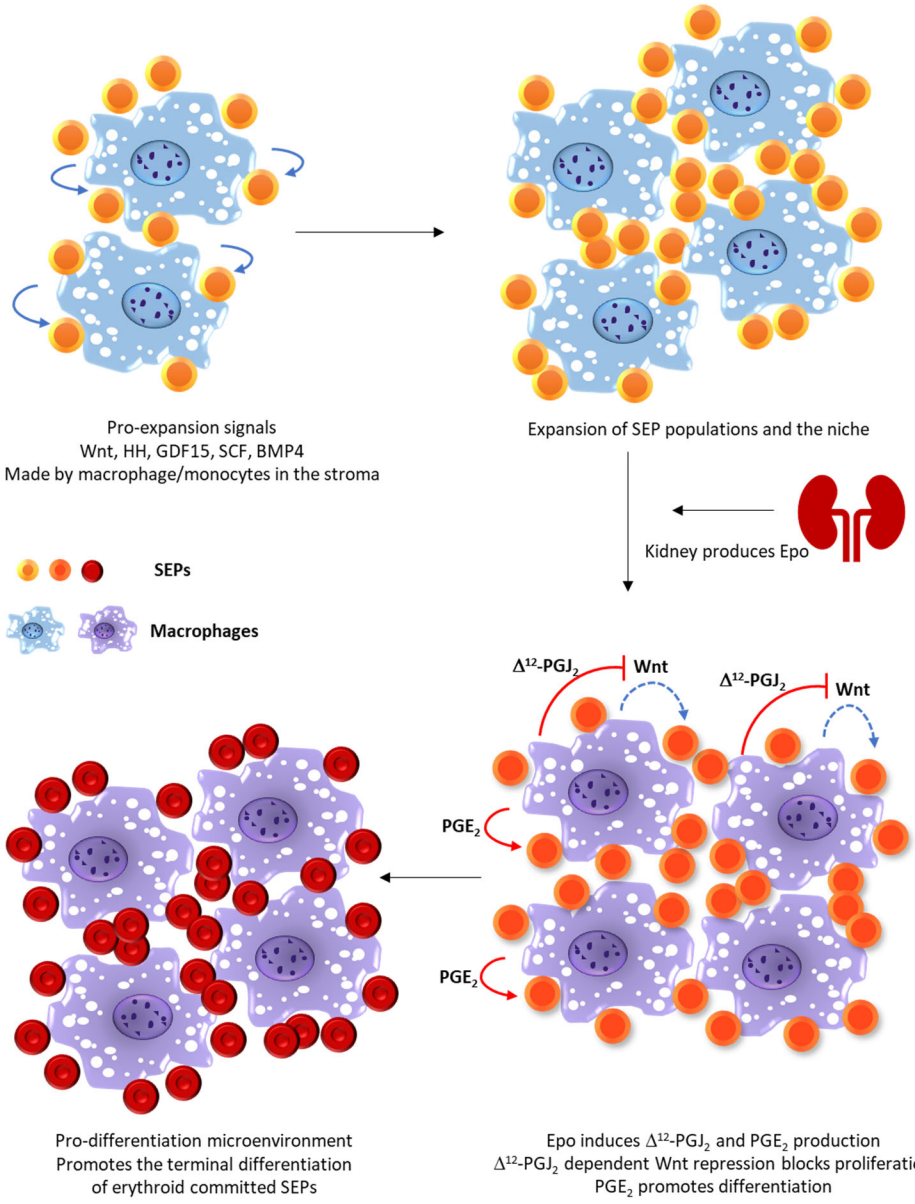

Figure **2-8**: **Schematic of Epo dependent microenvironmental signaling switch during stress erythropoiesis.**

2.5 References

1. Bresnick EH, Hewitt KJ, Mehta C, et al. Mechanisms of erythrocyte development and regeneration: implications for regenerative medicine and beyond. *Development.* 2018;145(1):

2. Nandakumar SK, Ulirsch JC and Sankaran VG. Advances in understanding erythropoiesis: evolving perspectives. *British journal of haematology.* 2016;173(2):206-218.

3. Paulson RF, Shi L and Wu DC. Stress erythropoiesis: new signals and new stress progenitor cells. *Curr Opin Hematol.* 2011;18(3):139-145.

4. Harandi OF, Hedge S, Wu DC, McKeone D and Paulson RF. Murine erythroid short-term radioprotection requires a BMP4-dependent, self-renewing population of stress erythroid progenitors. *J Clin Invest.* 2010;120(12):4507-4519.

5. Xiang J, Wu DC, Chen Y and Paulson RF. In vitro culture of stress erythroid progenitors identifies distinct progenitor populations and analogous human progenitors. *Blood.* 2015;125(11):1803-1812.

6. Lenox LE, Perry JM and Paulson RF. BMP4 and Madh5 regulate the erythroid response to acute anemia. *Blood.* 2005;105(7):2741-2748.

7. Perry JM, Harandi OF and Paulson RF. BMP4, SCF, and hypoxia cooperatively regulate the expansion of murine stress erythroid progenitors. *Blood.* 2007;109(10):4494-4502.

8. Perry JM, Harandi OF, Porayette P, et al. Maintenance of the BMP4-dependent stress erythropoiesis pathway in the murine spleen requires hedgehog signaling. *Blood.* 2009;113(4):911-918.

9. Chow A, Huggins M, Ahmed J, et al. CD169(+) macrophages provide a niche promoting erythropoiesis under homeostasis and stress. *Nature medicine.* 2013;19(4):429-436.

10. Liao C, Prabhu KS and Paulson RF. Monocyte-derived macrophages expand the murine stress erythropoietic niche during the recovery from anemia. *Blood.* 2018;132(24):2580-2593.

11. Ramos P, Casu C, Gardenghi S, et al. Macrophages support pathological erythropoiesis in polycythemia vera and beta-thalassemia. *Nature medicine.* 2013;19(4):437-445.

12. Seu KG, Papoin J, Fessler R, et al. Unraveling Macrophage Heterogeneity in Erythroblastic Islands. *Frontiers in immunology.* 2017;8(1140.

13. Li W, Wang Y, Zhao H, et al. Identification and transcriptome analysis of erythroblastic island macrophages. *Blood.* 2019;134(5):480-491.

14. Paulson RF. Epo receptor marks the spot. *Blood.* 2019;134(5):413-414.

15. Bennett LF, Liao C, Quickel MD, et al. Inflammation induces stress erythropoiesis through heme-dependent activation of SPI-C. *Science signaling.* 2019;12(598):

16. Boulter L, Govaere O, Bird TG, et al. Macrophage-derived Wnt opposes Notch signaling to specify hepatic progenitor cell fate in chronic liver disease. *Nature medicine.* 2012;18(4):572-579.

17. Sato N, Meijer L, Skaltsounis L, Greengard P and Brivanlou AH. Maintenance of pluripotency in human and mouse embryonic stem cells through activation of Wnt signaling by a pharmacological GSK-3-specific inhibitor. *Nature medicine.* 2004;10(1):55-63.

18. Hsieh JC, Kodjabachian L, Rebbert ML, et al. A new secreted protein that binds to Wnt proteins and inhibits their activities. *Nature.* 1999;398(6726):431-436.

19. Behrens J, von Kries JP, Kuhl M, et al. Functional interaction of beta-catenin with the transcription factor LEF-1. *Nature.* 1996;382(6592):638-642.

20. Schaefer KN and Peifer M. Wnt/Beta-Catenin Signaling Regulation and a Role for Biomolecular Condensates. *Developmental cell.* 2019;48(4):429-444.

21. Brault V, Moore R, Kutsch S, et al. Inactivation of the beta-catenin gene by Wnt1-Cre-mediated deletion results in dramatic brain malformation and failure of craniofacial development. *Development.* 2001;128(8):1253-1264.

22. Ventura A, Kirsch DG, McLaughlin ME, et al. Restoration of p53 function leads to tumour regression in vivo. *Nature.* 2007;445(7128):661-665.

23. Hao S, Xiang J, Wu DC, et al. Gdf15 regulates murine stress erythroid progenitor proliferation and the development of the stress erythropoiesis niche. *Blood advances.* 2019;3(14):2205-2217.

24. Kenny PA, Enver T and Ashworth A. Receptor and secreted targets of Wnt-1/beta-catenin signalling in mouse mammary epithelial cells. *BMC cancer.* 2005;5(3.

25. Nairz M, Sonnweber T, Schroll A, Theurl I and Weiss G. The pleiotropic effects of erythropoietin in infection and inflammation. *Microbes and infection.* 2012;14(3):238-246.

26. Nairz M, Schroll A, Moschen AR, et al. Erythropoietin contrastingly affects bacterial infection and experimental colitis by inhibiting nuclear factor-kappaB-inducible immune pathways. *Immunity.* 2011;34(1):61-74.

27. Luo B, Gan W, Liu Z, et al. Erythropoeitin Signaling in Macrophages Promotes Dying Cell Clearance and Immune Tolerance. *Immunity.* 2016;44(2):287-302.

28. Moldes M, Zuo Y, Morrison RF, et al. Peroxisome-proliferator-activated receptor gamma suppresses Wnt/beta-catenin signalling during adipogenesis. *The Biochemical journal.* 2003;376(Pt 3):607-613.

29. Vallee A and Lecarpentier Y. Crosstalk Between Peroxisome Proliferator-Activated Receptor Gamma and the Canonical WNT/beta-Catenin Pathway in Chronic Inflammation and Oxidative Stress During Carcinogenesis. *Frontiers in immunology.* 2018;9(745.

30. Rajakariar R, Hilliard M, Lawrence T, et al. Hematopoietic prostaglandin D2 synthase controls the onset and resolution of acute inflammation through PGD2 and 15-deoxyDelta12 14 PGJ2. *Proceedings of the National Academy of Sciences of the United States of America.* 2007;104(52):20979-20984.

31. Forman BM, Tontonoz P, Chen J, et al. 15-Deoxy-delta 12, 14-prostaglandin J2 is a ligand for the adipocyte determination factor PPAR gamma. *Cell.* 1995;83(5):803-812.

32. Shiraki T, Kamiya N, Shiki S, et al. Alpha,beta-unsaturated ketone is a core moiety of natural ligands for covalent binding to peroxisome proliferator-activated receptor gamma. *The Journal of biological chemistry.* 2005;280(14):14145-14153.

33. Matsushita N, Aritake K, Takada A, et al. Pharmacological studies on the novel antiallergic drug HQL-79: II. Elucidation of mechanisms for antiallergic and antiasthmatic effects. *Japanese journal of pharmacology.* 1998;78(1):11-22.

34. Sakamoto J, Kimura H, Moriyama S, et al. Activation of human peroxisome proliferator-activated receptor (PPAR) subtypes by pioglitazone. *Biochemical and biophysical research communications.* 2000;278(3):704-711.

35. Wright HM, Clish CB, Mikami T, et al. A synthetic antagonist for the peroxisome proliferator-activated receptor gamma inhibits adipocyte differentiation. *The Journal of biological chemistry.* 2000;275(3):1873-1877.

36. Funk CD. Prostaglandins and leukotrienes: advances in eicosanoid biology. *Science.* 2001;294(5548):1871-1875.

37. Durand EM and Zon LI. Newly emerging roles for prostaglandin E2 regulation of hematopoiesis and hematopoietic stem cell engraftment. *Current opinion in hematology.* 2010;17(4):308-312.

38. Goessling W, North TE, Loewer S, et al. Genetic interaction of PGE2 and Wnt signaling regulates developmental specification of stem cells and regeneration. *Cell.* 2009;136(6):1136-1147.

39. Nocka KH, Ottman OG and Pelus LM. The role of marrow accessory cell populations in the augmentation of human erythroid progenitor cell (BFU-E) proliferation by prostaglandin E. *Leukemia research.* 1989;13(7):527-534.

40. Pelus LM and Hoggatt J. Pleiotropic effects of prostaglandin E2 in hematopoiesis; prostaglandin E2 and other eicosanoids regulate hematopoietic stem and progenitor cell function. *Prostaglandins & other lipid mediators.* 2011;96(1-4):3-9.

41. Trompouki E, Bowman TV, Lawton LN, et al. Lineage regulators direct BMP and Wnt pathways to cell-specific programs during differentiation and regeneration. *Cell.* 2011;147(3):577-589.

42. Bessis M. [Erythroblastic island, functional unity of bone marrow]. *Revue d'hematologie.* 1958;13(1):8-11.

43. Chasis JA and Mohandas N. Erythroblastic islands: niches for erythropoiesis. *Blood.* 2008;112(3):470-478.

44. Manwani D and Bieker JJ. The erythroblastic island. *Current topics in developmental biology.* 2008;82(23-53.

45. Mohandas N and Chasis JA. The erythroid niche: molecular processes occurring within erythroblastic islands. *Transfusion clinique et biologique : journal de la Societe francaise de transfusion sanguine.* 2010;17(3):110-111.

46. Wang J, Hayashi Y, Yokota A, et al. Expansion of EPOR-negative macrophages besides erythroblasts by elevated EPOR signaling in erythrocytosis mouse models. *Haematologica.* 2018;103(1):40-50.

47. Cui Y, Riedlinger G, Miyoshi K, et al. Inactivation of Stat5 in mouse mammary epithelium during pregnancy reveals distinct functions in cell proliferation, survival, and differentiation. *Molecular and cellular biology.* 2004;24(18):8037-8047.

48. Bennett LF, Liao C and Paulson RF. Stress Erythropoiesis Model Systems. *Methods in molecular biology.* 2018;1698(91-102.

Chapter 3

PERK and mTORC1 Signaling Pathways Regulated Protein Translation Promotes Differentiation of Stress Erythroid Progenitors

Abstract

Stress erythropoiesis is a process that rapidly generates large numbers of erythrocytes in response to anemic stress. The rapid proliferation and synchronous differentiation of stress erythroid progenitors (SEPs) requires robust translational control to support the rapid cell growth and the large-scale production of hemoglobin. However, the underlying mechanisms of translational regulation remain elusive. The protein kinase RNA-like endoplasmic reticulum kinase (PERK) is a eukaryotic translation-initiation factor 2 alpha (eIF2α) kinase that regulates global protein synthesis in response to ER stress. Here we show a novel role of PERK in regulating erythroid differentiation. Previously, we showed that Epo induced the production of PGE_2 by macrophages in the niche. And PGE_2 promoted the differentiation of SEPs. Here we show that PGE_2 acts by mobilizing intracellular Ca^{2+} stores, which activates the PERK signaling pathway. The ultimate target of PERK signaling is the activation of the mTORC1 complex. Global protein synthesis rate was dramatically increased in SEPs through PERK induced mTORC1 activation. The increased protein translation fuels the SEP differentiation, which restores erythropoietic homeostasis.

3.1 Introduction

Tissue oxygenation relies on efficient oxygen transport through erythrocytes. Mature erythrocytes have the average lifespan of 120 days. Under homeostatic conditions, about 1% erythrocytes are recycled through phagocytosis and replaced by new erythrocytes daily[1]. This dynamic process maintains optimal erythrocyte concentration and oxygen delivery. Stress conditions like low oxygen or anemia induces an adaptive response, stress erythropoiesis. In mice, stress erythropoiesis mainly occurs in extramedullary sites such as spleen and liver[2,3,4]. Steady state erythropoiesis undergoes a relatively long cell fate decision path in the hematopoietic hierarchy[1]. In contrast, stress erythropoiesis shortens the process by generating a unique erythroid lineage committed progenitor population, the stress erythroid progenitors (SEPs), directly from short term reconstituting hematopoietic stem cells (ST-HSCs, CD34+Kit+Sca1+Lin-)[2,5,6]. The SEPs respond to a distinct series of signals, including bone morphogenetic protein 4 (BMP4), Hedgehog, stem cell factor (SCF), growth and differentiation factor 15 (GDF15), canonical Wnts, prostaglandin E_2 (PGE_2) and Erythropoietin (Epo)[2,7,8,9]. Orchestrated by precise coordination of different signals, SEPs efficiently replenish the blood system with new erythrocytes and alleviate tissue hypoxia. First, the most immature CD34+CD133+Kit+Sca1+ SEP population expands rapidly. Despite being erythroid restricted, they maintain their ability of self-renewal and express many stem cell markers. This immature population then gives rise to a transition population, CD34-CD133-Kit+Sca1+ SEPs, in response to Epo and other transition signals. The transition SEPs continue to differentiate and generate CD34-CD133-Kit+Sca1- stress BFU-E progenitors, which further mature into new erythrocytes. The high rate of generating new erythrocytes in stress erythropoiesis suggests a hyperactive cell division process, which requires increased protein translation rate. Therefore, appropriate translational regulations are crucial for stress erythropoiesis.

In response to stress, including hypoxia, iron deficiency, starvation and viral infection, an important signaling network termed the integrated stress response (ISR) is activated to restore cellular homeostasis. Activation of ISR leads to phosphorylation of eIF2α at Ser-51, which inhibits eIF2-GTP-Met-tRNA$_i^{Met}$ ternary complex formation and results in reduced initiation of global translation[10]. However, phosphorylated eIF2α (P-eIF2α) selectively promotes translation of mRNAs contain upstream open reading frames (uORFs) in the 5'-untranslated region (5'-UTR), such as activating transcription factor 4 (ATF4)[11]. ATF4 acts as main effector of ISR to induces the expression of genes involved in cell survival and stress adaptation. Timely termination of ISR, which maintains long-term homeostasis, is also required, since prolonged phosphorylation of eIF2α induces apoptosis. ISR is embedded with a negative feedback mechanism as ATF4 also promotes the expression of growth arrest and DNA damage-inducible protein-34 (GADD34), which regulates the dephosphorylation of eIF2α[12]. Therefore, cells are able to resume normal protein synthesis once stresses are resolved. The dual capability of attenuation and restoration of protein synthesis is the basic mechanism of the ISR. There are four eIF2α kinases that govern distinct environmental stresses in the ISR: Protein kinase RNA-like endoplasmic reticulum kinase (PERK), double-stranded RNA-dependent protein kinase (PKR), heme-regulated eIF2α kinase (HRI), and general control non-derepressible 2 (GCN2). PERK is responsible for ER stress which could be induced by various stimuli including hypoxia, increased reactive oxygen species and disturbance of Calcium balance[13]. Disruption of ER lumen environment leads to increased unfolded and misfolded proteins, which induced PERK dependent unfolded protein response (UPR). UPR reduces the protein load in ER through P-eIF2α/ATF4 mediated global translation repression and cell cycle arrest[14]. Also, UPR promotes ER abundance and potentiates ER protein folding capacity to help cells recover from the stress. Intriguingly, it has been reported that PERK/eIF2α/ATF4 signaling pathway implements cytoprotection function

by activating mTORC1, which promotes protein translation and cell survival, during chronic ER stress[15].

Here, we identified PERK as an important mediator in regulating the rapid erythroid differentiation during stress erythropoiesis. In response to Epo, PERK is activated by ER Ca^{2+} depletion. The increased PERK activity promotes the protein translation by maintaining high mTORC1 activity in SEPs. As a result, the SEP pool is rapidly expanded through active cell division, which benefits from the efficient and precise translational regulation.

3.2 Materials and methods

Mice

C57BL/6 mice, B6.SJL-*P*tprc^{a} Pepc^{b}/BoyJ mice, B6J.129(Cg)-*Gt(ROSA)16Sor*$^{tm1.1(CAG-cas9*,-EGFP)Fezh}$/J mice (TgCas9-GFP mice) and B6;129-*Gt (ROSA)26Sor*$^{tm1(cre/ERT)Nat}$/J mice (Rosa26-CreERT mice) were purchased from The Jackson Laboratory. ATF4^{tm1Tow}/J mice (referred to as ATF4$^{-/-}$ mice) were a gift from Dr. Tim M. Townes. All strains were back crossed onto C57BL/6 background. C57BL/6 mice with loxP sites flanking exon7-9 of PERK gene (referred to as PERK$^{fl/fl}$ mice) were obtained from Dr. Douglas R. Cavener. Homozygous PERK$^{fl/fl}$ mice were crossed with Rosa26-CreERT mice to generate PERK$^{fl/fl}$;Rosa26-CreERT mutants (referred to as PERK$^{-/-}$ mice). Isolated bone marrow cells were treated with 5μM 4-hydroxytamoxifen (Sigma Aldrich) for 24 hours to induce deletion of PERK *in vitro*. All animal procedures are approved by Institutional Animal Care and Use Committee (IACUC) of the Pennsylvania State University.

Cell culture

Isolated murine bone marrow cells were cultured in stress erythropoiesis expansion media (SEEM) for 5 days and switched to stress erythropoiesis differentiation media (SEDM) for 3 days. SEEM contains Gibco IMDM (Invitrogen) supplemented with 10% fetal bovine serum (Gemini Bio-Products), 1% penicillin-streptomycin, 10 μg/ml insulin, 200 μg/ml transferrin, 2mM L-glutamine, 0.01g/ml bovine serum albumin, 7 μl/L 2-mercaptoethanol, 30 ng/ml GDF15 (Novoprotein), 15 ng/ml BMP4 (R&D systems), 50 ng/ml SCF (Goldbio) and 25 ng/ml SHH (GoldBio). SEDM contains Gibco IMDM, all supplements in SEEM and 3U/ml Epo. Cells were incubated at 2% O_2, 5% CO_2 when cultured in SEDM.

Human bone marrow mononuclear cells (MNCs) (Stemcell Technologies) were thawed at 37°C water according to the Stemcell Technologies instructions. MNCs were enumerated and cell concentrations were adjusted to 5×10^5 cells/mL. MNCs were cultured in SEEM to expand human SEPs and then switched to SEDM to induce differentiation. Recombinant human factors, including 30 ng/ml GDF15 (R&D systems), 15 ng/ml BMP4 (R&D systems), 50 ng/ml SCF (Goldbio) and 25 ng/ml SHH (R&D systems), were supplemented in SEEM for human cell cultures. All other components and supplements were the same as murine SEEM. 3U/ml Epo was supplemented to human SEEM to make human SEDM. All culture conditions and procedures were the same murine stress erythropoiesis cultures.

The PERK inhibitor (GSK2606414) is a gift from Dr. Douglas R. Cavener. All PGE_2 receptor antagonists are used as 10 times of the IC_{50}.

Bone marrow transplant (BMT)

For BMT, PERKfl/fl;Rosa26-CreERT bone marrow cells were isolated and cultured in SEEM with 4-OHT for 24 hours to generate $PERK^{-/-}$ cells. $PERK^{fl/fl}$ cells were also treated with 4-OHT as control. Recipient mice were lethally irradiated (950 cGy) and transplanted with unfractionated or sorted donor bone marrow cells with indicated cell numbers.

Flow cytometry and cell sorting

Cells were collected and labeled with indicated antibodies. A list of antibodies was provided in supplemental Table 3-1. Dead cells were determined by zombie yellow fixable viability dye (BioLegend) staining. LSR-II Fortessa Flow cytometer (BD Biosciences) was used for flow cytometry analysis. All flow cytometry data were analyzed with FlowJo software. Astrios (Becton Dickinson) cell sorter was used for cell sorting.

Table **3-1**: **Flow cytometry antibody list**.

Antibodies	**Fluorochrome**	**Source**	**Catalog No.**
CD34	Alexa Fluor 647	BD	560230
CD133	PE	eBiosciences	12133182
CD133	PE-Cy7	BioLegend	141210
Kit (c-kit)	Brilliant Violet 421	BioLegend	1058282
Sca1 (Ly-6A/E)	PE-Cy7	BioLegend	122514
Sca1 (Ly-6A/E)	FITC	Biolegend	108106
Phospho-S6	Alexa Fluor 647	eBioscience	17900742
Phospho-4EBP1	Alexa Fluor 647	eBioscience	50910742

c-Myc	Alexa Fluor 647	Cell Signaling Technology	13871
ATF4	FITC	Abcam	Ab150236
CD16/32	N/A	Biolegend	101302

Calcium flux flow cytometry

In vitro cultured bone marrow cells were pre-stained with viability dye and SEP markers before processing to Ca^{2+} indicator staining. Cells were resuspended in HBSS with 1% FBS at $5x10^6$ cells/ml. Each 1ml suspension was loaded with 1μl of 4mg/ml Fluo-3 AM (ThermoFisher) and 1μl of 10mg/ml Fura Red AM (ThermoFisher). Cells were incubated at 37 for 30min. Fluo-3 fluorescence was detected by 488 laser with 530/30 filter. The fluorescence signal of Fluo-3 is Ca^{2+} dependent. Fura Red fluorescence was detected by 488 laser with 670/14 filter. The fluorescence signal of Fura Red at Ex/Em 472/657nm is Ca^{2+} independent and serves as dye loading control. The Calcium positive population percentage was calculated as $Calcium^{pos}$ = $Fluo\text{-}3^{pos}$ / ($Fluo\text{-}3^{pos}$ + $Fura\ Red^{pos}$). Baseline (untreated sample) $Calcium^{pos}$ population percentage was subtracted from sample (treated with Epo or PGE_2) $Calcium^{pos}$ population percentage to normalize the results.

CellTrace CFSE cell labeling

Bone marrow cells were isolated and immediately labeled with CellTrace CFSE by following the manufacture instructions (CellTraceTM Cell Proliferation Kits, Invitrogen).

Labeled cells were transplanted into CD45.1 recipients. On indicated days, spleen cells were collected and stained with other cell surface markers before flow cytometry analysis. CFSE were detect by using LSR-II Fortessa Flow cytometer (BD Biosciences) with 488nm laser and 530/30 filter.

Stress BFU-E colony assay

Isolated spleen cells or *in vitro* cultured bone marrow cells were plated in methylcellulose media (M3334, StemCell Technologies). Stress BFU-Es were scored after 5 days incubation. Stress BFU-E culture conditions and stress BFU-E colony enumeration procedures were previously described[50].

Western Blotting

Western blot analysis was performed by using the following primary antibodies: anti-phosphorylated eIF2α (#9721, Cell Signaling Technology) at 1:1000 dilution, anti-total eIF2α (#5324, Cell Signaling Technology) at 1:1000 dilution, anti-phosphorylated PERK (#3179, Cell Signaling Technology) at 1:1000 dilution, anti-total PERK (#3192, Cell Signaling Technology) at 1:1000 dilution, anti-PTGER3 (#ab21227, abcam) at 1:500, anti-β-tubulin (#2146, Cell Signaling Technology) at 1:2000 dilution and anti-β-actin (sc-47778, Santa Cruz Biotechnology) at 1:2000 for overnight at 4°C. Secondary antibody was used at 1:5000 dilution.

CRISPR/Cas9 knockdown of PTGER3

Lentivirus vectors were cloned with sgRNA targeting 5'-TGCTCGTGTCGCGCAGCTACCGG -3' (g1) or 5'- GCTGGCGCTCACCGACTTAGTGG -3' (g2) were purchased from VectorBuilder. TgCas9-GFP BM cells were transduced with lentivirus expressing scramble sgRNA (S), g1 sgRNA or g2 sgRNA. Transduced cells were cultured in SEEM and SEDM as described in cell culture section. The PTGER3 knockdown efficiency was determined by western blot targeting the EP3 receptor protein.

Quantitative reverse transcription PCR (RT-qPCR)

Total RNA was isolated by using TriZol reagent (Invitrogen). Complementary DNA (cDNA) was generated by using the qScript cDNA SuperMix (Quanta Biosciences). qPCR was done by using StepOnePlus Real-Time PCR System (Applied Biosystems). A list of TaqMan probes is provided in supplemental Table 3-2.

Table **3-2**: **TaqMan probe list**.

Gene	**Catalog No.**
18s	Hs99999901_s1
Nrf1	Mm01135606_m1
Nrf2	Mm00477784_m1
Gadd34	Mm01205601_g1
CReP	Mm00551747_m1
CHOP	Mm01135937_g1
Nrf1 (Human)	Hs00602161_m1
Nrf2 (Human)	Hs00975961_g1

Gadd34 (Human)	Hs00169585_m1
CReP (Human)	Hs03044848_m1
CHOP(Human)	Hs00358796_g1
LAT1	Mm00441516_m1
LAT3	Mm01336378_m1
LARS	Mm00506560_m1
CD98	Mm00500521_m1
ASCT2	Mm00436603_m1
SNAT2	Mm00628416_m1
SNAT9	Mm00724649_m1
CAT1	Mm01219063_m1

3.3 Results

Epo/PGE_2 induced intracellular Ca^{2+} increase is required for stress erythropoiesis.

Our previous work demonstrated that Epo induces PGE_2 production in EBI macrophages. The upregulated PGE_2 is the key transition signal that initiates the differentiation of early stage SEPs. When PGE_2 production was blocked by adding the PGE_2 synthase inhibitor in *in vitro* cultures, SEPs showed significantly fewer stress BFU-E formation (see Chapter2, Figure 2-7G). These observations suggest that Epo mediated microenvironmental PGE_2 is required for differentiation of SEPs. However, the underlying mechanisms of PGE_2 action remain largely obscure. There are four PGE_2 receptors, EP1-4. Each of the receptors coupling with distinct G

proteins and activating distinct downstream signaling pathways upon PGE_2 binding. EP1 receptor elevates intracellular Ca^{2+} through coupling with Gq and receptor-activated Ca^{2+} channels (RACC), which leads a calcium influx from extracellular resources. EP3 receptor coupling with Gi and increases inositol 1, 4, 5-trisphosphate (IP3), which causes Ca^{2+} mobilization from ER storage[16]. Both EP2 and EP4 receptor can activate the cyclic adenosine monophosphate (cAMP) and protein kinase A (PKA) signaling pathway via Gs. Whereas EP4 receptor is also able to activate phosphoinositide-3-kinase (PI3K) through coupling with Gi. We first examined the expression level of the four EP receptors in SEPs. EP1 is undetectable in SEPs. EP2, EP3 and EP4 had significantly higher expression in early stage CD34+CD133+Kit+Sca1+ SEPs in compare to the more mature CD34-CD133-Kit+Sca1+ SEPs (Figure 3-1 A-C), indicating that PGE_2 targets the immature SEPs and promotes their differentiation. We tested whether the EP receptor dependent signaling pathways affect stress erythropoiesis by inhibiting each EP receptor. We observed that all EP receptor antagonists were able to repress the formation of stress BFU-Es except EP1 antagonist (Figure 3-1D). In mouse embryo, the emergence of HSCs in AGM depends on the PKA target, cAMP response element-binding protein (CREB), and BMP signaling[17]. As PGE_2 has been demonstrated to play an important role in HSC formation and proliferation, the PGE_2-EP2/EP4 is a potential upstream of PKA-CREB signaling pathway in hematopoietic system. It is important to address the possible role of EP2/EP4 mediated SEP proliferation in further study. Intriguingly, a recent study showed that myeloid-based HSCs have higher intracellular Ca^{2+} in compare to lymphoid-based HSCs. Furthermore, all HSCs contains much lower Ca^{2+} than MPPs and Lin-Sca1-Kit+ committed progenitors, which generate common myeloid, megakaryocyte-erythroid and granulocyte-macrophage progenitors[18]. The low intracellular Ca^{2+} in HSCs protects them from exhaustion. These observations suggest a mechanism that myeloid progenitors require high intracellular Ca^{2+} concentration to remain active, which may also apply to the proliferative SEPs. To explore the hypothesis, we first

examined the intracellular Ca^{2+} levels in cultured SEPs. We found that both Epo and PGE_2 were able to increase intracellular Ca^{2+} levels in SEPs (Figure 3-1E). Intriguingly, PGE_2 rapidly induced the elevation of Ca^{2+} within 2 hours. However, it took 48 hours to detect a significant increase of intracellular Ca^{2+} when cells were treated with Epo. These data are in line with our recent findings that Epo induced PGE_2 production peaks from 48 hours. We next tested whether PGE_2 induced Ca^{2+} through both EP1 and EP3 receptors. EP1 antagonist (SC51322) and EP3 antagonist (L-798,106) were used to block corresponding Ca^{2+} mobilization pathways. We found that both EP1 antagonist and EP3 antagonist were able to significantly block the Ca^{2+} increase in response to both Epo and PGE_2 (Figure 3-1E). Since the SEPs don't express EP1 receptor, the effects of EP1 antagonist must be mediated by its effects on other cells, so we focused on the role of EP3 receptor in regulating Ca^{2+} flux. We extended the investigation to human stress erythropoiesis by using *in vitro* cultured human bone marrow (BM) mononuclear cells. Both the EP3 dependent Ca^{2+} increase and BFU-E formation in response to Epo were observed in human SEP cultures (Figure 3-1F, 3-1G). These observations indicate that differentiation of SEPs require Epo induced elevation of intracellular Ca^{2+} through PGE_2/EP3 signaling pathway.

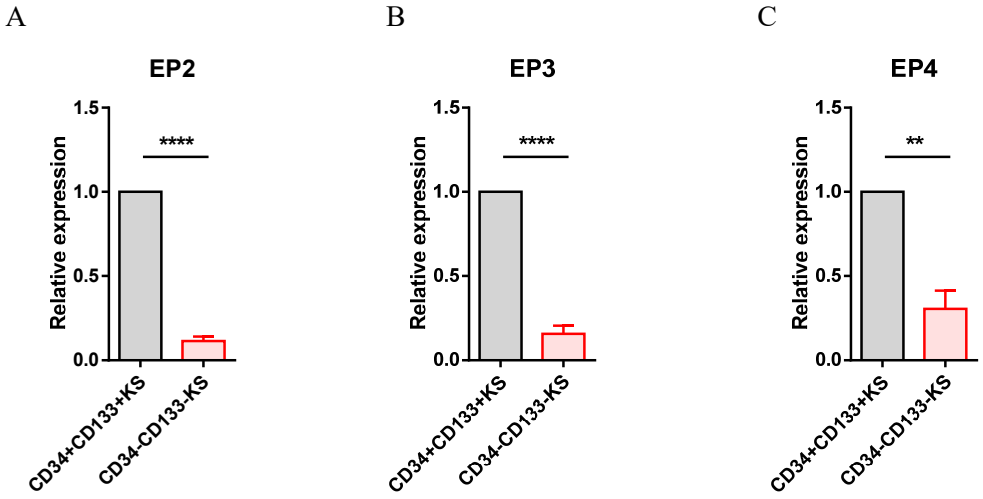

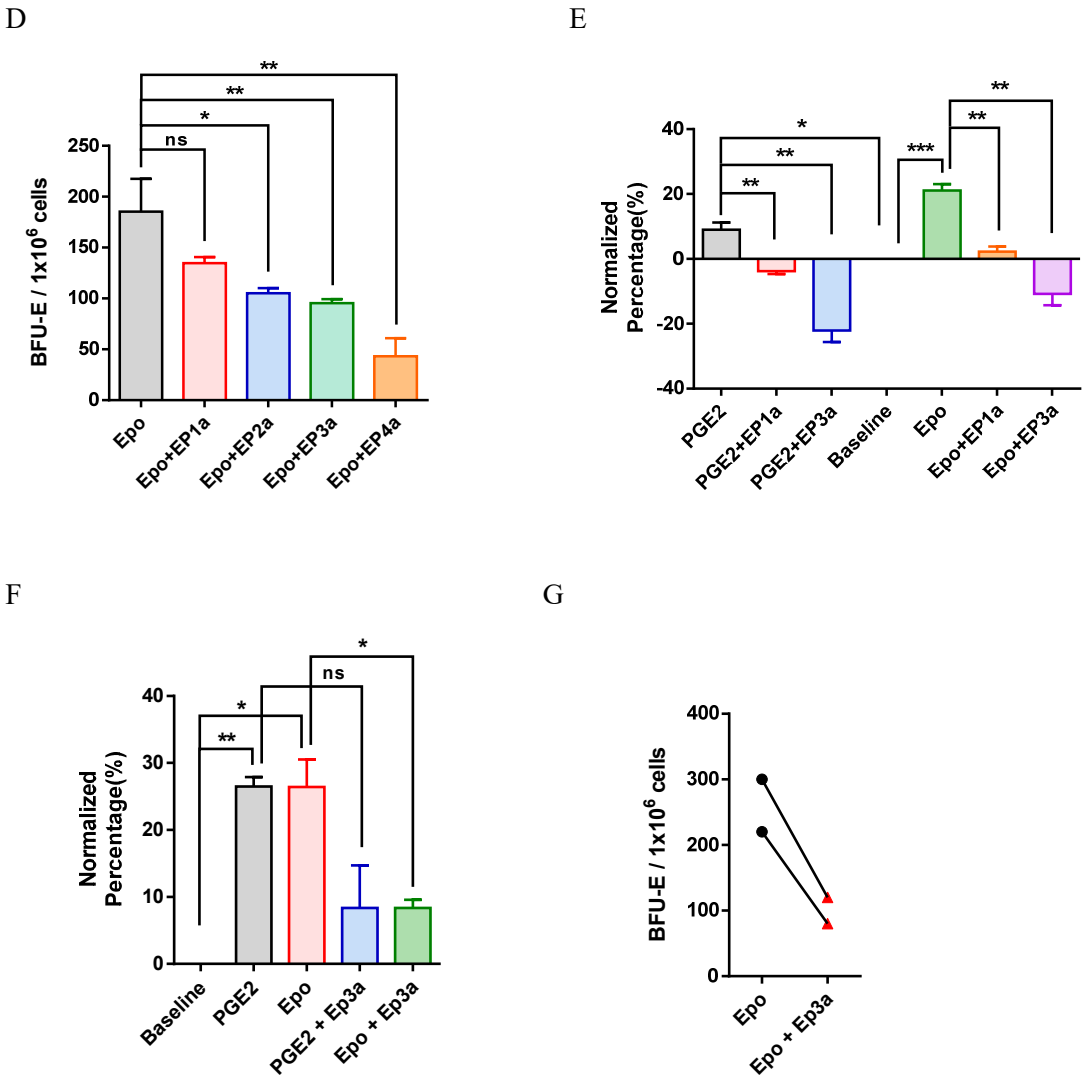

Figure **3-1**: **Epo dependent PGE_2 regulates Ca^{2+} mobilization in SEPs**.

(A-C). mRNA expression of EP receptors in sorted CD34+CD133+Kit+Sca1+ SEPs (CD34+CD133+KS) and CD34-CD133-Kit+Sca1+ SEPs (CD34-CD133-KS). EP2 (A), EP3 (B), EP4 (C). Student t-test (2-tailed). Data represent means ± SEM. ** p< 0.01, **** p< 0.0001.

(D). Stress BFU-E colony assay of mouse SEPs treated with Epo ± EP receptor antagonists. 5μM EP1 antagonist (EP1a, SC51322), 1μM EP2 antagonist (EP2a, AH6809), 1μM EP3 antagonist (EP3a, L-798,106) and 5μM EP4 antagonist (EP4a, AH23848) were supplemented in SEDM as indicated. Student t-test (2-tailed). Data represent means ± SEM. ns, not significant, * p< 0.05, ** p< 0.01.

(E). Flow cytometry analysis of Ca^{2+} positive population in mouse SEPs. Cells were treated with 50nM 16,16-dimethyl PGE_2 (PGE_2) ± EP1a or ± EP3a; Epo ± EP1a or ± EP3a as indicated. SEPs cultured in SEEM were used as baseline. Student t-test (2-tailed). Data represent means ± SEM. * $p< 0.05$, ** $p< 0.01$, *** $p< 0.001$. Ca^{2+} positive populations were gated on Kit+Sca1+.
(F). Flow cytometry analysis of Ca^{2+} positive population in human BM mononuclear cell derived SEPs. Cells were treated with PGE_2 ± EP3a or Epo ± EP3a as indicated. SEPs cultured in SEEM were used as baseline. Student t-test (2-tailed). Data represent means ± SEM. ns, not significant, * $p< 0.05$, ** $p< 0.01$. Ca^{2+} positive populations were gated on Kit+CD133+.
(G). Stress BFU-E colony assay of human SEPs treated with Epo ± EP3a.

Intracellular Ca^{2+} flux activates PERK signaling pathway

PERK kinase is known can be activated by mobilization of ER Ca^{2+} stores in various tissues [19,20]. Our observation that Epo/PGE_2 mobilizes ER Ca^{2+} suggests that PGE_2/EP3 dependent intracellular Ca^{2+} flux may affect PERK activity in SEPs. In order to confirm the increased intracellular Ca^{2+} can activates PERK signaling pathway in SEPs, we sorted out Ca^{2+} positive SEPs and Ca^{2+} negative SEPs from *in vitro* cultures after Epo treatment. We found that PERK/eIF2α/ATF4 target genes were highly correlated with Ca^{2+} positive SEP population (Figure 3-2 A-E). Using phosphorylated eIF2α as an indicator, we observed that EP3 antagonist treatment reduced the Epo/PGE_2 dependent PERK activity (Figure 3-2F, 3-2G). Next, we knocked down EP3 in SEPs by using the CRISPR-Cas9 gene editing system (Figure 3-3A). We observed all PERK/eIF2α/ATF4 target genes were significantly repressed with EP3 knockdown except GADD34 where the decrease was not significant (Figure 3-3 B-F). We observed a similar loss of expression, when EP3 signaling was blocked by an EP3 antagonist (Figure 3-3 I-M). In response to Epo, immature CD34+CD133+Kit+Sca1+ SEPs rapidly acquire the ability to

differentiate and mature into later stage CD34-CD133-Kit+Sca1- stress BFU-E progenitors. Intriguingly, we observed that knock down of EP3 resulted in the accumulation of early stage CD133+Kit+Sca1+ SEPs in the Epo containing SEDM (Figure 3-3G), which led to fewer differentiated stress BFU-Es (Figure 3-3H). Taken together, these observations demonstrate that Epo dependent PGE_2 activates EP3 signaling that leads to Ca^{2+} mobilization from ER to cytoplasm. This increased intracellular Ca^{2+} is able to activate PERK and the corresponding downstream signaling pathway.

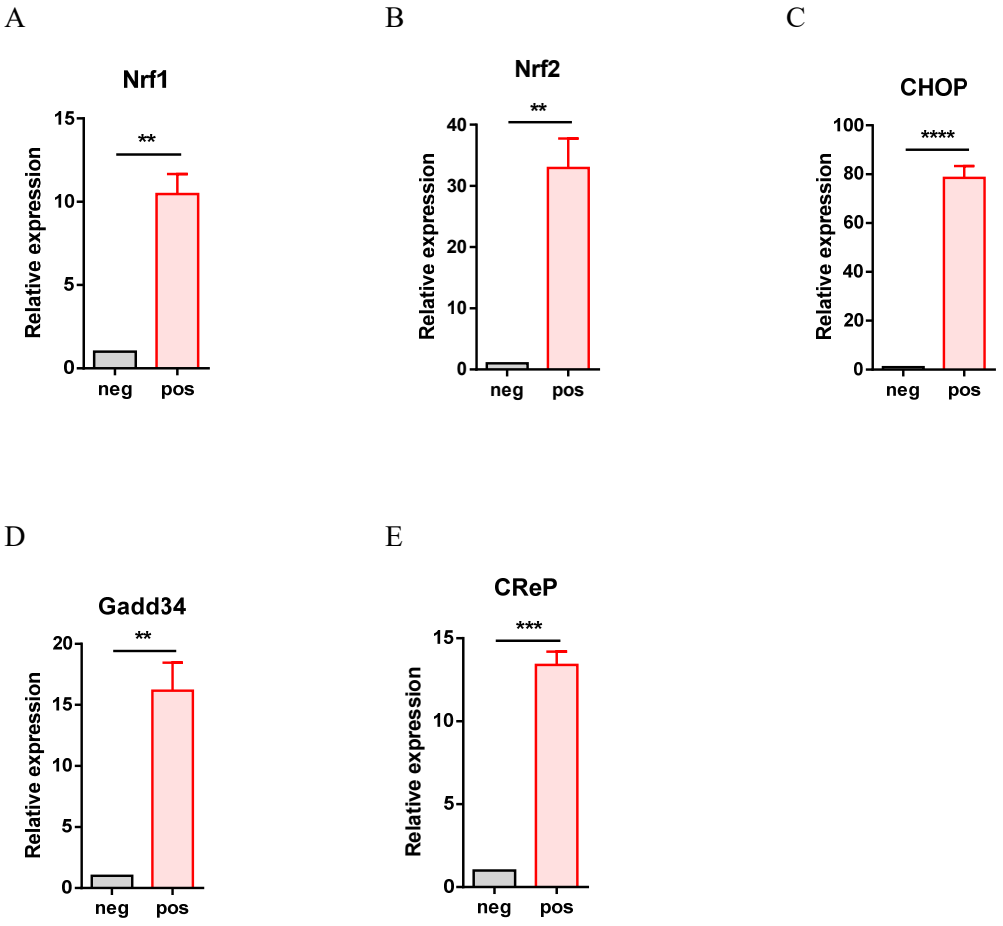

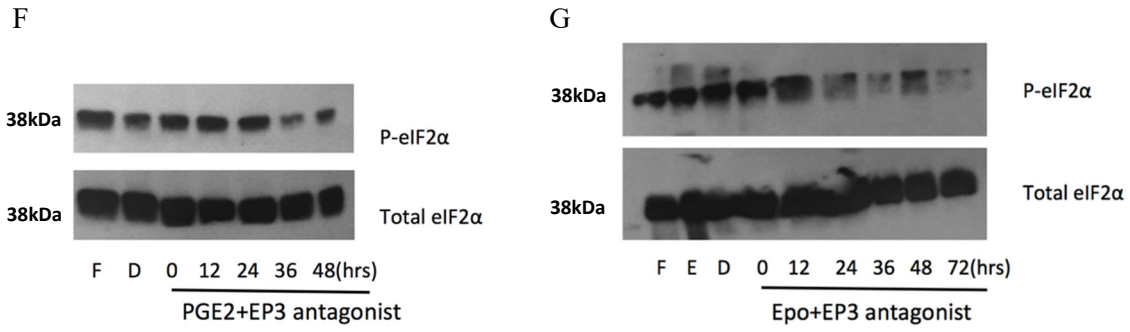

Figure **3-2**: **EP3 dependent Ca^{2+} activity is positive correlated with PERK signaling pathway**.

(A-E). mRNA expression of PERK signaling pathway target genes in sorted Ca^{2+} positive Kit+Sca1+ SEPs (pos) or Ca^{2+} negative Kit+Sca1+ SEPs (neg). Student t-test (2-tailed). Data represent means ± SEM. ** $p< 0.01$, *** $p< 0.001$, **** $p< 0.0001$.

(F). Western blot analysis of P-eIF2α and total eIF2α in *in vitro* cultured BM cells treated with PGE_2 + EP3a for indicated time period. F: fresh BM cells, D: differentiation day 3 BM cells.

(G). Western blot analysis of P-eIF2α and total eIF2α in *in vitro* cultured BM cells treated with Epo + EP3a for indicated time period. F: fresh BM cells, E: expansion day 5 BM cells, D: differentiation day 3 BM cells.

A

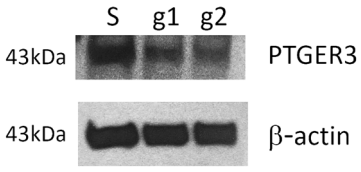
S
g1
g2
43kDa
PTGER3
43kDa
β-actin

B

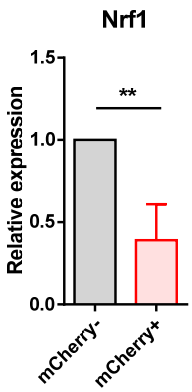
Nrf1
Relative expression
1.5
1.0
0.5
0.0
**
mCherry-
mCherry+

C

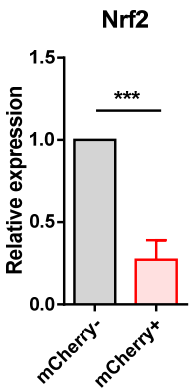
Nrf2
Relative expression
1.5
1.0
0.5
0.0
***
mCherry-
mCherry+

D

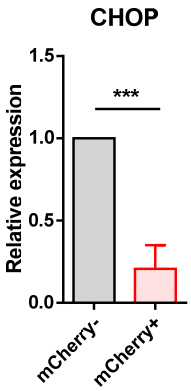
CHOP
Relative expression
1.5
1.0
0.5
0.0
***
mCherry-
mCherry+

E

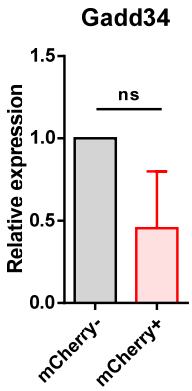
Gadd34
Relative expression
1.5
1.0
0.5
0.0
ns
mCherry-
mCherry+

F

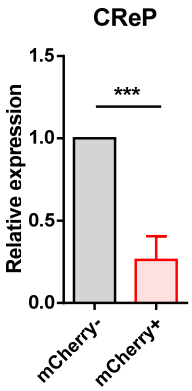
CReP
Relative expression
1.5
1.0
0.5
0.0
***
mCherry-
mCherry+

G

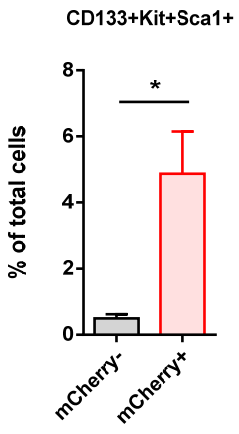
CD133+Kit+Sca1+
% of total cells
8
6
4
2
0
*
mCherry-
mCherry+

H

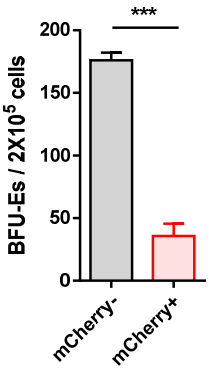
BFU-Es / 2X10^5 cells
200
150
100
50
0
***
mCherry-
mCherry+

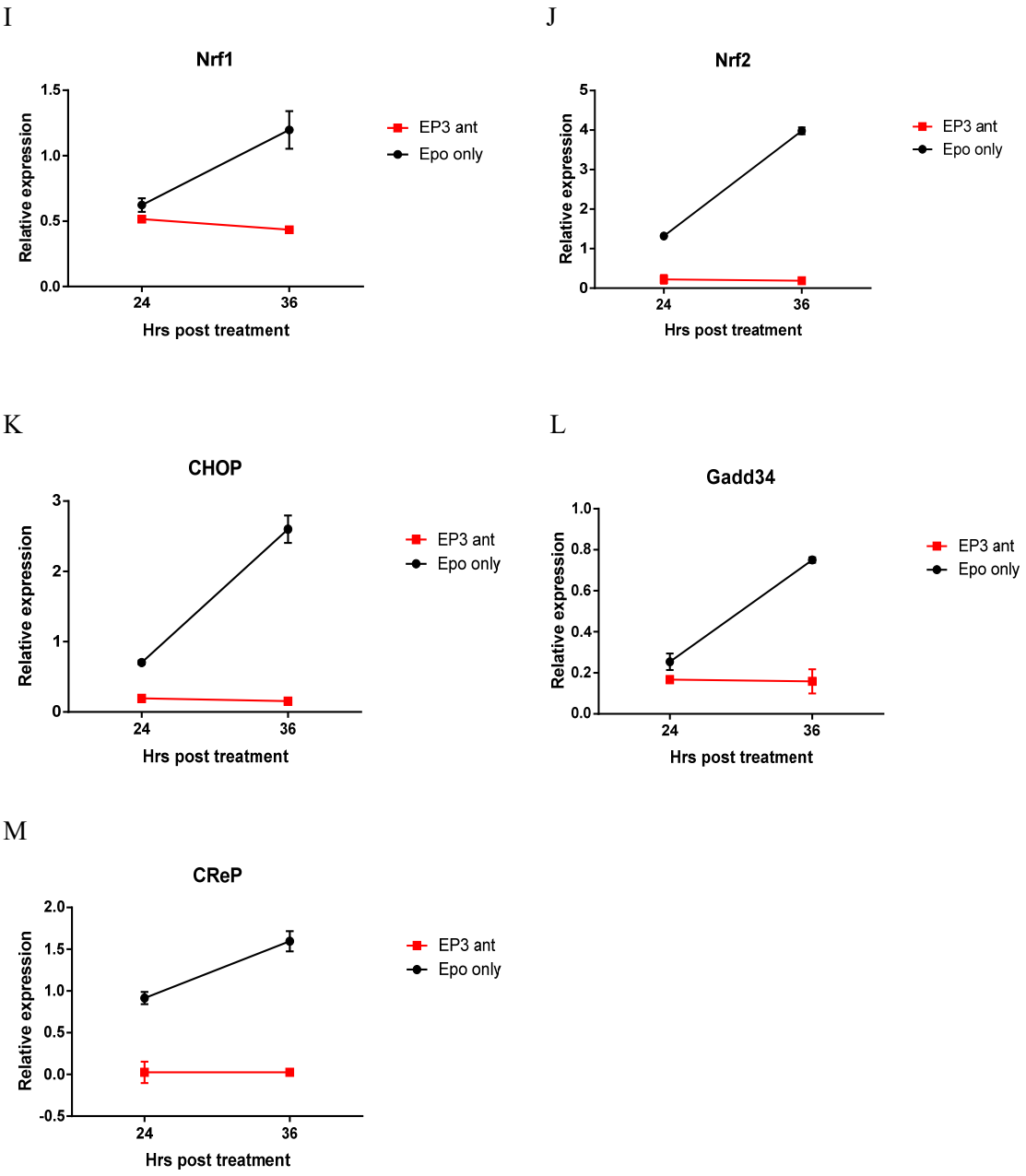

Figure **3-3**: **Perturbation of EP3 receptor leads to reduced PERK signaling pathway activity.**

(A). Western blot analysis of EP3 receptor (PTGER3) knockdown efficiency. S: scramble guide RNA (control), g1: PTGER3 guide RNA1, g2: PTGER3 guide RNA2.

(B -F). mRNA expression of PERK signaling pathway target genes in sorted EP3 receptor knockdown Kit+Sca1+ SEPs (mCherry+) or control Kit+Sca1+ SEPs (mCherry-). Student t-test (2-tailed). Data represent means ± SEM. ns, not significant, ** $p< 0.01$, *** $p< 0.001$.
(G). Flow cytometry analysis of CD133+Kit+Sca1+ population in EP3 knockdown SEPs (mCherry+) and control SEPs (mCherry-). Student t-test (2-tailed). Data represent means ± SEM. * $p< 0.05$.
(H). Stress BFU-E colony assay of sorted EP3 receptor knockdown Kit+Sca1+ SEPs (mCherry+) or control Kit+Sca1+ SEPs (mCherry-). Student t-test (2-tailed). Data represent means ± SEM. *** $p< 0.001$.
(I - M). mRNA expression of PERK signaling pathway target genes in *in vitro* cultured BM cells treated with Epo (Epo only) or Epo + EP3a (EP3 ant) for 24 hours and 36 hours.

PERK signaling is required for SEP differentiation during stress erythropoiesis.

PERK is one of the kinases that implements the ISR[21]. Previous studies found that mutations of several components of the PERK pathway cause defects in erythropoiesis[22,23]. In order to characterize the role of PERK pathway in stress erythropoiesis, we utilized both PERK inhibitor and PERK conditional knockout mice. Similar to blocking EP3 signaling, we observed that SEPs accumulated at early stages (Kit+Sca1+) *in vitro* and failed to differentiate into stress BFU-Es (Figure 3-4A, 3-4B) when cultured in the presence of PERK inhibitor (GSK2606414) in Epo containing SEDM. Consistent with the findings in murine SEP cultures, *in vitro* cultured human BM mononuclear cells showed a similar developmental blockage in response to PERK inhibitor. Notably, human SEPs were specifically blocked in the earliest stage (CD34+CD133+Kit+) and exhibited more severe defects in stress BFU-E formation than murine cultures when treated with PERK inhibitor (Figure 3-4C, 3-4D). When we transplanted 100,000 unfractionated BM cells into lethally irradiated recipients, we found 75% of recipients

transplanted with $PERK^{-/-}$ donor cells were unable to survive (Figure 3-4E). In order to better investigate the mechanisms, we used 500,000 $PERK^{-/-}$ donor cells to improve the survival. Though the recipients were able to survive after bone marrow transplantat (BMT) in this condition, they produced fewer stress BFU-E in comparison to recipients transplanted with $PERK^{fl/fl}$ donor cells (Figure 3-4F). When we genotyped the BFU-Es from $PERK^{-/-}$ group, we found PERK allele were not fully deleted in these BFU-Es (Figure 3-4G). PERK dependent phosphorylation of eIF2α selectively promotes translation of ATF4 in the ISR. ATF4 mutant mice were reported to have anemic phenotypes in embryo and fetal liver. In addition, they exhibited a weak erythroid response to PHZ induced acute hemolytic anemia[22]. Our previous work also showed that ATF4 knockout mice exhibited delayed recovery after BMT. In order to investigate the role of ATF4 in stress erythropoiesis in more detail, we cultured $ATF4^{-/-}$ and control BM cells in SEP cultures. In response to Epo, ATF4 protein increases in SEPs as measured by intracellular flow. This increase is blocked by PERKi (Figure 3-4H), indicating that ATF4 is one of the downstream targets of PERK during stress erythropoiesis. Consistent with the defects observed when PERK is inhibited, $ATF4^{-/-}$ SEPs were blocked at the Kit+Sca1+ stage in SEDM and gave rise to significantly fewer stress BFU-Es (Figure 3-4I, 3-4J). These observations suggest that PERK promotes SEP differentiation in response to Epo through activating the downstream effector ATF4.

A

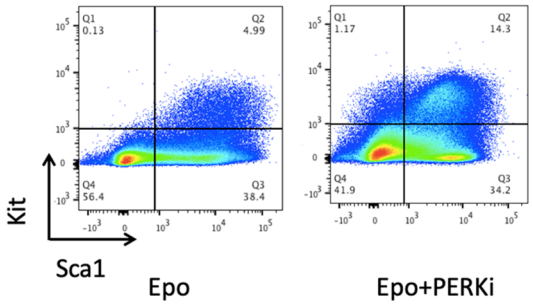
Q1
0.13
Q2
4.99
Q4
56.4
Q3
38.4
Q1
1.17
Q2
14.3
Q4
41.9
Q3
34.2
Kit
Sca1
Epo
Epo+PERKi

B

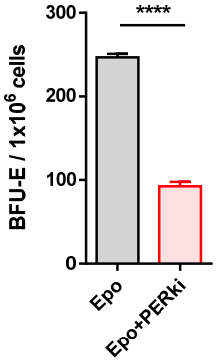
****
BFU-E / 1x10^6 cells
300
200
100
0
Epo
Epo+PERKi

C

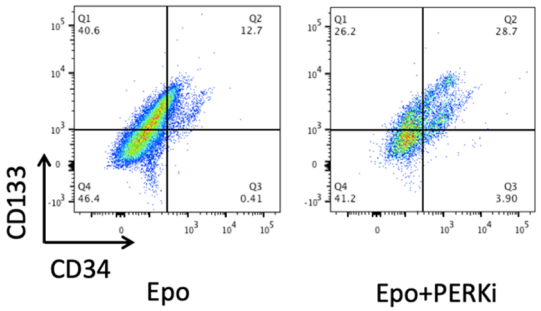
Q1
40.6
Q2
12.7
Q4
46.4
Q3
0.41
Q1
26.2
Q2
28.7
Q4
41.2
Q3
3.90
CD133
CD34
Epo
Epo+PERKi

D

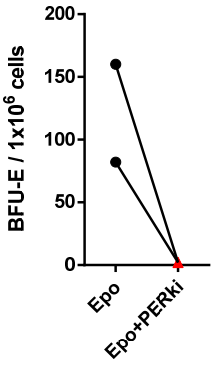
BFU-E / 1x10^6 cells
200
150
100
50
0
Epo
Epo+PERKi

E

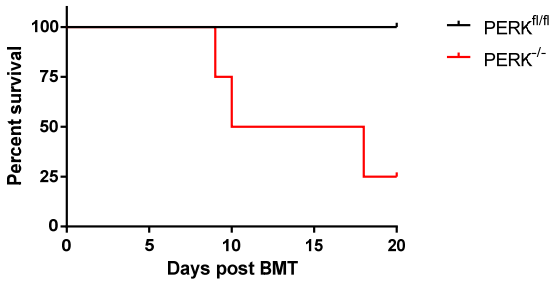
Percent survival
100
75
50
25
0
0
5
10
15
20
Days post BMT
PERK^fl/fl
PERK^-/-

F

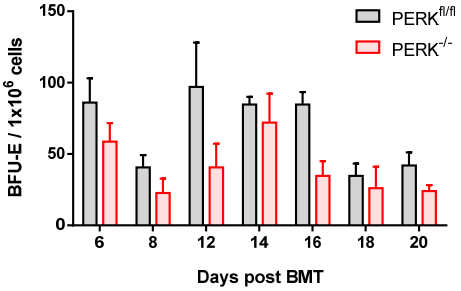
BFU-E / 1x10^6 cells
150
100
50
0
6
8
12
14
16
18
20
Days post BMT
PERK^fl/fl
PERK^-/-

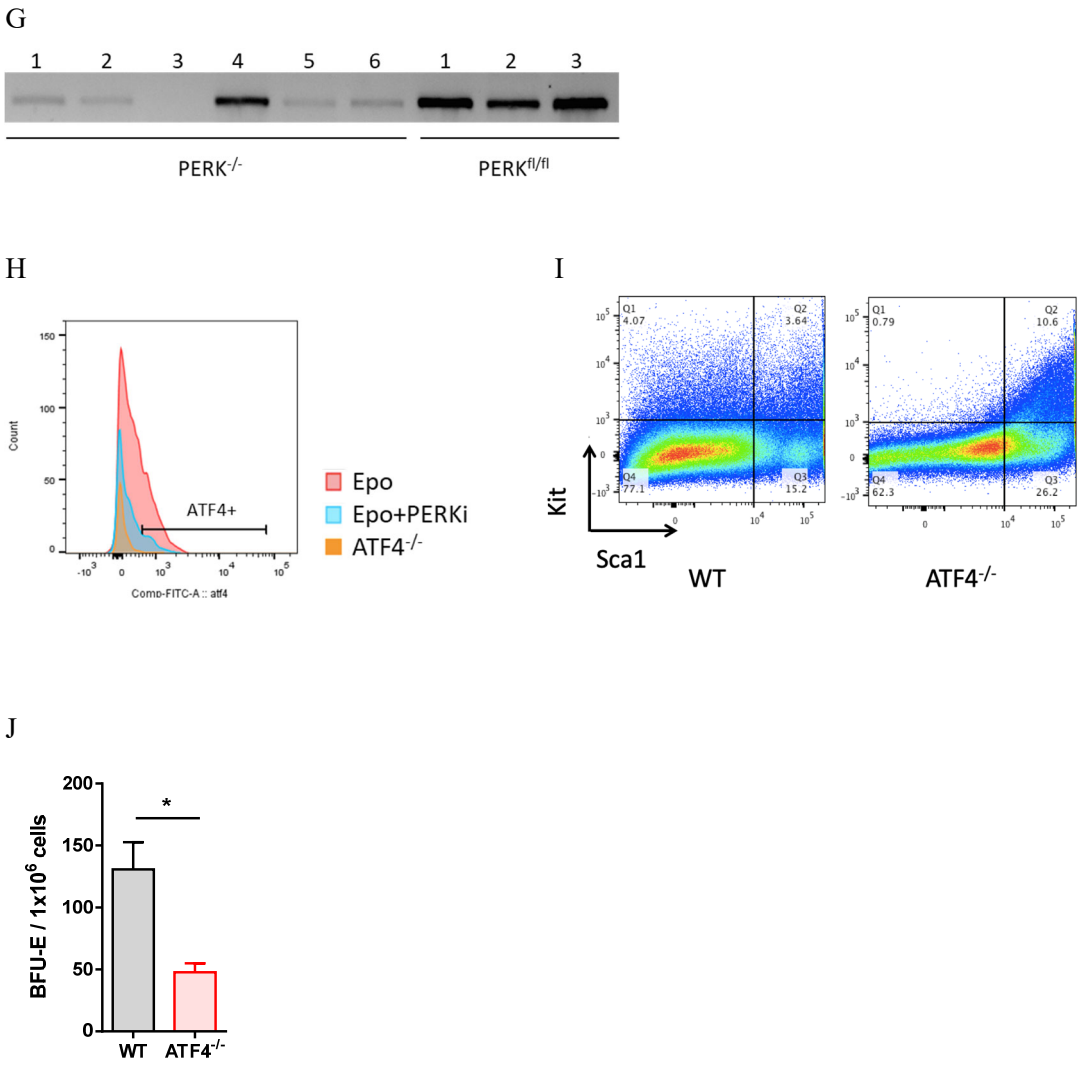

Figure **3-4**: **PERK and ATF4 are required for SEP differentiation.**

(A). Flow cytometry analysis of *in vitro* cultured mouse BM cells treated with Epo ± 1μM PERK inhibitor (PERKi, GSK2606414).

(B). Stress BFU-E colony assay of *in vitro* cultured mouse BM cells treated with Epo ± PERKi. Student t-test (2-tailed). Data represent means ± SEM. *** $p < 0.001$.

(C). Flow cytometry analysis of *in vitro* cultured human mononuclear BM cells treated with Epo ± PERKi. Expression of CD34 and CD133 was gated on Kit+.

(D). Stress BFU-E colony assay of *in vitro* cultured human mononuclear BM cells treated with Epo ± PERKi.

(E). Survival of recipients transplanted with $PERK^{fl/fl}$ or $PERK^{-/-}$ BM cells after lethal irradiation. 100,000 donor cells were transplanted into recipient mice. n=8 mice per group.
(F). Stress BFU-E colony assay of spleen cells in recipients received $PERK^{fl/fl}$ or $PERK^{-/-}$ BM cells on indicated days after BMT. 500,000 donor cells were transplanted into recipient mice.
(G). PCR analysis of PERK allele knockout efficiency in stress BFU-Es on day 14 after BMT. The colonies were from the same set of experiments in (F). Forward primer TCTGGCTTTCACTCCTCACAGC and reverse primer AAAGGAGGAAGGTGGAATTTGGA were used to detect floxed PERK allele.
(H). Flow cytometry analysis of intracellular ATF4 expression in *in vitro* cultured BM cells. Epo: WT BM cells treated with Epo, Epo + PERKi: WT BM cells treated with Epo + PERKi, $ATF4^{-/-}$: $ATF4^{-/-}$ BM cells treated with Epo. Expression of ATF4 was gated on Kit+Sca1+.
(I). Flow cytometry analysis of WT and $ATF4^{-/-}$ BM cells cultured in SEDM.
(J). Stress BFU-E colony assay of in vitro cultured WT and $ATF4^{-/-}$ BM cells from (I). Student t-test (2-tailed). Data represent means ± SEM. * $p< 0.05$.

Activation of PERK induces high translation rate and high proliferation rate in SEPs.

In the ISR, activation of PERK leads to global translation attenuation by phosphorylating eIF2α[24]. Paradoxically, eIF2α selectively promotes the translation of ATF4, which in turn increases the expression of GADD34. GAD34 negatively feeds back to dephosphorylate eIF2α and restores protein synthesis[25]. Thus, the survival of cells is regulated through eIF2α - ATF4 pathway dependent combination of repression and activation of global and preferential protein translation in ISR. High translational efficiency is required for SEPs to generate large numbers of erythrocytes, indicating that PERK/eIF2α/ATF4 dependent translational regulation may play a role in stress erythropoiesis. We first examined the global protein translation rate by

labeling SEPs with an alkyne analog of puromycin, O-propargyl-puromycin (OPP). OPP incorporates into newly translated proteins and stops the translation. We observe that the mean fluorescence intensity (MFI) of OPP in $PERK^{fl/fl}$ SEP donors started to rise from day 6 after BMT. This increase of translation peaks at day 8, then gradually declined in the following 4 days (Figure 3-5A). This dynamic process of global protein synthesis synchronized nicely with the production of PGE_2 in spleen after BMT (see Chapter2, Figure 2-7B), indicating that PGE_2 may play an important role in translational control by acting on PERK in SEPs. In $PERK^{-/-}$ donors, the increased global protein synthesis rate was compromised at day 6 and day 8. Correspondingly, recipients received $PERK^{-/-}$ cells had significantly fewer donor cells and lower spleen weights at these time points (Figure 3-5 B-D). We observed that the protein translation rate in $PERK^{-/-}$ donors were improved from day 10. Donor derived cells and spleen weights were still moderately less in recipients transplanted with $PERK^{-/-}$ cells on day 10 and day 12. These observations might due to the limited knockout efficiency of the PERK allele. There was a small fraction of cells contained wildtype allele in the $PERK^{-/-}$ donors. These cells proliferated normally and were able to reach an adequate number after 10 days to compensate the defects caused by the PERK mutant cells. We also tested the proliferation rate of SEPs by labeling donor cells with the fluorescent cell tracing reagent, CellTrace CFSE, which binds to intracellular amines and will be gradually diluted along with cell division. $PERK^{fl/fl}$ or $PERK^{-/-}$ donor cells were labeled with CellTrace CFSE prior to transplantation. When followed the CFSE fluorescence intensity in donor SEPs, we observed that most of $PERK^{-/-}$ donor SEPs exhibited low proliferation rates as shown by the retention of high CFSE fluorescence. The differences were more predominant on day 8 and day 10 (Figure 3-5E), by when the translational activity of $PERK^{fl/fl}$ SEPs was high and the cell number increased dramatically (Figure 3-5 A-C). Taken together, these findings suggest that PERK regulated increase of global protein translation is required by the rapid cell proliferation of SEPs.

A

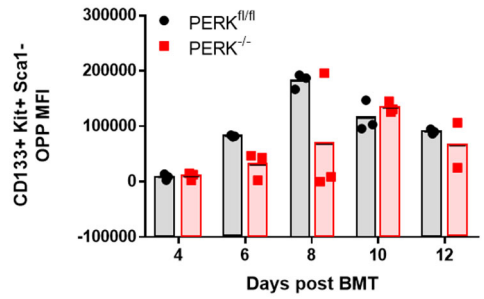
CD133+ Kit+ Sca1- OPP MFI
300000
200000
100000
0
-100000
PERK^fl/fl
PERK^-/-
4
6
8
10
12
Days post BMT

B

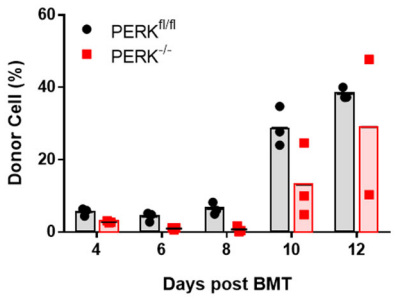
Donor Cell (%)
60
40
20
0
PERK^fl/fl
PERK^-/-
4
6
8
10
12
Days post BMT

C

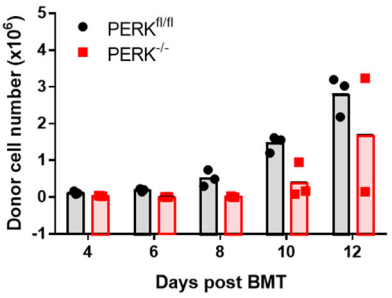
Donor cell number (x10^6)
5
4
3
2
1
0
-1
PERK^fl/fl
PERK^-/-
4
6
8
10
12
Days post BMT

D

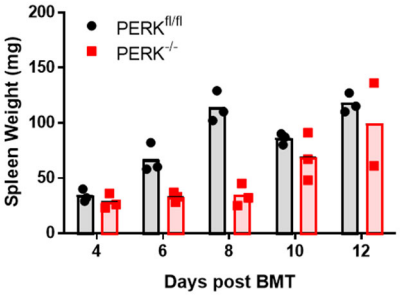
Spleen Weight (mg)
200
150
100
50
0
PERK^fl/fl
PERK^-/-
4
6
8
10
12
Days post BMT

E

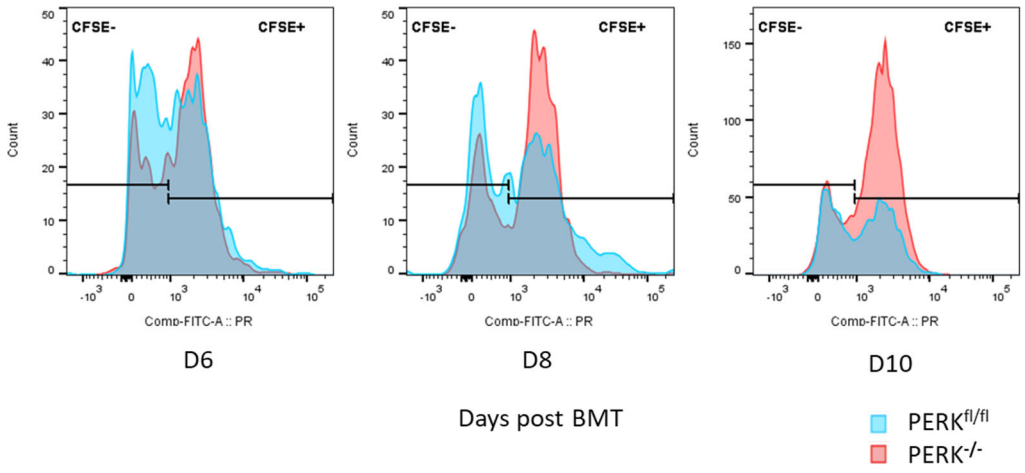
CFSE-
CFSE+
Count
Comp-FITC-A :: PR
D6
D8
D10
Days post BMT
PERK^fl/fl
PERK^-/-

Figure **3-5**: **PERK is required for global protein translation and proliferation of SEPs.** (A-D). 500,000 donor cells from $PERK^{fl/fl}$ or $PERK^{-/-}$ BM were transplanted into CD45.1 recipient mice. Flow cytometry analysis of OPP mean fluorescence intensity of donor CD133+Kit+Sca1+ SEPs after BMT (A). Donor cell percentage (B), absolute donor cell number (C) and spleen weight (D) were analyzed on indicated days.
(E). Flow cytometry analysis of cell proliferation rate after BMT. $PERK^{fl/fl}$ or $PERK^{-/-}$ BM cells were labeled with CellTrace CFSE reagent before transplanting in to CD45.1 recipient mice. The CFSE fluorescence intensity of Kit+Sca1+ donor SEP were analyzed on indicated days.

PERK promotes SEP differentiation through activating mTORC1 signaling pathway.

ATF4 induces adaptive gene transcription by binding to ISR-targeted promoters[26]. It has been demonstrated that ATF4 induces anabolism by promoting the expression of genes encoding selective amino acid transporters and aminoacyl-tRNA synthetases[24]. Previous work reported leucine supplementation is an effective treatment for Diamond-Blackfan anemia (DBA), in which erythroid progenitors have reduced translational capability caused by mutations in ribosomal protein genes[27]. This implies that amino acid availability and translational regulation is important in erythropoiesis. We first examined the expression of amino acid transporter genes and aminoacyl-tRNA synthetase genes. We observed that leucine transporters, leucine tRNA synthetase, glutamine transporters and arginine transporters all had the highest gene expression levels on day 8 after BMT (Figure 3-6 A-H). These peaks overlapped nicely with the phosphorylated PERK peak and global translation peak (Figure 3-6I and Figure 3-5A). In contrast, the expression levels of the amino acid transporter genes and leucine tRNA synthetase gene in $PERK^{-/-}$ cells were significantly lower on day 8. These observations indicate that PERK

activity is required for the increases of amino acid transporters and aminoacyl-tRNA synthetases during the recovery from BMT.

mTORC1 is known as nutrient and redox sensor that promotes global protein synthesis[28]. Previous work in the field shows that the PERK/ATF4 ISR pathway communicates with the mTORC1 signaling pathway[29]. ATF4 mediates the increased expression of amino acid transporters for small neutral amino acids, branched-chain amino acids and aromatic amino acids[30], which leads to increased intracellular amino acid flux and activates mTORC1 signaling pathway. Furthermore, treatment of mice with mTORC1 inhibitors restricts stress erythropoiesis, which further underscores the role of this pathway in stress erythropoiesis. To characterize the correlation between PERK signaling pathway and mTORC1 signaling pathway, we analyzed the mTORC1 activity by using $PERK^{fl/fl}$ and $PERK^{-/-}$ mice. We first analyzed the expression of phosphorylated ribosomal S6 protein (P-S6), phosphorylated 4E-BP1 (P-4EBP1) and the mTORC1 target, Myc in the *in vitro* cultured SEPs. The three indicators were barely expressed during the expansion stage (SEEM condition) in all $PERK^{fl/fl}$ and $PERK^{-/-}$ SEP subpopulations (Figure 3-7 A-F). However, in $PERK^{fl/fl}$ cells, we observed significant increases of P-S6, P-4EBP1 and Myc in the most immature CD34+CD133+Kit+Sca1+ SEPs in response to Epo (SEDM condition) (Figure 3-7 A-C left panels). Intriguingly, the increase of P-S6, P-4EBP1 and Myc in later stage CD34-CD133-Kit+Sca1+ SEPs and CD34-CD133-Kit+Sca1- BFU-E progenitors were not as significant as CD34+CD133+Kit+Sca1+ SEPs (Figure 3-7 A-C middle and right panels). In $PERK^{-/-}$ cells, the increase of P-S6, P-4EBP1 and Myc in all subpopulations were moderate in response to Epo (Figure 3-7 D-F). When compared to $PERK^{fl/fl}$ SEPs, we found all $PERK^{-/-}$ SEPs expressed lower levels of P-S6, P-4EBP1 in SEDM (Figure 3-7G, 3-7H). There was no significant difference of the Myc fluorescent intensity between the two groups (Figure 3-7I). Consistent with the PERK inhibitor findings, $PERK^{-/-}$ cells exhibited significantly increased immature CD34+CD133+Kit+Sca1+ SEPs accompanied with decreased CD34-CD133-

Kit+Sca1+ SEPs and CD34-CD133-Kit+Sca1- BFU-E progenitors (Figure 3-7J). Taken together, these observations suggest that the PERK mutation leads to low mTORC1 signaling pathway activity in immature SEPs, which may contribute to the impaired differentiation in PERK mutant cells.

We extended the *in vitro* analysis to *in vivo* BMT model. Consistent with the previous PERK activity and amino acid transporter data, we observed high fluorescence intensity of P-S6, P-4EBP1 and Myc in donor derived CD133+Kit+Sca1+ SEPs on day 8 in $PERK^{fl/fl}$ cells (Figure 3-8 A-C). P-4EBP1 and Myc fluorescence intensity were increased until day 12. In contrast, $PERK^{-/-}$ CD133+Kit+Sca1+ SEPs failed to generate comparable fluorescence intensity of P-S6 and P-4EBP1 on day 8. The fluorescence intensity of P-4EBP1 in $PERK^{-/-}$ donor SEPs remained low until day 12. In concordance with the *in vitro* observations, the difference of Myc fluorescence intensity between $PERK^{-/-}$ and $PERK^{fl/fl}$ donor SEPs were minor in all time points after BMT (Figure 3-8C). The later stage CD133-Kit+Sca1- SEPs had lower fluorescence intensity in all three mTORC1 activity indicators in compare to CD133+Kit+Sca1+ SEPs (Figure 3-8 D-F). Despite of the lower P-S6 levels in $PERK^{-/-}$ SEPs on day 8, the fluorescence intensity of P-S6, P-4EBP1 and Myc showed no differences between $PERK^{fl/fl}$ and $PERK^{-/-}$ cells in the later stage SEP populations. These observations suggest that Epo mainly induces mTORC1 signaling pathway activity in immature SEPs, which possibly results from PERK/ATF4 mediated amino acid influx. The increased mTORC1 signaling pathway activity facilitates the global protein translation in the early stage SEPs and enables their further differentiation.

A

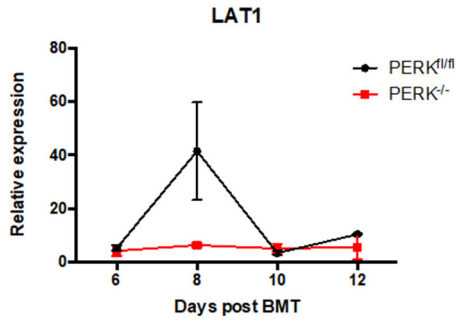
LAT1
Relative expression
Days post BMT
PERKfl/fl
PERK-/-

B

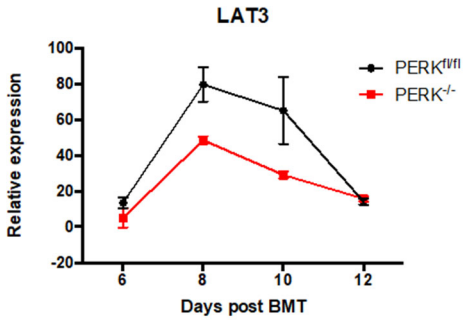
LAT3
Relative expression
Days post BMT
PERKfl/fl
PERK-/-

C

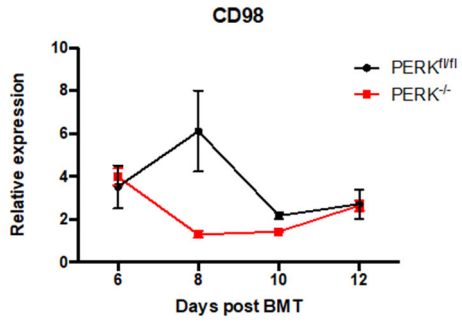
CD98
Relative expression
Days post BMT
PERKfl/fl
PERK-/-

D

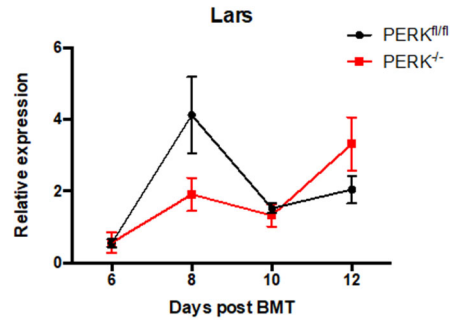
Lars
Relative expression
Days post BMT
PERKfl/fl
PERK-/-

E

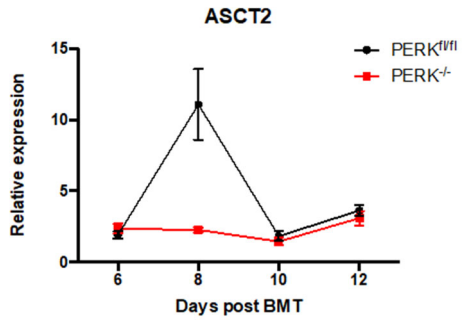
ASCT2
Relative expression
Days post BMT
PERKfl/fl
PERK-/-

F

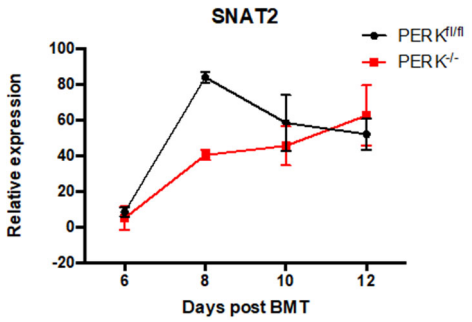
SNAT2
Relative expression
Days post BMT
PERKfl/fl
PERK-/-

G

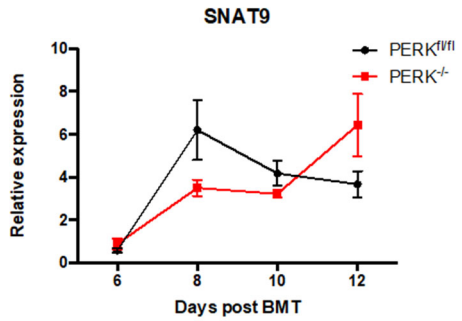

H

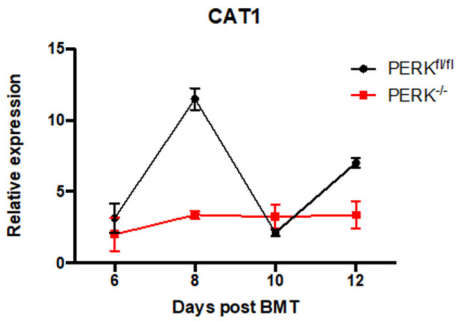

I

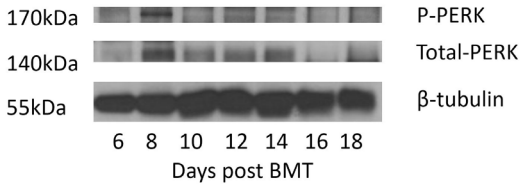

Figure **3-6**: **PERK signaling pathway regulates amino acid transporters and aminoacyl-tRNA synthetases during stress erythropoiesis.**

(A-H). mRNA expression of genes regulating leucine, glutamine, arginine transporters and leucyl-tRNA synthetase. Leucine regulatory genes: LAT1, LAT3, CD98, leucyl-tRNA synthetase gene: LARS, glutamine regulatory genes: ASCT2, SNAT2, arginine regulatory genes: SNAT9, CAT1.

(I). Western blot analysis of phosphorylated PERK (P-PERK) and total PERK (Total-PERK) in spleen cells after BMT.

A

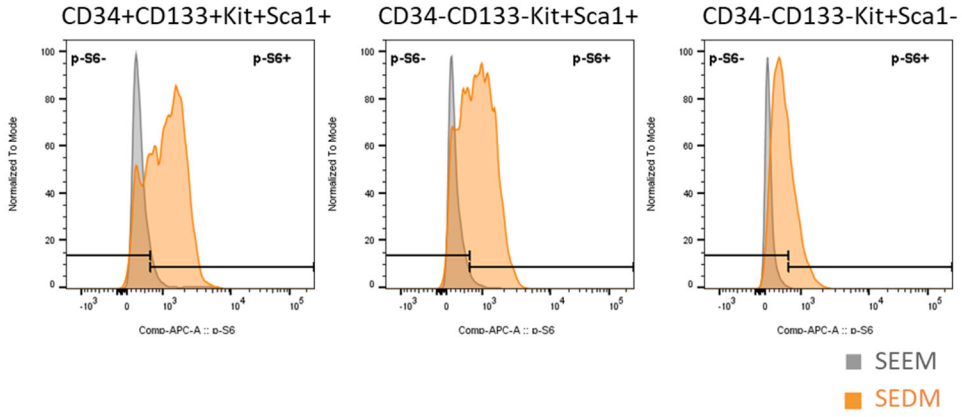
CD34+CD133+Kit+Sca1+
CD34-CD133-Kit+Sca1+
CD34-CD133-Kit+Sca1-
p-S6-
p-S6+
Normalized To Mode
Comp-APC-A :: p-S6
SEEM
SEDM

B

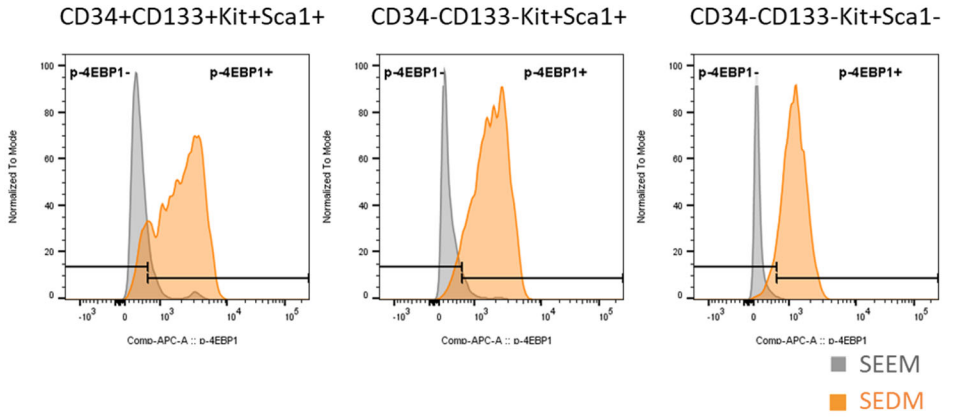
CD34+CD133+Kit+Sca1+
CD34-CD133-Kit+Sca1+
CD34-CD133-Kit+Sca1-
p-4EBP1-
p-4EBP1+
Normalized To Mode
Comp-APC-A :: p-4EBP1
SEEM
SEDM

C

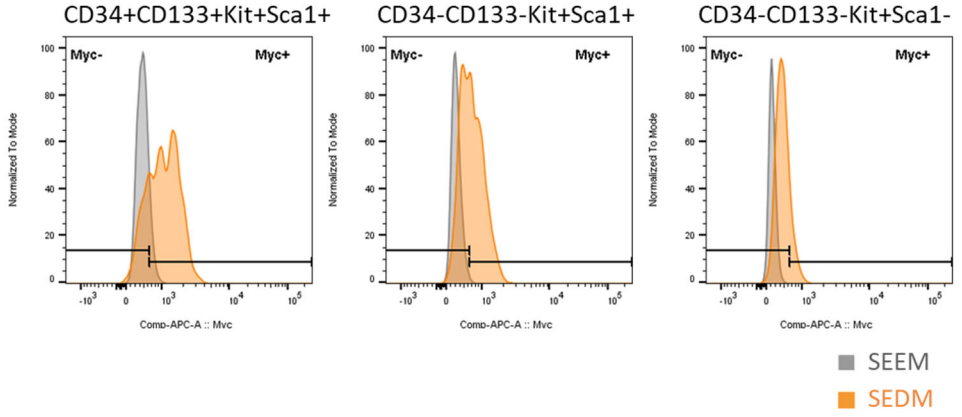
CD34+CD133+Kit+Sca1+
CD34-CD133-Kit+Sca1+
CD34-CD133-Kit+Sca1-
Myc-
Myc+
Normalized To Mode
Comp-APC-A :: Myc
SEEM
SEDM

D

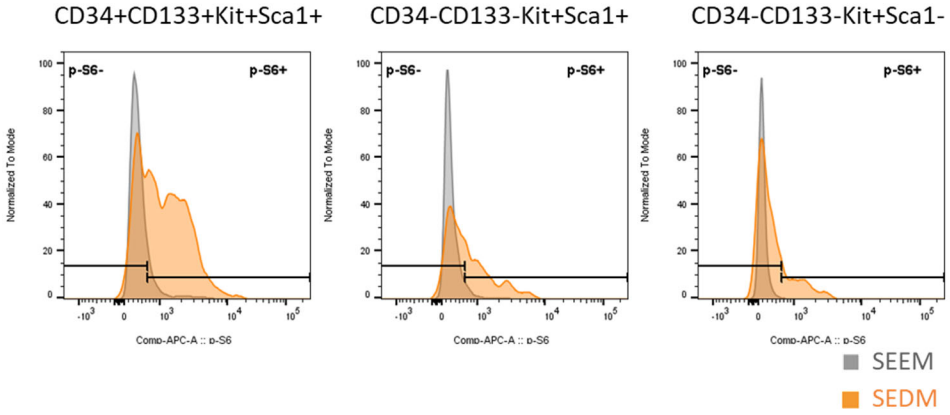
CD34+CD133+Kit+Sca1+
CD34-CD133-Kit+Sca1+
CD34-CD133-Kit+Sca1-
p-S6-
p-S6+
Normalized To Mode
Comp-APC-A :: p-S6
SEEM
SEDM

E

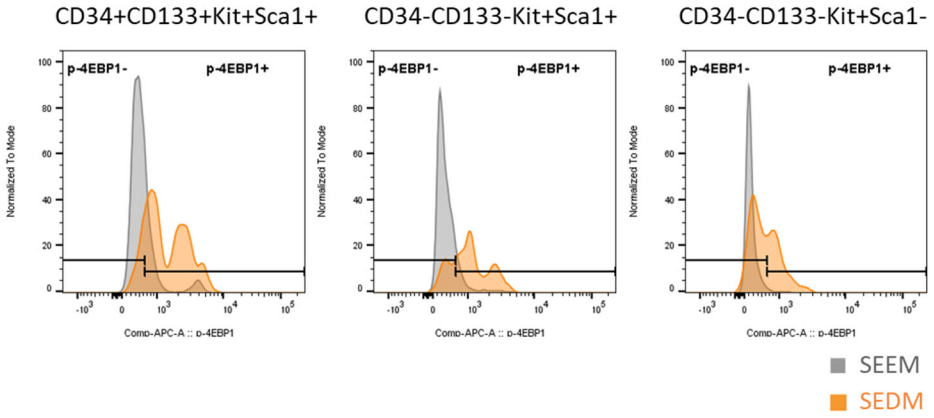
CD34+CD133+Kit+Sca1+
CD34-CD133-Kit+Sca1+
CD34-CD133-Kit+Sca1-
p-4EBP1-
p-4EBP1+
Normalized To Mode
Comp-APC-A :: p-4EBP1
SEEM
SEDM

F

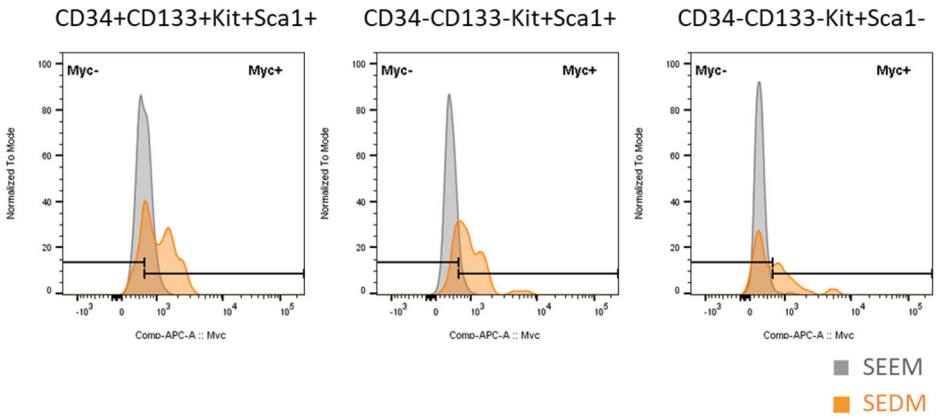
CD34+CD133+Kit+Sca1+
CD34-CD133-Kit+Sca1+
CD34-CD133-Kit+Sca1-
Myc-
Myc+
Normalized To Mode
Comp-APC-A :: Myc
SEEM
SEDM

G

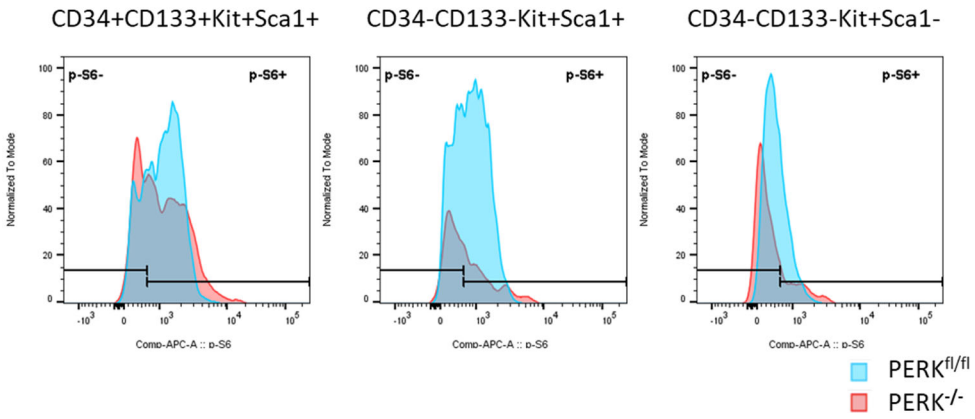
CD34+CD133+Kit+Sca1+
CD34-CD133-Kit+Sca1+
CD34-CD133-Kit+Sca1-
p-S6-
p-S6+
Normalized To Mode
Comp-APC-A :: p-S6
PERK^fl/fl
PERK^-/-

H

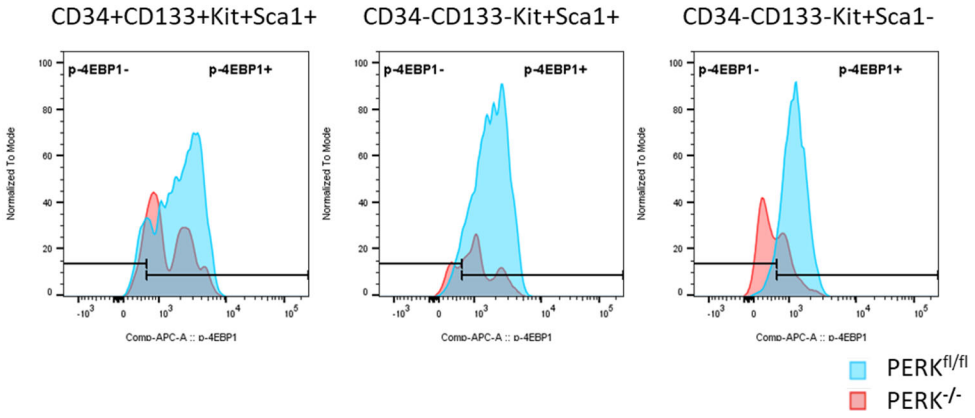
CD34+CD133+Kit+Sca1+
CD34-CD133-Kit+Sca1+
CD34-CD133-Kit+Sca1-
p-4EBP1-
p-4EBP1+
Normalized To Mode
Comp-APC-A :: p-4EBP1
PERK^fl/fl
PERK^-/-

I

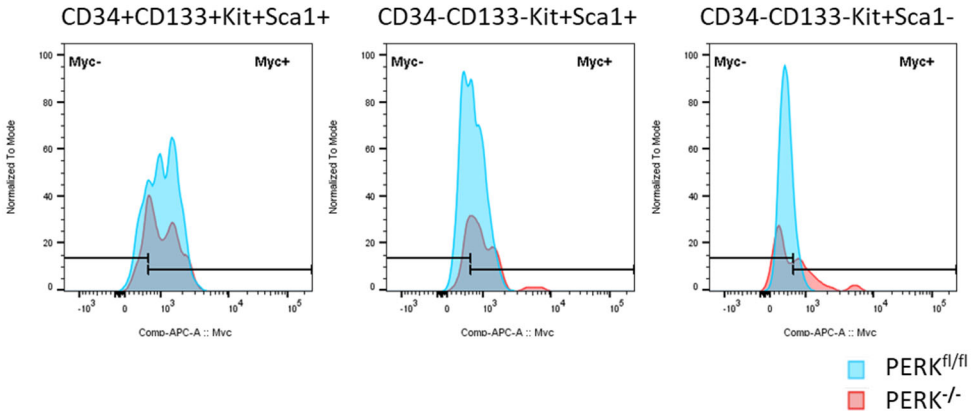
CD34+CD133+Kit+Sca1+
CD34-CD133-Kit+Sca1+
CD34-CD133-Kit+Sca1-
Myc-
Myc+
Normalized To Mode
Comp-APC-A :: Myc
PERK^fl/fl
PERK^-/-

J

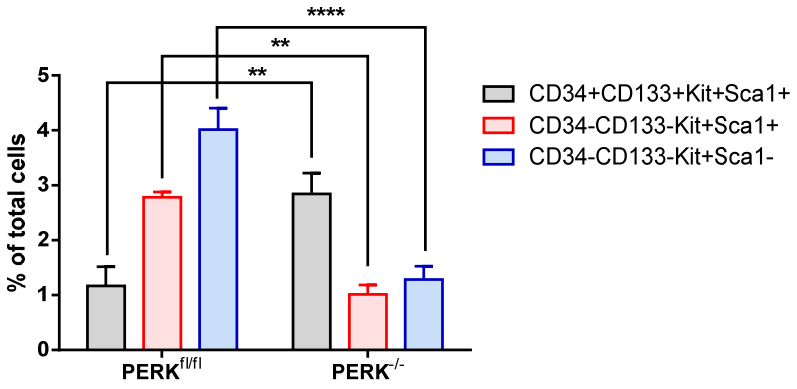

Figure **3-7**: **PERK regulates activity of mTORC1 signaling pathway *in vitro*.**

(A-F). Flow cytometry analysis of intracellular P-S6, P-4EBP1 and Myc expression in $PERK^{fl/fl}$ or $PERK^{-/-}$ BM cells cultured in SEEM or SEDM. CD34+CD133+Kit+Sca1+: immature SEPs, CD34-CD133-Kit+Sca1+: later stage SEPs, CD34-CD133-Kit+Sca1-: stress BFU-E progenitors.

(A-C). Comparison of mTORC1 activity indicator fluorescence intensity in SEEM and SEDM of $PERK^{fl/fl}$ SEPs. P-S6 (A), P-4EBP1 (B), Myc (C).

(D-F). Comparison of mTORC1 activity indicator fluorescence intensity in SEEM and SEDM of $PERK^{-/-}$ SEPs. P-S6 (D), P-4EBP1 (E), Myc (F).

(G-I). Comparison of mTORC1 activity indicator fluorescence intensity in $PERK^{fl/fl}$ and $PERK^{-/-}$ SEPs cultured in SEDM. P-S6 (G), P-4EBP1 (H), Myc (I).

(J). Percentage of SEP subpopulations in $PERK^{fl/fl}$ and $PERK^{-/-}$ BM cells cultured in SEDM. Two-way ANOVA followed by Bonferroni's multiple comparisons. Data represent means ± SEM. ** $p< 0.01$, **** $p< 0.0001$.

A

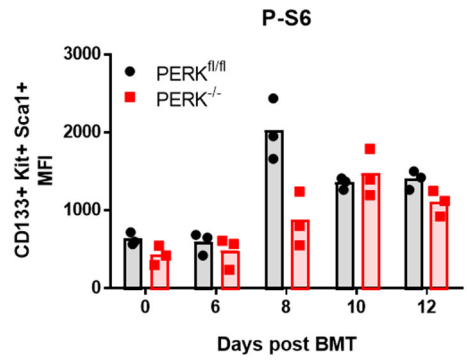
P-S6
CD133+ Kit+ Sca1+ MFI
PERK^fl/fl
PERK^-/-
3000
2000
1000
0
0
6
8
10
12
Days post BMT

B

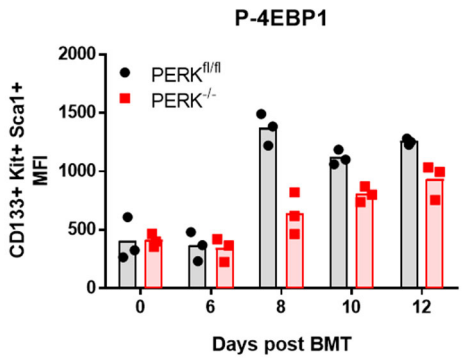
P-4EBP1
CD133+ Kit+ Sca1+ MFI
PERK^fl/fl
PERK^-/-
2000
1500
1000
500
0
0
6
8
10
12
Days post BMT

C

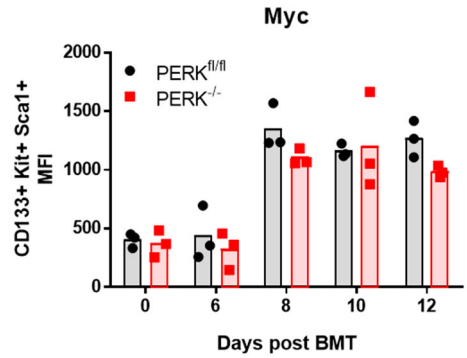
Myc
CD133+ Kit+ Sca1+ MFI
PERK^fl/fl
PERK^-/-
2000
1500
1000
500
0
0
6
8
10
12
Days post BMT

D

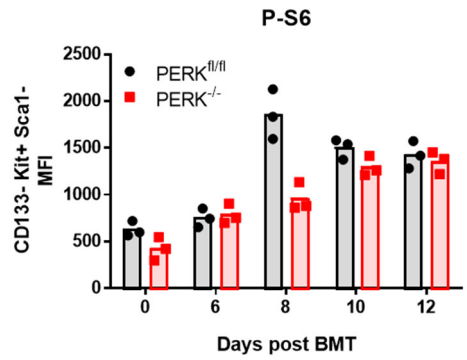
P-S6
CD133- Kit+ Sca1- MFI
PERK^fl/fl
PERK^-/-
2500
2000
1500
1000
500
0
0
6
8
10
12
Days post BMT

E

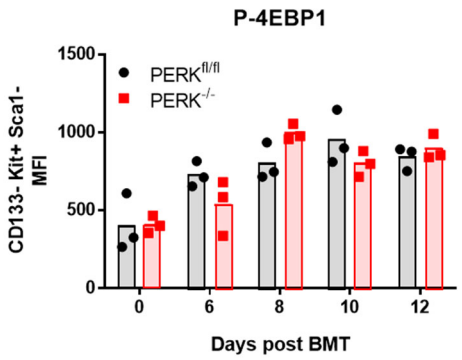
P-4EBP1
CD133- Kit+ Sca1- MFI
PERK^fl/fl
PERK^-/-
1500
1000
500
0
0
6
8
10
12
Days post BMT

F

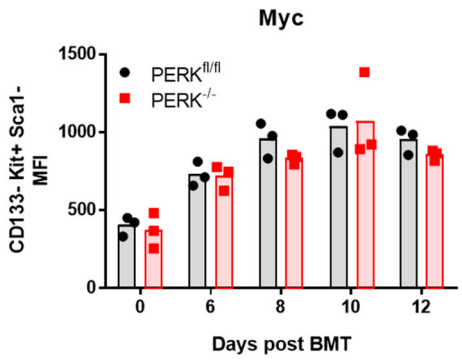

Figure **3-8**: **PERK regulates activity of mTORC1 signaling pathway *in vivo*.**
500,000 donor cells from PERK$^{fl/fl}$ or PERK$^{-/-}$ BM were transplanted into CD45.1 recipient mice. (A-C). Flow cytometry analysis of mean fluorescence intensity of mTORC1 activity indicators in donor CD133+Kit+Sca1+ SEPs after BMT. P-S6 (A), P-4EBP1 (B), Myc (C).
(D-F). Flow cytometry analysis of mean fluorescence intensity of mTORC1 activity indicators in donor CD133-Kit+Sca1- SEPs after BMT. P-S6 (D), P-4EBP1 (E), Myc (F).

3.4 Discussion

Gene expression is the key process in regulating cell growth and development. Research focused on transcription regulation has revealed key transcriptional regulatory mechanisms. However, post-transcriptional regulation remains largely obscure. Different cell types have distinct requirements of global protein synthesis rate and translation of specific mRNAs. Dysregulation of translation is related to various of diseases including cancer and blood disorders[31,32,33]. Previous work showed that protein synthesis rate undergoes remarkable changes during hematopoiesis[34]. HSCs require low protein synthesis rate to maintain homeostasis. Either increasing protein synthesis by *Pten* deletion or further reducing protein synthesis by mutating

Rpl24 ribosome significantly impairs HSC reconstitution capability[34,35]. Intriguingly, protein synthesis rate is much higher in lineage committed progenitors including CMPs, GMPs and MEPs[34]. In terminal erythroid differentiation, translational regulation is even more crucial since erythroblasts require high efficiency of hemoglobin synthesis[36]. SEPs are actively dividing to give rise to new erythrocytes during stress erythropoiesis. Increased translation rate is required to generate adequate protein for constructing new cells. Our data showed that the protein synthesis rate is dramatically increased during recovery process after BMT. Accompanied with the high cell proliferation rate, increased SEP numbers and increasing spleen size, our findings suggest that the elevated translation enables the rapid differentiation of SEPs. The appropriate regulation of protein synthesis also includes suppression of neoplastic proliferation. Cancer cells synthesize protein more efficiently through dysregulating translation initiation[37]. Our work gives another example of maintaining tissue homeostasis by proper translational regulation. The protein synthesis rate gradually reduced after day 8 post BMT. This trend is consistent with the serum Epo level and spleen PGE_2 level (see Chapter2, Figure 2-7B), the two key transition signals drives SEP differentiation, suggesting that Epo and PGE_2 may act as regulators that initiate the translational control machinery. After maximizing the pool of immature SEPs required for relieving anemic stress, negative feedback inhibits these responses as SEPs differentiate. Therefore, this hyperactive erythropoiesis process is able to rapidly replenish erythrocytes without inducing polycythemia.

mTORC1 is one of the master regulators of cell growth and development. It integrates various environmental signals, including nutrients, growth factors and intracellular ATP, to regulate protein synthesis[38]. Previous studies showed that mutations in components of mTORC1 pathway impaired erythroid development in mice[39,40,41]. Consistent with the protein synthesis regulation, increased mTORC1 activity depletes HSCs[35,42]. Notably, erythroid cells are extraordinarily sensitive to mTORC1 activity. Inhibition of mTORC1 results in significant

decrease of protein synthesis in erythroid cells while has minimal impact on other hematopoietic lineages like granulocytes[43]. Under phenylhydrazine induced hemolytic stress, mTORC1 inhibition leads to 50% mortality with significant decreases of late stage erythroid progenitors in spleen and circulating reticulocytes[41]. Paradoxically, hyperactivation of mTORC1 also impairs erythroid differentiation by inducing macrocytic anemia[41]. These data suggested that accurate regulation of mTORC1 is critical for erythropoiesis. Our findings extended the regulatory role of mTORC1 into early stage erythropoiesis. We demonstrated that Epo dependent mTORC1 signaling pathway is required for the differentiation of SEPs. Early stage CD34+CD133+Kit+Sca1+ SEPs quickly differentiate into a transition population, CD34-CD133-Kit+Sca1+ SEPs, during stress erythropoiesis. The transition SEPs continue to give rise to the stress BFU-E progenitor, CD34-CD133-Kit+Sca1+ SEPs. With low mTORC1 activity, we observed fewer numbers of early stage CD34+CD133+Kit+Sca1+ SEPs, which have impaired capability of generating both transition SEPs and the later stress BFU-E progenitors. DBA and 5q-syndrome are ribosomopathies characterized by ribosome protein haploinsufficiency caused anemia[44]. The low protein synthesis rate in erythroid lineages can be mitigated by L-leucine supplementation, which is a classical cue of mTORC1 activation[45,46]. Our data is consistent with the evidence that mTORC1 dependent translational control is important for erythroid proliferation and differentiation. However, further investigation of mTORC1 regulated protein synthesis in stress erythropoiesis are necessary to delineate the precise role for mTORC1 activation in stress erythropoiesis and how it is regulated, as unregulated mTORC1 can initiate tumorigenesis[31,33].

In many circumstances, mTORC1 coordinates with other signaling pathways to regulate cell growth. This interaction between mTORC1 and the different ISR pathways underscores the wide potential for these pathways to regulate translation during development. In contrast to our example of the positive interaction between PERK and mTORC1 in the regulation of cell proliferation and differentiation, HRI signaling pathway inhibits mTORC1 signaling pathway in

iron deficiency (ID) model. HRI is important in regulating hemoglobin synthesis in ID through sensing the availability of heme[47]. Recent work from Zhang et al showed that, in addition to activating downstream P-eIF2a and ATF4 to specifically increase the expression of genes required for redox homeostasis and erythroid differentiation, HRI signaling pathway also inhibits mTORC1 to prevent global protein synthesis to limit the expansion of early erythroblasts[48,49]. Ablation of P-eIF2α or ATF4 lead to increased mTORC1 activity and ineffective erythropoiesis. In this case, inhibition of mTORC1 is able to improve erythroid differentiation in iron deficient HRI mutants and P-eIF2a mutants[48,49]. The cooperation of these two signaling pathways regulates erythroid differentiation in ID without having redundant globin induced proteotoxicity or excessive protein synthesis induced macrocytic anemia.

In conclusion, our data identifie PGE_2-dependent mobilization of ER Ca^{2+} as an initiating step for the increase in protein translation. Ca^{2+} dependent activation of PERK/eIF2α/ATF4 pathway is well known as the regulator in response to ER stress. Although PERK mediates inhibition of global protein synthesis to reduce unfolded proteins in ER stress, in this study, we observed PERK dependent increase of protein synthesis in SEPs. The underlying mechanism for this elevated translation is that the PERK pathway increases the expression of amino acid transporters and tRNA synthases, including the leucine transporter and leucine tRNA synthetase, which activate mTORC1 signaling pathway activity (Figure 3-9). These findings suggest a new role of PERK in translational regulation. By activating mTORC1 signaling pathway, PERK promotes global protein translation in early erythroid progenitors to achieve the active cell division in stress erythropoiesis.

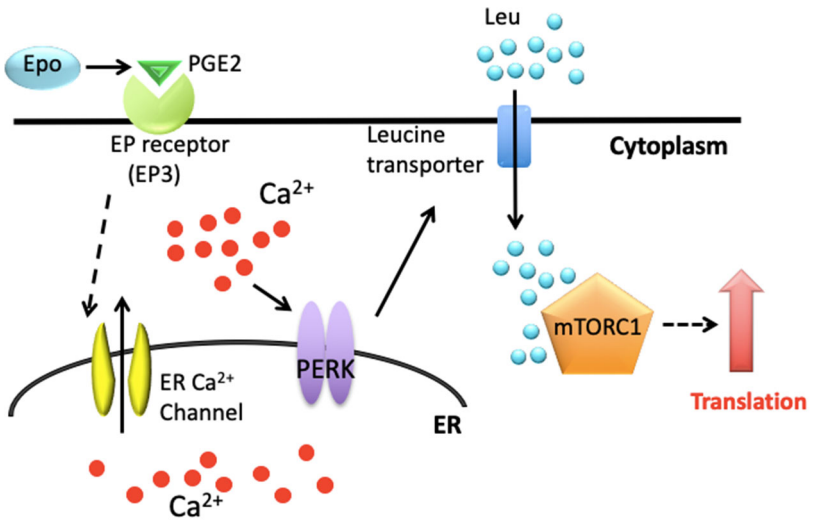

Figure **3-9**: **Schematic of PERK and mTORC1 signaling pathway regulated protein translation in SEPs**.

3.5 References

1. Dzierzak, E. & Philipsen, S. Erythropoiesis: Development and differentiation. *Cold Spring Harb. Perspect. Med.* (2013) doi:10.1101/cshperspect.a011601.
2. Paulson, R. F., Shi, L. & Wu, D. C. Stress erythropoiesis: New signals and new stress progenitor cells. *Curr. Opin. Hematol.* (2011) doi:10.1097/MOH.0b013e32834521c8.
3. Lenox, L. E., Shi, L., Hegde, S. & Paulson, R. F. Extramedullary erythropoiesis in the adult liver requires BMP-4/Smad5-dependent signaling. *Exp. Hematol.* (2009) doi:10.1016/j.exphem.2009.01.004.
4. Ploemacher, R. E. & van Soest, P. L. Morphological investigation on phenylhydrazine-induced erythropoiesis in the adult mouse liver. *Cell Tissue Res.* (1977) doi:10.1007/BF00219567.
5. Xiang, J., Wu, D. C., Chen, Y. & Paulson, R. F. In vitro culture of stress erythroid progenitors identifies distinct progenitor populations and analogous human progenitors. *Blood* (2015) doi:10.1182/blood-2014-07-591453.
6. Harandi, O. F., Hedge, S., Wu, D. C., Mckeone, D. & Paulson, R. F. Murine erythroid short-term radioprotection requires a BMP4-dependent, self-renewing population of stress erythroid progenitors. *J. Clin. Invest.* (2010) doi:10.1172/JCI41291.
7. Lenox, L. E., Perry, J. M. & Paulson, R. F. BMP4 and Madh5 regulate the erythroid response to acute anemia. *Blood* (2005) doi:10.1182/blood-2004-02-0703.
8. Perry, J. M., Harandi, O. F. & Paulson, R. F. BMP4, SCF, and hypoxia cooperatively regulate the expansion of murine stress erythroid progenitors. *Blood* (2007) doi:10.1182/blood-2006-04-016154.
9. Porayette, P. & Paulson, R. F. BMP4/Smad5 dependent stress erythropoiesis is required for the expansion of erythroid progenitors during fetal development. *Dev. Biol.* (2008) doi:10.1016/j.ydbio.2008.01.047.
10. Lu, P. D., Harding, H. P. & Ron, D. Translation reinitiation at alternative open reading frames regulates gene expression in an integrated stress response. *J. Cell Biol.* (2004) doi:10.1083/jcb.200408003.
11. Vattem, K. M. & Wek, R. C. Reinitiation involving upstream ORFs regulates ATF4 mRNA translation in mammalian cells. *Proc. Natl. Acad. Sci. U. S. A.* (2004) doi:10.1073/pnas.0400541101.
12. Pakos-Zebrucka, K. *et al.* The integrated stress response. *EMBO Rep.* (2016) doi:10.15252/embr.201642195.
13. Rozpedek, W. *et al.* The Role of the PERK/eIF2α/ATF4/CHOP Signaling Pathway in Tumor Progression During Endoplasmic Reticulum Stress. *Curr. Mol. Med.* (2016) doi:10.2174/1566524016666160523143937.

14. Raven, J. F. *et al.* PKR and PKR-like endoplasmic reticulum kinase induce the proteasome-dependent degradation of cyclin D1 via a mechanism requiring eukaryotic initiation factor 2α phosphorylation. *J. Biol. Chem.* (2008) doi:10.1074/jbc.M709677200.

15. Guan, B. J. *et al.* Translational control during endoplasmic reticulum stress beyond phosphorylation of the translation initiation factor eif2. *J. Biol. Chem.* (2014) doi:10.1074/jbc.M113.543215.

16. Reader, J., Holt, D. & Fulton, A. Prostaglandin E 2 EP receptors as therapeutic targets in breast cancer. *Cancer Metastasis Rev.* (2011) doi:10.1007/s10555-011-9303-2.

17. Kim, P. G. *et al.* Flow-induced protein kinase A-CREB pathway acts via BMP signaling to promote HSC emergence. *J. Exp. Med.* (2015) doi:10.1084/jem.20141514.

18. Luchsinger, L. L. *et al.* Harnessing Hematopoietic Stem Cell Low Intracellular Calcium Improves Their Maintenance In Vitro. *Cell Stem Cell* (2019) doi:10.1016/j.stem.2019.05.002.

19. Zhu, S., McGrath, B. C., Bai, Y., Tang, X. & Cavener, D. R. PERK regulates Gq protein-coupled intracellular Ca2+ dynamics in primary cortical neurons. *Mol. Brain* (2016) doi:10.1186/s13041-016-0268-5.

20. Wang, R. *et al.* Insulin secretion and Ca2+ dynamics in β-cells are regulated by PERK (EIF2AK3) in concert with calcineurin. *J. Biol. Chem.* (2013) doi:10.1074/jbc.M113.503664.

21. Moenner, M., Pluquet, O., Bouchecareilh, M. & Chevet, E. Integrated endoplasmic reticulum stress responses in cancer. *Cancer Research* (2007) doi:10.1158/0008-5472.CAN-07-1705.

22. Masuoka, H. C. & Townes, T. M. Targeted disruption of the activating transcription factor 4 gene results in severe fetal anemia in mice. *Blood* (2002) doi:10.1182/blood.V99.3.736.

23. Harding, H. P. *et al.* Ppp1r15 gene knockout reveals an essential role for translation initiation factor 2 alpha (eIF2α) dephosphorylation in mammalian development. *Proc. Natl. Acad. Sci. U. S. A.* (2009) doi:10.1073/pnas.0809632106.

24. Han, J. *et al.* ER-stress-induced transcriptional regulation increases protein synthesis leading to cell death. *Nat. Cell Biol.* (2013) doi:10.1038/ncb2738.

25. Chen, J. J. Translational control by heme-regulated eIF2α kinase during erythropoiesis. *Current Opinion in Hematology* (2014) doi:10.1097/MOH.0000000000000030.

26. Dey, S. *et al.* Both transcriptional regulation and translational control of ATF4 are central to the integrated stress response. *J. Biol. Chem.* (2010) doi:10.1074/jbc.M110.167213.

27. Kamimae-Lanning, A. N. & Kurre, P. L-leucine alleviates Diamond-Blackfan anemia. *Blood* (2012) doi:10.1182/blood-2012-07-443978.

28. Sarbassov, D. D. & Sabatini, D. M. Redox regulation of the nutrient-sensitive raptor-mTOR pathway and complex. *J. Biol. Chem.* (2005) doi:10.1074/jbc.M506096200.

29. Reiling, J. H. & Sabatini, D. M. Increased mTORC1 Signaling UPRegulates Stress. *Molecular Cell* (2008) doi:10.1016/j.molcel.2008.02.011.

30. Harding, H. P. *et al.* An integrated stress response regulates amino acid metabolism and resistance to oxidative stress. *Mol. Cell* (2003) doi:10.1016/S1097-2765(03)00105-9.

31. Hsieh, A. C. *et al.* Genetic Dissection of the Oncogenic mTOR Pathway Reveals Druggable Addiction to Translational Control via 4EBP-eIF4E. *Cancer Cell* (2010) doi:10.1016/j.ccr.2010.01.021.

32. Barna, M. *et al.* Suppression of Myc oncogenic activity by ribosomal protein haploinsufficiency. *Nature* (2008) doi:10.1038/nature07449.

33. Hsieh, A. C. *et al.* The translational landscape of mTOR signalling steers cancer initiation and metastasis. *Nature* (2012) doi:10.1038/nature10912.

34. Signer, R. A. J., Magee, J. A., Salic, A. & Morrison, S. J. Haematopoietic stem cells require a highly regulated protein synthesis rate. *Nature* (2014) doi:10.1038/nature13035.

35. Yilmaz, Ö. H. *et al.* Pten dependence distinguishes haematopoietic stem cells from leukaemia-initiating cells. *Nature* (2006) doi:10.1038/nature04703.

36. Alvarez-Dominguez, J. R., Zhang, X. & Hu, W. Widespread and dynamic translational control of red blood cell development. *Blood* (2017) doi:10.1182/blood-2016-09-741835.

37. Ruggero, D. Translational control in cancer etiology. *Cold Spring Harb. Perspect. Biol.* (2013) doi:10.1101/cshperspect.a012336.

38. Laplante, M. & Sabatini, D. M. MTOR signaling in growth control and disease. *Cell* (2012) doi:10.1016/j.cell.2012.03.017.

39. Murakami, M. *et al.* mTOR Is Essential for Growth and Proliferation in Early Mouse Embryos and Embryonic Stem Cells. *Mol. Cell. Biol.* (2004) doi:10.1128/mcb.24.15.6710-6718.2004.

40. Magee, J. A. *et al.* Temporal changes in PTEN and mTORC2 regulation of hematopoietic stem cell self-renewal and leukemia suppression. *Cell Stem Cell* (2012) doi:10.1016/j.stem.2012.05.026.

41. Knight, Z. A., Schmidt, S. F., Birsoy, K., Tan, K. & Friedman, J. M. A critical role for mTORC1 in erythropoiesis and anemia. *Elife* (2014) doi:10.7554/eLife.01913.

42. Zhang, J. *et al.* PTEN maintains haematopoietic stem cells and acts in lineage choice and leukaemia prevention. *Nature* (2006) doi:10.1038/nature04747.

43. Liu, X. *et al.* Regulation of mitochondrial biogenesis in erythropoiesis by mTORC1-mediated protein translation. *Nat. Cell Biol.* (2017) doi:10.1038/ncb3527.

44. Narla, A. & Ebert, B. L. Ribosomopathies: Human disorders of ribosome dysfunction. *Blood* (2010) doi:10.1182/blood-2009-10-178129.

45. Payne, E. M. *et al.* L-leucine improves the anemia and developmental defects associated

with Diamond-Blackfan anemia and del(5q) MDS by activating the mTOR pathway. *Blood* (2012) doi:10.1182/blood-2011-10-382986.

46. Janes, M. R. *et al.* Effective and selective targeting of leukemia cells using a TORC1/2 kinase inhibitor. *Nat. Med.* **16**, 205–213 (2010).

47. Chen, J. J. & London, I. M. Regulation of protein synthesis by heme-regulated eIF-2α kinase. *Trends in Biochemical Sciences* (1995) doi:10.1016/S0968-0004(00)88975-6.

48. Zhang, S. *et al.* HRI coordinates translation by eIF2αP and mTORC1 to mitigate ineffective erythropoiesis in mice during iron deficiency. *Blood* (2018) doi:10.1182/blood-2017-08-799908.

49. Zhang, S. *et al.* HRI coordinates translation necessary for protein homeostasis and mitochondrial function in erythropoiesis. *Elife* (2019) doi:10.7554/eLife.46976.

50. Bennett, L. F., Liao, C. & Paulson, R. F. Stress erythropoiesis model systems. in *Methods in Molecular Biology* (2018). doi:10.1007/978-1-4939-7428-3_5.

Chapter 4

Discussion and future directions

4.1 Discussion

Anemia is a global health problem that causes significant morbidity and mortality. The most commonly used therapy for anemia patients is repeated blood transfusion. However, the large amount of iron delivered by transfusion increases the risk of iron overload, which can induce inflammatory response syndrome[1]. In addition, there is a risk of infection with contaminated blood products. Previous studies suggest that prolonged storage of red blood cells increases the risk of multiorgan failure, thromboembolism and infections[2,3]. To conquer the limitations of current treatment, new therapies that target the generation of adequate amounts of normal erythrocytes would provide long-term efficacy with minimum adverse effects for these congenital anemias. One approach to identify new targets for therapy is to better understand the mechanisms of stress erythropoiesis. Stress erythropoiesis, which is distinct from steady state erythropoiesis, is capable of generating large amounts of new erythrocytes in a short-term. SEPs undergo series of symmetric and asymmetric divisions in response to corresponding stress erythroid signals and eventually develop into mature erythrocytes. Both an *in vitro* culture system and an *in vivo* BMT model are nicely established in our laboratory to study stress erythropoiesis[4]. In our stress erythropoiesis model, SEPs can engraft, self-renew and only give rise to cells in the erythroid lineage. The *in vitro* stress erythropoiesis culture system can also apply to human bone marrow cells[5]. These appropriate and applicable models of stress erythropoiesis enable us to investigate the mechanisms of erythroid response in anemia.

In chapter 2, we demonstrated an Epo dependent signal change in microenvironment macrophages. Macrophage derived canonical Wnt ligands increased at early stage of stress erythropoiesis and activate β-catenin in SEPs. Engagement of Wnt/β-catenin signaling pathway results in efficient proliferation of SEPs. The proliferating signals are suppressed when the levels of serum Epo is increased. Alternatively, Epo induces a set of differentiating signals in macrophages, including PGE_2 and PGJ_2. The two prostaglandins drive differentiation of SEPs through distinct mechanisms. PGJ_2 acts as ligand of PPARγ, which antagonizes Wnt ligands, while PGE_2 promotes SEP differentiation independently. With the Epo dependent transition of the two sets of microenvironmental signals, SEPs are able to rapidly expand and differentiate into abundant erythrocytes. Accumulating evidence about the erythroid niche emphasize the role of EBI macrophages during development and steady state erythropoiesis. Here, we extend the findings into stress erythropoiesis. Since stress erythropoiesis is a hyperdynamic process of generating new erythrocytes, distinct microenvironmental signals are required to facilitate the rapid maturation of SEPs. For decades, Epo has been known as the hallmark signal that regulates differentiation of erythroid progenitors. However, the underlying mechanism remains obscure. Recent work identified that a subtype of macrophages that expresses high level of EpoR constitutes the EBIs[6], suggesting that macrophages could be the targets of Epo instead of or in addition to erythroid progenitors. Our findings further confirmed the hypothesis that Epo is able to directly act on EBI macrophages. The presence of Epo shuffles the microenvironmental signals to mediate the differentiation of SEPs. The identification of novel Epo dependent microenvironmental signals in this work indicates that further research focusing on the correlation between SEPs and the microenvironment is needed. The erythroid niche might be more comprehensive than we currently know. In addition to EBI macrophages, the niche may require the coordination of other cell types and signals to fulfill the rapid growth and maturation of SEP.

In chapter 3, we further investigated PGE_2 mediated SEP differentiation. In response to Epo, increased PGE_2 is able to promote intracellular Ca^{2+} mobilization through binding to EP3 receptor. The increased Ca^{2+} flux activates a stress sensor, PERK. The PERK signaling pathway is required for the differentiation of SEPs. In fact, PERK dependent ATF4 regulates the amino acid influx in SEPs. Increased intracellular amino acids activate mTORC1 signaling pathway, which promotes global protein translation. The high rate of protein synthesis in SEPs fuels the rapid differentiation of the cells and results in efficient generation of mature erythrocytes. In this study, we built the connections between PERK and mTORC1 signaling pathway in stress erythropoiesis. The integration of these two pathways in regulating cell differentiation was poorly studied in previous research. Also, we interpreted PERK function in translational control in an innovative way. In our model, rather than ceasing general protein translation as observed in other stress cases, PERK promotes translation in SEPs by cooperating with mTORC1. These findings provide more comprehensive understanding in PERK signaling pathway and lead to questions of the balance between inhibition and elevation of protein translation in stress responses and how that might relate to chronic diseases. We observed that mTORC1 signaling pathway is activated in response to the transition signal Epo, which emphasizes the importance of mTORC1 in stress erythropoiesis. Since mTORC1 can integrate various signals and regulate cell growth in multiple ways, it leads to more questions about the potential mechanisms of mTORC1 regulated SEPs differentiation.

4.2 Future directions

4.2.1 IL4 regulated PPARγ and macrophage/microenvironment transition in stress erythropoiesis

PGD_2 is widely expressed in the central nervous system[7]. The effects of PGD_2 has been suggested to play both pro-inflammatory and anti-inflammatory roles in different disease models[8]. Similar to other PGs, PGD_2 exerts its activity through binding to G protein coupled receptors. In fact, the various effects of PGD_2 depends on the expression location and expression level of PGD_2 receptors (DPs). DP1 has been demonstrated plays a role in recruiting inflammatory lymphocytes and eosinophils in asthma[9]. DP2 is also called the chemoattractant receptor-homologous molecule expressed on Th2 cells (CRTH2). In addition to T helper 2 (Th2) cells, CRTH2 is also found in basophils and eosinophils[10]. Previous studies showed that CRTH2 mediates the inhibition of cAMP synthesis and can induce intracellular Ca^{2+} mobilization[11]. Our work showed that PGD_2 derived Δ12-PGJ_2 regulates PPARγ expression in macrophages (Chapter2 Figure 2-5). Intriguingly, we also observe a decrease of PPARγ expression in $CRTH2^{-/-}$ stroma cells in SEDM culture, which is consistent with impaired PPARγ expression when CRTH2 is antagonized by CAY10595 (Figure 4-1A). In addition, fewer stress BFU-Es were observed when CRTH2 is perturbed (Figure 4-1B) This finding indicates that in addition to giving rise to Δ12-PGJ_2, PGD_2 may also directly regulate PPARγ in EBI macrophages through CRTH2 mediated signaling pathways. One well documented Th2 cytokine is interleukin 4 (IL4). Previous study found that IL4 is able to induce the expression of PPARγ in macrophages[12]. We observed that IL4 increased the growth of stroma cells in SEEM culture (Figure 4-2A). The expression of PPARγ was also dramatically increased with the presence of IL4 (Figure 4-2B).

The supplementation of IL4 resulted in increased stress BFU-E colonies when Epo was not present (Figure 4-2C). However, this IL4 effect was totally diminished when Epo was present. The stress BFU-E number remained comparable in SEDM with or without the presence of IL4. In addition, the IL4 expression in spleen cells peaked at day 6 after BMT, which is in parallel with the serum Epo peak (Figure 4-2E and Chapter2 Figure 2-2C). These observations suggest that IL4 might be another important signal that induced by Epo during stress erythropoiesis. It may share part of the responsibility of elevating PPARγ in microenvironmental macrophages. A few intriguing questions arise from the current findings. First, the source of IL4 is not clear. Th2 cells are both recipient and producer of IL4[13]. Upon being activated by exogenous IL4, Th2 cells continue to produce additional IL4 to the system. It opens up the possibility that there are other cell types that participate in the modulation of the erythroid niche by releasing IL4 and cooperating with Th2 cells. Our unpublished data also showed that T cells support the EBIs in spleen. Another question is based on the observation that IL4 reduces the number of SEPs (Figure 4-2D), whereas promotes the formation of stress BFU-Es. It implies that IL4 limits the self-renewal capability of immature SEPs, while driving the rapid differentiation of SEPs. Further research is needed to understand the underlying mechanisms. It will also be interesting to know whether IL4 can directly act on SEPs or whether it promotes SEP differentiation through altering the microenvironment. Another question is the connection between IL4 and Epo during stress erythropoiesis. Although the current evidence indicates that IL4 responds to Epo, the *in vivo* trend of IL4 expression was not precisely in line with the serum Epo change after BMT. IL4 shows a transient peak on day 6 and rapidly declines to the basal level on day 8. In contrast, the serum Epo level is gradually decreased from day 6 to day 12. Therefore, one emerging question is about the possible negative regulation of IL4. The Th2 cytokine is known to induce the polarization of macrophages to the alternatively activated phenotype (M2 macrophages), which regulates the resolution of inflammation[14]. Both IL4 and IL4 induced PPARγ has been demonstrated to induce

the differentiation of monocytes into M2 macrophages[15,16]. Recent work showed that pro-inflammatory cytokines are able to trigger stress erythropoiesis without tissue hypoxia[17], suggesting that inflammatory signals play important roles in initiating stress erythroid response. Epo is able to induce production of anti-inflammatory cytokine IL-10 in hemorrhagic shock model[18]. Our lab also observed multiple anti-inflammatory cytokines are required for SEP differentiation. These findings implicate a strong correlation between inflammation and stress erythropoiesis. Therefore, the alteration of microenvironment in response to Epo may also include a transition from monocytes to M2 macrophages or from classically activated macrophages (M1 macrophages), which has pro-inflammatory function, to M2 macrophages. Our unpublished data also showed an increase in M2 macrophages accompanied with the decrease in M1 macrophages after Epo treatment.

Taken together, I hypothesize a new mechanism where Epo induces a transition from pro-inflammatory microenvironment to anti-inflammatory microenvironment to support the growth of SEPs (Figure 4-3). First, Epo increases the production of PGD_2 in EBI macrophages. Next, the PGD_2-CRTH2 binding induces the release of Th2 cytokines, including IL4. IL4 helps to expand the niche and promotes the transition from monocytes or M1 macrophages to M2 macrophages. The IL4 induced production of PPARγ also contributes to this macrophage polarization. As a result, the M2 macrophage predominant microenvironment benefits the SEP differentiation by inducing high levels of PPARγ in the niche and inducing required anti-inflammatory cytokines.

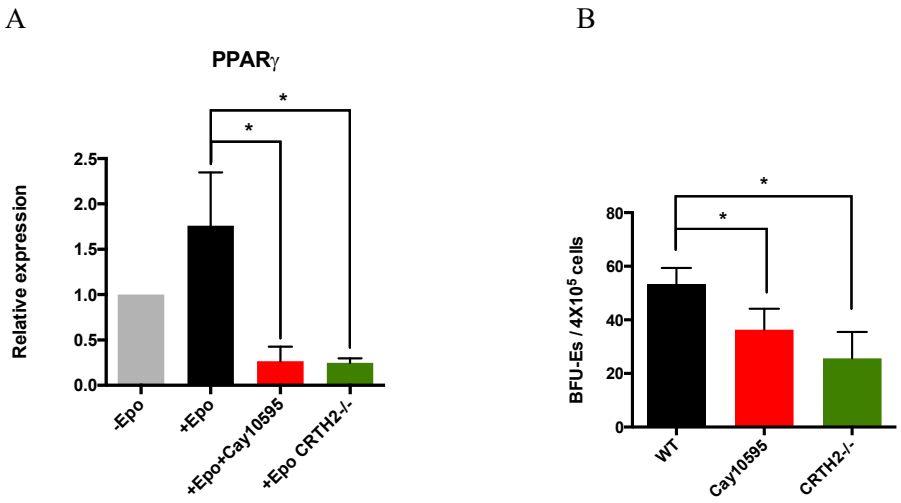

Figure **4-1**: **CRTH2 regulates PPARγ expression in stress erythropoiesis.**

(A). mRNA expression of PPARγ in *in vitro* cultured stroma cells. -Epo: WT cells in SEEM, +Epo: WT cells in SEDM, +Epo+Cay10595: WT cells in SEDM supplemented with Cay10595 (CRTH2 antagonist), +Epo CRTH2$^{-/-}$: CRTH2$^{-/-}$ cells in SEDM. Student t-test (2-tailed). Data represent means ± SEM. * $p < 0.05$.

(B). Stress BFU-E colony assay of *in vitro* cultured WT and ATF4$^{-/-}$ BM cells from (A). Student t-test (2-tailed). Data represent means ± SEM. * $p < 0.05$

A

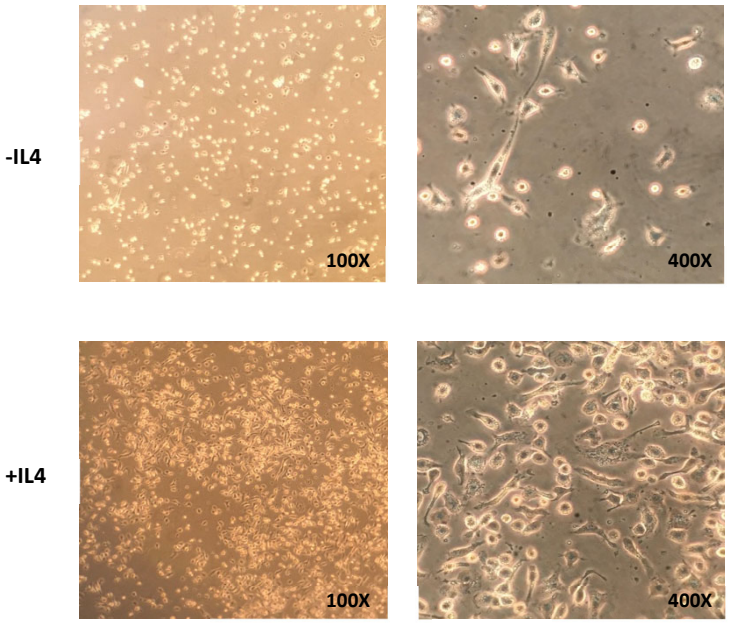
-IL4
100X
400X
+IL4
100X
400X

B

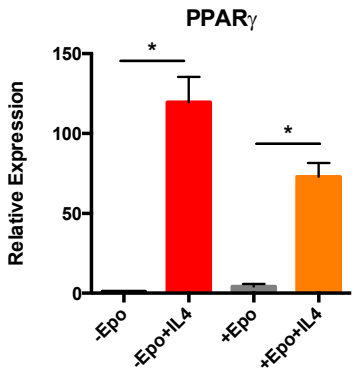
PPARγ
Relative Expression
150
100
50
0
*
*
-Epo
-Epo+IL4
+Epo
+Epo+IL4

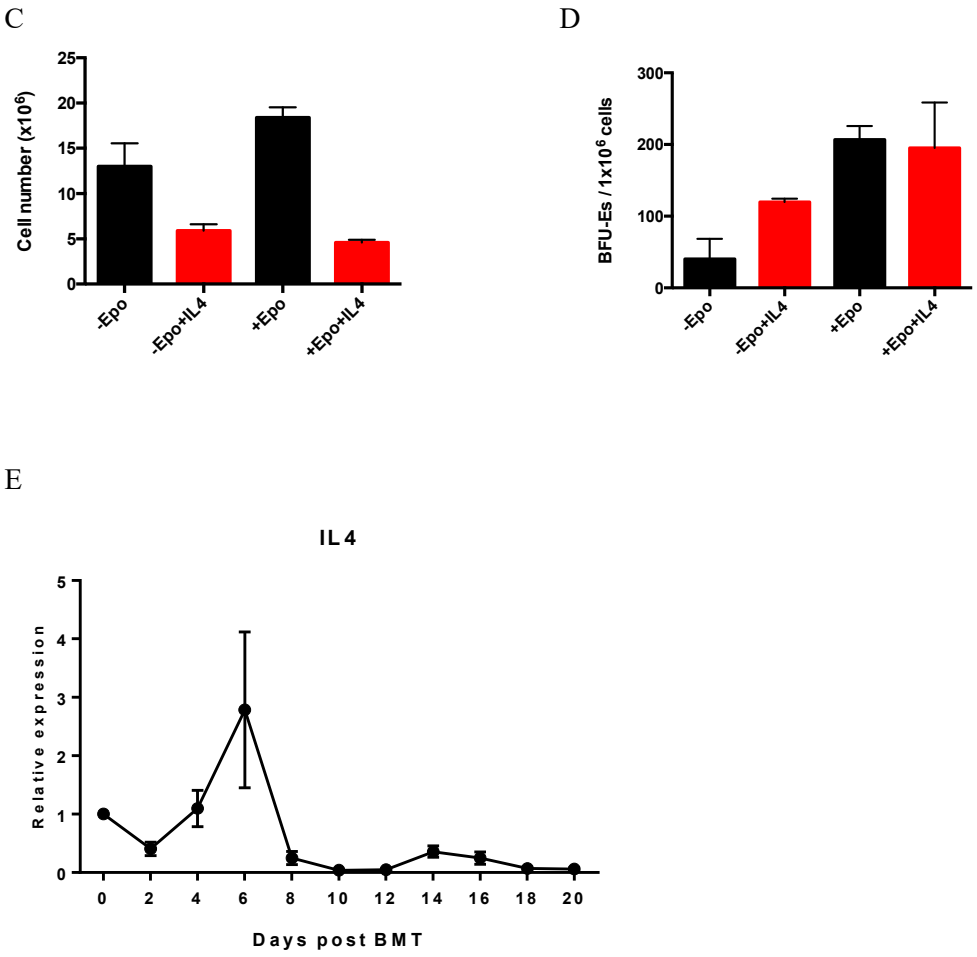

Figure **4-2**: **IL4 regulates PPARγ in microenvironment and differentiation of SEPs.**

(A). Representative microscopy images of in stroma cells in SEEM culture. Upper panels: SEEM culture without IL4. Bottom panels: SEEM culture supplemented with IL4.

(B). mRNA expression of PPARγ in *in vitro* cultured stroma cells treated ±Epo±IL4 as indicated. Student t-test (2-tailed). Data represent means ± SEM. * $p < 0.05$.

(C). Total SEP numbers in *in vitro* culture. Cells were treated with ±Epo±IL4 as indicated.

(D). Stress BFU-E colony assay of *in vitro* cultured SEPs from (C).

(E). mRNA expression of IL4 in spleen cells after BMT.

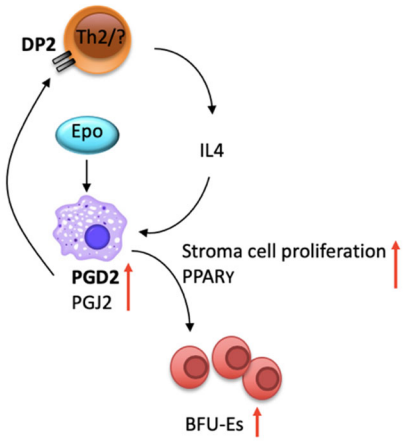

Figure **4-3**: **Proposed schematic of Epo dependent PGD_2/IL4 signaling in regulating niche and SEP development.**

4.2.2 mTORC1 regulated metabolic reprogramming in stress erythropoiesis

Actively dividing cells alter their metabolism according to the increased needs for energy and anabolic processes. Oxidative phosphorylation (OXPHOS) and glycolysis are two major bioenergetics pathways in mammalian cells. Under normal conditions, mitochondrial OXPHOS provides 70% of energy required by cells by generating 34 ATP molecules per reaction[19,20]. During rapid cell division, cellular metabolism changes to meet the increased energetic and anabolic requirements. Glycolysis is the preferred process in many types of actively dividing cells. In addition to immediately producing 2 ATP molecules, glycolysis generates multiple intermediates required by cell growth, including ribose for generating DNA and RNA, amino acids for generating proteins and glycerol for generating phospholipid cell membrane[21]. Cancer metabolism is one of the mostly well studied models of metabolic change. Cancer cells primarily

rely on glycolysis even with presence of oxygen and intact mitochondrial function[21]. This metabolic reprogramming is critical for doubling the biomass of cancer cells, which sustains the high proliferation rate in tumorigenesis. T cell activation also requires metabolic reprogramming[22]. The transition from quiescent naïve T cell to activated effector T cell is concomitant with increased cell size, proliferation and differentiation rate. The engagement of glycolysis enables anabolic growth and biomass accumulation required in these processes. Stress erythropoiesis is a hyperactive process of generating new erythrocytes, indicating that appropriate regulation of biosynthetic process is required by actively dividing SEPs.

We've discussed the role of mTORC1 in regulating global protein synthesis through coordinating with PERK signaling pathway. In addition to directly promoting protein translation, mTORC1 is also one of the key metabolic regulators. Activation of mTORC1 induces the translation of Myc and hypoxia-inducible factor1 alpha (HIF1α)[23,24]. These two transcription factors regulate the expression of key genes required by glycolysis, including glucose transporters and glycolytic enzymes[25,26]. It is also well documented that mTORC1 can initiate glycolysis by enhancing glutamine and glucose uptake[27]. Back to stress erythropoiesis, it will be interesting to investigate whether the activated mTORC1 in SEPs induces a metabolic change. Further studies could focus on characterizing metabolic phenotypes in different stages of stress erythropoiesis. Would there be a metabolic reprogramming once SEPs receive the transition signals? Would there be any changes in the biosynthesis of macromolecules, such as nucleotides, proteins and lipids, once SEPs acquire a new metabolic phenotype? One hypothesis is mTORC1 could induce the change from OXPHOS/glycolysis homeostatic status to glycolysis predominant status in SEPs. The increased glycolysis could fuel the rapid SEP differentiation by promoting the biosynthesis of essential constituents required by constructing new erythrocytes.

Previous work has demonstrated that transcription reprogramming plays a role in erythropoietic development[28–30]. However, the metabolic changes during erythropoiesis,

especially in stress erythropoiesis, have not been characterized. glucose-6-phosphate dehydrogenase (G6PD) deficiency and pyruvate kinase (PK) deficiency are two inherited anemia caused by variant genetic mutations in these two glycolytic enzymes. G6PD deficiency is the most common enzymatic blood disorder, which affects 400 million people worldwide[31]. By addressing the metabolic regulation questions in stress erythropoiesis, it's possible to characterize new metabolic transition signals derived from glycolytic metabolites in the future. Based on the findings, we might be able to identify potential metabolic targets for G6PD deficiency and PK deficiency treatments and provide references for further therapeutic research. In a broader perspective, mTORC1 function has been well studied in cancer cells and lymphoid cells[32,22]. Many drugs and treatments are designed for targeting mTORC1 signaling pathway. It is important to extend the mTORC1 regulatory roles into the erythropoiesis system, which would supplement the current knowledge of mTORC1 signaling pathway and advise relevant drug development to consider more about the comprehensive effect of mTORC1 in different cell types.

4.3 References

1. Shander, A., Javidroozi, M., Ozawa, S. & Hare, G. M. T. What is really dangerous: Anaemia or transfusion? *Br. J. Anaesth.* (2011) doi:10.1093/bja/aer350.
2. Zimrin, A. B. & Hess, J. R. Current issues relating to the transfusion of stored red blood cells. *Vox Sanguinis* (2009) doi:10.1111/j.1423-0410.2008.01117.x.
3. Spinella, P. C. *et al.* Duration of red blood cell storage is associated with increased incidence of deep vein thrombosis and in hospital mortality in patients with traumatic injuries. *Crit. Care* (2009) doi:10.1186/cc8050.
4. Bennett, L. F., Liao, C. & Paulson, R. F. Stress erythropoiesis model systems. in *Methods in Molecular Biology* (2018). doi:10.1007/978-1-4939-7428-3_5.
5. Xiang, J., Wu, D. C., Chen, Y. & Paulson, R. F. In vitro culture of stress erythroid progenitors identifies distinct progenitor populations and analogous human progenitors. *Blood* (2015) doi:10.1182/blood-2014-07-591453.
6. Li, W. *et al.* Identification and transcriptome analysis of erythroblastic island macrophages. *Blood* (2019) doi:10.1182/blood.2019000430.
7. Jowsey, I. R. *et al.* Mammalian class Sigma glutathione S-transferases: Catalytic properties and tissue-specific expression of human and rat GSH-dependent prostaglandin D2 synthases. *Biochem. J.* (2001) doi:10.1042/0264-6021:3590507.
8. Joo, M. & Sadikot, R. T. PGD synthase and PGD 2 in immune resposne. *Mediators of Inflammation* (2012) doi:10.1155/2012/503128.
9. Kabashima, K. & Narumiya, S. The DP receptor, allergic inflammation and asthma. *Prostaglandins Leukot. Essent. Fat. Acids* (2003) doi:10.1016/S0952-3278(03)00080-2.
10. Nagata, K. *et al.* CRTH2, an orphan receptor of T-helper-2-cells, is expressed on basophils and eosinophils and responds to mast cell-derived factor(s). *FEBS Lett.* (1999) doi:10.1016/S0014-5793(99)01251-X.
11. Narumiya, S. & FitzGerald, G. A. Genetic and pharmacological analysis of prostanoid receptor function. *Journal of Clinical Investigation* (2001) doi:10.1172/JCI200113455.
12. Huang, J. T. *et al.* Interleukin-4-dependent production of PPAR-γ ligands in macrophages by 12/15-lipoxygenase. *Nature* (1999) doi:10.1038/22572.
13. Jutel, M. *et al.* Bee venom immunotherapy results in decrease of IL-4 and IL-5 and increase of IFN-γ secretion in specific allergen-stimulated T cell cultures. *J. Immunol.* (1995).
14. Gordon, S. Alternative activation of macrophages. *Nature Reviews Immunology* (2003) doi:10.1038/nri978.
15. Bouhlel, M. A. *et al.* PPARγ Activation Primes Human Monocytes into Alternative M2

Macrophages with Anti-inflammatory Properties. *Cell Metab.* (2007) doi:10.1016/j.cmet.2007.06.010.

16. Odegaard, J. I. *et al.* Macrophage-specific PPARγ controls alternative activation and improves insulin resistance. *Nature* (2007) doi:10.1038/nature05894.

17. Diederich, M., Morceau, F. & Dicato, M. Pro-inflammatory cytokine-mediated anemia: Regarding molecular mechanisms of erythropoiesis. *Mediators of Inflammation* (2009) doi:10.1155/2009/405016.

18. Arimori, Y. *et al.* Role of heme oxygenase-1 in protection of the kidney after hemorrhagic shock. *Int. J. Mol. Med.* (2010) doi:10.3892/ijmm-00000430.

19. Mishra, P. & Chan, D. C. Mitochondrial dynamics and inheritance during cell division, development and disease. *Nature Reviews Molecular Cell Biology* (2014) doi:10.1038/nrm3877.

20. Robinson, G. L., Dinsdale, D., MacFarlane, M. & Cain, K. Switching from aerobic glycolysis to oxidative phosphorylation modulates the sensitivity of mantle cell lymphoma cells to TRAIL. *Oncogene* (2012) doi:10.1038/onc.2012.13.

21. Lunt, S. Y. & Vander Heiden, M. G. Aerobic Glycolysis: Meeting the Metabolic Requirements of Cell Proliferation. *Annu. Rev. Cell Dev. Biol.* (2011) doi:10.1146/annurev-cellbio-092910-154237.

22. Buck, M. D., O'Sullivan, D. & Pearce, E. L. T cell metabolism drives immunity. *Journal of Experimental Medicine* (2015) doi:10.1084/jem.20151159.

23. Zhu, H. *et al.* PKM2 enhances chemosensitivity to cisplatin through interaction with the mTOR pathway in cervical cancer. *Sci. Rep.* (2016) doi:10.1038/srep30788.

24. Düvel, K. *et al.* Activation of a metabolic gene regulatory network downstream of mTOR complex 1. *Mol. Cell* (2010) doi:10.1016/j.molcel.2010.06.022.

25. Kim, J. W., Tchernyshyov, I., Semenza, G. L. & Dang, C. V. HIF-1-mediated expression of pyruvate dehydrogenase kinase: A metabolic switch required for cellular adaptation to hypoxia. *Cell Metab.* (2006) doi:10.1016/j.cmet.2006.02.002.

26. Wang, R. *et al.* The Transcription Factor Myc Controls Metabolic Reprogramming upon T Lymphocyte Activation. *Immunity* (2011) doi:10.1016/j.immuni.2011.09.021.

27. Rolf, J. *et al.* AMPKα1: A glucose sensor that controls CD8 T-cell memory. *Eur. J. Immunol.* (2013) doi:10.1002/eji.201243008.

28. Iwasaki, H. *et al.* The order of expression of transcription factors directs hierarchical specification of hematopoietic lineages. *Genes Dev.* (2006) doi:10.1101/gad.1493506.

29. Ebina, W. & Rossi, D. J. Transcription factor-mediated reprogramming toward hematopoietic stem cells. *EMBO J.* (2015) doi:10.15252/embj.201490804.

30. Khajuria, R. K. *et al.* Ribosome Levels Selectively Regulate Translation and Lineage Commitment in Human Hematopoiesis. *Cell* (2018) doi:10.1016/j.cell.2018.02.036.

31. Cappellini, M. & Fiorelli, G. Glucose-6-phosphate dehydrogenase deficiency. *The Lancet* (2008) doi:10.1016/S0140-6736(08)60073-2.

32. Kim, L. C., Cook, R. S. & Chen, J. MTORC1 and mTORC2 in cancer and the tumor microenvironment. *Oncogene* (2017) doi:10.1038/onc.2016.363.

VITA

Yuanting Chen

Education

- **Ph.D. in Biological and Biomedical Sciences** — **08/2013 – present**
  The Huck Institutes of Life Sciences — Pennsylvania State University — State College, PA
- **M.S. in Internal Medicine** — **09/2011 – 06/2013**
  The First Affiliated Hospital — Zhejiang University — Hangzhou, China
- **B.S. in Biological Sciences** — **09/2007 – 06/2011**
  Department of Biological Sciences — Xiamen University — Xiamen, China

Publications

1. Paulson RF, Ruan B, Hao S, **Chen Y**. Stress Erythropoiesis is a Key Inflammatory Response. ***Cells***, 2020. 9:634.
2. Xiang J, Wu D, **Chen Y**, Paulson RF. In vitro culture of stress erythroid progenitors identifies distinct progenitor populations and analogous human progenitors. ***Blood***, 2015. 125(11):1803-12
3. Qin N, Yang F, Li A, Prifti E, Chen Y, Shao L, Guo J, Le Chatelier E, Yao J, Wu L, Zhou J, Ni S, Liu L, Pons N, Batto JM, Kennedy SP, Leonard P, Yuan C, Ding W, **Chen Y**, Hu X, Zheng B, Qian G, Xu W, Ehrlich SD, Zheng S, Li L. Alterations of the human gut microbiome in liver cirrhosis. ***Nature***, 2014.9:513(7516).
4. Huang F, Guo J, Zou Z, Liu J, Cao B, Zhang S, Li H, Wang W, Sheng M, Liu S, Pan J, Bao C, Zeng M, Xiao H, Qian G, Hu X, Chen Y, **Chen Y**, Zhao Y, Liu Q, Zhou H, Zhu J, Gao H, Yang S, Liu X, Zheng S, Yang J, Diao H, Cao H, Wu Y, Zhao M, Tan S, Guo D, Zhao X, Ye Y, Wu W, Xu Y, Penninger JM, Li D, Gao GF, Jiang C, Li L. Angiotensin II plasma levels are linked to disease severity and predict fatal outcomes in H7N9-infected patients. ***Nat Commun***, 2014. 5: 3595.

Manuscripts in preparation

1. **Chen Y**, Xiang J, Qian F, Bastihalli DT, Ruan B, Hao S, Prabhu KS, Paulson RF. Macrophage Epo-receptor signaling alters the splenic niche to promote erythroid differentiation. Under revision.
2. **Chen Y**, Xiang J, Ruan B, Xin P, Trebak M, Paulson RF. Critical roles of PGE2 dependent Calcium dynamics and PERK signaling mediated translational reprogramming in anemia. In preparation.

Conference Presentations

1. **Chen Y**, Xiang J, Paulson RF. Role of PGE2 dependent Perk kinase signaling in stress erythropoiesis. Gordon Research Conference on Red Cells, Jun 2015, Holderness, NH
2. **Chen Y**, Xiang J, Paulson RF. Translational regulation by PGE2-PERK signaling pathway during stress erythropoiesis. 2016 Hemoglobin Switching Conference, Sep 2016, Pacific Grove, CA
3. **Chen Y**, Xiang J, Paulson RF. New roles of Epo dependent PGE_2- PERK signaling pathway in translational control during stress erythropoiesis. Gordon Research Conference on Red Cells, Jul 2017, Newport, RI
4. **Chen Y**. Prostaglandin E2 and PERK Signaling Pathways Regulate Differentiation of Stress Erythroid Progenitors. 60th Annual Red Cell Meeting, Oct 2018, New Haven, CT
5. **Chen Y**. Epo Regulate Niche Signaling to Promote Expansion and Differentiation of Stress Erythroid Progenitors. 61st Annual Red Cell Meeting, Oct 2019, Rochester, NY

Scholarships, Honors and Awards

- 2019 CAS Graduate Student Competitive Grant Program Award, College of Agricultural Sciences, Pennsylvania State University
- 2017 and 2016 Huck Travel Award, Huck Institutes of Life Sciences, Pennsylvania State University
- 2016 CAS Travel Award, College of Agricultural Sciences, Pennsylvania State University

Teaching experience

- Teaching assistant at Pennsylvania State University, University Park, PA — **08/2016- 12/2016**
  Course: BIOL 230W, Molecular and Cellular Biology lab.
- Teaching assistant at Pennsylvania State University, University Park, PA — **01/2017- 05/2017** & **08/2018-12/2018** & **01/2019-05/2019**
  Course: MICRB 107, Elementary Microbiology lab.